IMMUNOSUPPRESSIVE PROPERTIES OF WHARTON'S JELLY DERIVED MESENCHYMAL STROMAL CELLS IN THE TREATMENT OF GRAFT VERSUS HOST DISEASE IN RAT MODEL

by

YELICA VIRGINIA LOPEZ RODRIGUEZ

DVM, Universidad Centroccidental Lisandro Alvarado, 1999

AN ABSTRACT OF A DISSERTATION

submitted in partial fulfillment of the requirements for the degree

DOCTOR OF PHILOSOPHY

Department of Anatomy and Physiology.

College of Veterinary Medicine

KANSAS STATE UNIVERSITY
Manhattan, Kansas

2013

Abstract

Graft Versus Host Disease (GVHD) is the major complication following hematopoietic stem cell transplantation. GVHD is activated by immunocompetent T cells presented in the donor grafted tissue. Due to the increased use of bone marrow transplantation to treat diverse malignancies, the incidence of GVHD has shown a notable increase. Depending of the degree of immunological mismatch between donor and host, 50-70 % of patients develop GVHD after allogeneic Bone Marrow Transplantation (BMT). Once GVHD develops, mortality reaches up to 50% in humans. Several studies using Mesenchymal Stromal Cells (MSCs) to prevent and treat GVHD have produced controversial results. It is thought that distinct MSCs sources used in those studies might be an important factor that produces different outcomes. For cellular therapy, the most attractive characteristics of MSCs are their reduced immunogenic potential, and their abilities to modulate immune responses. This dissertation addressed the hypothesis that Wharton's jelly cells (WJCs) would prevent the pathology and death associated with GVHD after BMT. To accomplish this, I created a clinically relevant model of GVHD by transplanting allogeneic bone marrow across minor histocompatibility antigen (HA) barriers in the rat. To enhance alloreactive T-cell stimulation, bone marrow (BM) was co-administered with a fraction of $CD8^+$ cells magnetically selected from spleen to induce GVHD. Bone marrow tissue was isolated from a donor rat Fischer 344 (F344, RT1lv) and transplanted into lethally irradiated (10 Gray) Lewis rat (LEW, RT1l). Once GVHD was induced, MSCs derived from umbilical cord WJCs were either co-transplanted at day 0 with bone marrow, or given on day 2 post-BMT intravenously. The prophylactic potential of WJCs in an *in vivo* GVHD model was assessed as survival time, clinical symptomatology occurrence, and histopathology injuries in target tissues. Results indicate that while co-administration of WJCs with hematopoietic cells on day 0 failed to alleviate GVHD associated symptomatology and mortality. WJCs administered on day 2 post-induction ameliorated GVHD-associated symptomatology, improved engraftment and survival.

Keywords: graft versus host disease, umbilical cord mesenchymal stromal cells, Wharton's jelly cells, GVHD rat model.

IMMUNOSUPPRESSIVE PROPERTIES OF WHARTON'S JELLY DERIVED MESENCHYMAL STROMAL CELLS IN THE TREATMENT OF GRAFT VERSUS HOST DISEASE IN RAT MODEL

by

YELICA VIRGINIA LOPEZ RODRIGUEZ

DVM, Universidad Centroccidental Lisandro Alvarado, 1999

A DISSERTATION

submitted in partial fulfillment of the requirements for the degree

DOCTOR OF PHILOSOPHY

Department of Anatomy and Physiology.

College of Veterinary Medicine

KANSAS STATE UNIVERSITY
Manhattan, Kansas

2013

Approved by:

Major Professor
Mark L Weiss

Copyright

Abstract

Graft Versus Host Disease (GVHD) is the major complication following hematopoietic stem cell transplantation. GVHD is activated by immunocompetent T cells presented in the donor grafted tissue. Due to the increased use of bone marrow transplantation to treat diverse malignancies, the incidence of GVHD has shown a notable increase. Depending of the degree of immunological mismatch between donor and host, 50-70 % of patients develop GVHD after allogeneic Bone Marrow Transplantation (BMT). Once GVHD develops, mortality reaches up to 50% in humans. Several studies using Mesenchymal Stromal Cells (MSCs) to prevent and treat GVHD have produced controversial results. It is thought that distinct MSCs sources used in those studies might be an important factor that produces different outcomes. For cellular therapy, the most attractive characteristics of MSCs are their reduced immunogenic potential, and their abilities to modulate immune responses. This dissertation addressed the hypothesis that Wharton's jelly cells (WJCs) would prevent the pathology and death associated with GVHD after BMT. To accomplish this, I created a clinically relevant model of GVHD by transplanting allogeneic bone marrow across minor histocompatibility antigen (HA) barriers in the rat. To enhance alloreactive T-cell stimulation, bone marrow (BM) was co-administered with a fraction of $CD8^+$ cells magnetically selected from spleen to induce GVHD. Bone marrow tissue was isolated from a donor rat Fischer 344 (F344, RT1lv) and transplanted into lethally irradiated (10 Gray) Lewis rat (LEW, RT1l). Once GVHD was induced, MSCs derived from umbilical cord WJCs were either co-transplanted at day 0 with bone marrow, or given on day 2 post-BMT intravenously. The prophylactic potential of WJCs in an *in vivo* GVHD model was assessed as survival time, clinical symptomatology occurrence, and histopathology injuries in target tissues. Results indicate that while co-administration of WJCs with hematopoietic cells on day 0 failed to alleviate GVHD associated symptomatology and mortality. WJCs administered on day 2 post-induction ameliorated GVHD-associated symptomatology, improved engraftment and survival.

Keywords: graft versus host disease, umbilical cord mesenchymal stromal cells, Wharton's jelly cells, GVHD rat model.

Table of Contents

List of Figures

List of Tables

Acknowledgements

I would like to acknowledge my alma mater the Universidad Centroccidental Lisandro Alvarado in Barquisimeto-Venezuela for providing the economic support for my studies. To my colleagues in the Department of Basic Science at Veterinary School, especially who were in charge of my academic responsibilities for the past 5 years: Professors Marygnacia Suárez, Bernardo Vásquez, Gloria Cánepa, Celeste Flores, Johilmer Alvarez and Eduard Martínez, thank you.

I would like to express my sincere gratitude to my advisor, Dr. Mark. L Weiss, for giving me the opportunity to work in his lab towards my doctoral degree. He offered invaluable assistance, support and guidance. Far from home, Dr. Weiss was like a second father to me. I will keep good memories from Dr. Weiss' lab for the rest of my life.

Deepest gratitude is due to the members of the supervisory committee Dr. Duane Davis, Dr. Maria Ferrer, Dr. Dudley McCaw, and Dr. Michael Kenney

Thanks also to my graduate friends, Kreeson Packthongsuk, Sivasai Balivada, Lakshmi Deepthi Uppalapati, Cesar Caballero and Hamad Alshetaiwi, in my most difficult moments you were always there for me to encourage me to keep going.

I would like to thanks to the current Dr. Weiss's lab members Dr. Hong He (Uncle He), John Hirt, Katrina Fox, Robbie Smith, Jason Orr and especially to Phuoc Bui (Van) who was my right hand in all the transplantation procedures and helped me a lot taking care the rats. My sincere thanks to past Weiss' lab member Kiran Seshareddy, who guided me through the stem cells manipulation and isolation techniques. I would like to extend my sincere thanks to the faculty and administrative staff at the department of Anatomy and Physiology and especially to Kansas State Animal Resource Facility's workers Dr. Tracy Miesner, Dr. Susan Rose, Dr. Sally Olsen and James Dille.

Special thanks to my mom Rosa and Ytalo Carazut for taking care of my most precious treasure, my little daughter Luz Celeste, during the course of my studies

Dedication

To my little Daughter

Chapter 1- Introduction

1.1 Background and Significance

Hematopoietic stem cell transplantation (HSCT) is the current transplant indication for patients suffering specific congenital or acquired hematologic disorders [1], such as leukemia [2,3,4], multiple myeloma [5,6], aplastic anemia [7,8,9], thalassemia [10, 11], severe immunodeficiency syndrome [12,13] and more recently, human immunodeficiency virus (HIV) [14,15]. Currently, HSCT is performed from autologous, syngeneic and allogeneic donor sources [16] and hematopoietic cells are typically collected from bone marrow (BM), umbilical cord blood or peripheral blood after mobilization [1, 16, 17]. The aim of HSCT is replacing the damaged hematopoietic compartments with functional hematopoietic stem cells which are capable of reconstituting hematopoietic niches after myeloablative conditioning regimens [1, 17]. Therapeutic efficacy of HSCT in patients with hematologic malignancies is attributed, in part, to responses mediated by donor T cells and natural killer (NK) cells, which lead to the graft versus leukemia (GVL) effect [18]. Unfortunately, induction of GVL is accompanied often by the development of graft versus host disease (GVHD). GVHD is a post-transplant life-threatening disorder that affects 30-75% of the patients receiving allogeneic HSCT from disparate human leucocyte antigen (HLA) donors [19]. A GVHD-like syndrome also has been described after haploidentical HSCT, syngeneic [20] and even autologous HSCT [21]. Therefore, GVHD represents a major complication which affects successful HSCT outcomes [22]. The severity of GVHD correlates with the stem cell source, MHC disparity across minor and major antigens [23], the age of the patient, sex mismatch between donor and recipient [24], conditioning regimen [25], any GVHD prophylaxis used [26], degree of immunosuppression [27], number of transfused donor T cells [28], and intestinal microflora and endotoxin [29].

GVHD is a syndrome resulting from disparities for minor and major histocompatibility antigens [30]. Classically, based upon time of clinical symptomatology manifestation, GVHD has been described as acute (aGVHD) if symptoms appear before 100 days post-HSCT, or chronic (cGVHD), if clinical indicators appear beyond 100 days after HSCT [31]. However, a new consensus for GVHD diagnosis and grading for clinical trials, which is based on clinical manifestation rather than presentation time, is currently accepted by NIH. This consensus

includes a third classification of GVHD founded in the concomitant presentation of clinical signals of both acute and chronic GVHD [32, 33, 34].

Epithelial tissues are the target for GVHD [35]. Clinical signals and histopathological damage typically occur in skin, gastrointestinal mucosa and liver [34]. However, many studies have reported GVHD-related afflictions on varied organs such as pancreas [36], lung [37, 38, 39, 40], kidney [39, 40], spleen [39] and cardiovascular system [40]. In contrast, cGVHD is considered a pleiotropic syndrome, whose target is mainly connective tissue and clinical and histopathological manifestations include fibrosis [34].

Although GVHD might involve multiple immune reactions [41], a general agreement is that this disorder is generated by the recognition of donor T cells to alloantigens present in immunocompromised hosts who are unable to reject donor cells after myeloablative regimens [42]. Under this notion, GVHD pathophysiology is driven by cytopathic donor T cells, which react to genetically disparate host polymorphic antigens and can be presented by antigen-presenting cells (APCs) from host, donor or both [34,41]. Hematopoietic derived APCs [43], also known as professional APC [44], such as B cells, tissue macrophages and Langerhans cells, play an important role in triggering aGVHD [45]. Recent investigation supports the notion that a subpopulation of stromal APCs (nonhematopoietic, also called nonprofessional APCs), such as follicular dendritic cells [46], fibroblasts, myofibroblasts, and pericytes [47], may play an underestimated role in GVHD pathogenesis [44, 47]. Scientific evidence presented by Tobuai *et al*. 2012 suggest that vascular endothelial and certain epithelial cells are the putative nonhematopoietic APCs with the capacity to directly stimulate donor T cells and induce GVHD [48].

Typically, GVHD pathophysiology is described in sequential stages. The first stage is set by the preparative immunosuppressive regimen of chemotherapy and/or radiotherapy, which damages host tissues, and causes hypercytokinemia [49]. In the second stage, APCs from donor and host, along with inflammatory cytokines, trigger activation of donor T cells, which proliferate and differentiate into effector cells. In the third stage, activated donor T cells drive cytotoxicity against target host tissue [50]. Radiation-induced vascular endothelium injury [40, 51] and innate immunity are also considered triggering factors for GVHD progress [52]. Components of the innate immune system, such as epithelial barriers, soluble molecules and cells, are being studied as potential factors that play a role in GHVD induction in target tissues

[52, 53]. In a rat model of aGVHD, Koltun *et al*. found a positive correlation between small intestine epithelial permeability and GVHD occurrence [54]. Activation in target tissues of complement and Toll-Like Receptor (TLR) plays a role of recognition of associated molecular patterns (PAMPs) from the intestinal microflora and may intensify aGVHD syndrome [55]. Complement activation has been reported in murine models of aGVHD [56]. The role of innate immune cells, such as eosinophils, mast cells and neutrophils, and macrophages, in GVHD pathogenesis has been dissected in several studies [57, 58, 59, 60, 61, 62].

New theories argue that a pool of host radio-resistant immune cells may be involved in cGVHD pathogenesis [63, 64, 65], therefore cGVHD may be driven by autoimmune components [34, 63, 66]. In a cGVHD model Lee *et al*. showed that hosts receiving T-cell depleted BM develop an autoimmune disorder driven by host T cells originated from radio-resistant intra-thymic precursors which, despite a reduction in dendritic cells (DC) after high-dose irradiation, escape the intra-thymic mechanisms of self-antigen removal (negative selection) [64]. Currently researchers are making efforts to find reliable biomarkers for the detection of GVHD [67, 68]. Recently, the protein Elafin was discovered as a novel marker for cutaneous GVHD which might predict GVHD severity [69]. However to date, diagnostic, staging and grading of GVHD are based on clinical manifestation and posterior confirmation is based on histopathology studies [19].

1.2 Methods of Preventing GVHD

1.2.1. Immunosuppressive drugs.

GVHD is one of the main causes of non-relapsed mortality in patients receiving allogeneic HSCT (allo-HSCT) [70]. GVHD development is determined by immunocompetent cells present in the allograft that recognize donor alloantigens and activate once they interact with APC, and thus generate an immune response against host target tissue [71, 72]. Most transplantation protocols include strategies to induce immunosuppression in the host and immunotolerance of donor tissues, and thus prevent or reduce clinical manifestations of GVHD [73]. Though, the optimal strategy to reestablish the immune system has not been defined [74].

Administration of immunosuppressive drugs to reduce the incidence of aGVHD in patients receiving allogeneic HSCT is considered a standard practice [75]. Various drugs either

prevent activation of donor T cells such as cyclosporine, tacrolimus, sirolimus (rapamycin), methotrexate, mycophenolate mofet and cytotoxic T-lymphocyte antigen 4 (CTLA-4), or act on effector cells, such as daclizumab and infliximab, are currently used in GVHD prophylaxis [76]. Corticosteroids, alone or in combination with other immunosuppressive drugs, are the first-line treatment of aGVHD [73], and methylprednisone is most frequently used [24]. However, steroid toxicity and collateral effects result in allograft loss, refractory condition to steroids and infections [77].

1.2.2. Graft T-cell depletion.

Another strategy to reduce incidence of GVHD involves removing T cells of the graft (T-cell depletion) [24]. Nevertheless, hematopoietic reconstitution, mortality and occurrence of opportunistic infections [78] represent a problem in host receiving T-cell depleted grafts [79]. In addition, in the case of an underlying malignant disease, manipulation of the graft by depletion of T cells might reduce the desired GVL effect and increase risk of relapse of the underlying disease [79].

1.2.3. Immunotolerance mediated by Tregs.

Another approach to control GVHD is by means of regulatory T cells (Tregs), a subpopulation of T cells which have the capacity of modulate immune responses by regulating the effector cells activation, expansion and differentiation [80].. In a phase I dose-escalation clinical trial Brusntein *et al*. demonstrated that infusion of ex vivo expanded umbilical cord blood (UCB)- derived Tregs selected after double umbilical cord blood transplantation (UCBT) and nonmyeloablative conditioning regimen, reduced incidence of grade II-IV aGVHD. They have shown that in murine model of aGVHD, Tregs are able to suppress CD8+ effector cells in target organs [80]. However, because Tregs can inhibit host antitumor responses leading to neoplasia recurrence, tolerance induced by Tregs might be insufficient to control underlying malignant diseases [81].

1.2.4. MSCs infusions

Mesenchymal stromal cells (MSCs) are a heterogeneous cell population derived from the embryonic connective tissue, mesenchyme, which constitutes the structural support, or stroma, of different organs [82]. MSCs are defined following the International Society for Cell Therapy

(ISCT) guideline as a population of cells which adheres to plastic culture flasks, express particular surface markers antigens and are capable to differentiate along mesenchymal lineages such as fat, bone and cartilage [83].

Though absent of specific or standard surface markers, MSC recognition is made possible by several mechanisms. Most practically, recognition is apparent within culture due to their ability to adhere to plastic tissue culture dishes [83]. Within assays, MSCs are recognized by the expression of certain mesenchymal surface markers such as cluster of differentiation (CD) CD105 (Sh2 or endoglin), CD73 (SH3 or SH4), CD90, CD44. Additionally, MSCs are negative for expression of hematopoietic markers CD34 and CD45 [83]. Recognition of MSCs via their ability to differentiate into specific tissue of mesodermal lineages, such as bone, cartilage and fat, may also be accomplished [83]. Several studies have reported the capacity of MSCs to overcome the typical mesenchymal cell fate by trans-differentiating into cells of endodermal [84] and neuroectodermal origin [85].However, donor age affects both proliferation and differentiation potentials [86]. For example, an *in vitro* comparison of rat Wharton's jelly cells (WJCs) versus adult bone marrow derived MSCs showed a superior capacity of fetal sources of MSCs (WJCs) to differentiate towards cardiomyocyte lineage [87]. MSCs play a fundamental role in cell turnover and maintaining homeostasis within tissues *in vivo* [88]. The abilities of MSCs to suppress the activation, expansion and maturation of immunocompetent cells T cells, B cells, natural killer and dendritic cells [89], made them an attractive cell therapy to control immunologic disorders [90, 91].

1.2.5. Adult versus Fetal MSCs

MSCs were initially isolated from adult bone marrow (BM), where they constitute about 0.01 to 0.001% of mononuclear cells [92]. However, cells with comparable characteristics also have been found in almost every tissue, close to blood vessel walls [93]. Comparative studies of BM-derived MSCs versus fetal sources MSCs have established similarities between both sources of cells [94, 95]. MSCs from fetal sources are exceptional due to their proliferative and less differentiated state than the ones from adult origin [96]. Baksh *et al*. found that umbilical cord perivascular MSCs (UCPVCs) had a higher proliferative capacity than BM-derived MSCs [94]. Comparative studies of proliferation performed by Lu *et al.* in 2006 revealed that BM-derived MSCs manifested slower population doubling time (PDT) than umbilical cord-derived MSCs

[97]. Mitchell *et al*. found that porcine WJCs cultured for more than 80 population doubling time (PDT) do not show senescence, change in morphology or lose their capacity to differentiate into neurons [85].

In the present dissertation, the goal is to evaluate the effect of administration of Wharton's jelly cells (WJCs) on the prophylaxis of graft versus host disease (GVHD) after allo-HSCT. Specifically, this study aimed to first, I describe a protocol to isolate and expand WJCs from rat umbilical cord. Second, I developed a minor antigen mismatch model of GVHD. Third, I evaluated the treatment effect of WJCs derived from rat umbilical cord to ameliorate clinical manifestation of GVHD, and to improve survival time in recipients following total body irradiation (TBI) and allo-HSCT. Finally, I measured the effect of WJCs in improving hematopoietic compartment reconstitution.

1.2.6. MSCs and the Immune System

The reduced immunogenicity related to MSCs might be explained in part to their immunophenotype associated with low expression of MHC class I antigens and no expression of MHC class II [98], together with no expression of co-stimulatory molecules CD40, CD80 and CD86, which are decisive for the activation of T cells and the development of a successful immune response [99]. Due to MSCs expression of MHC class I molecules, they may potentially activate T cells, but in the absence of appropriated co-stimulation by a second signal, any lasting engagement of the T cell receptor on T helper (Th) cells would lead to state of unresponsiveness or anergy, which contributes to tolerance [99].

Different studies have shown that MSCs can regulate both adaptive and innate immune responses [100, 101, 102, 103]. Studies performed *in vitro* and *in vivo* have shown the capacities of MSC to exert a potent immunomodulatory effect on many cells of the immune system [100]. Even though mechanisms underlying these effects remain to be fully elucidated, the immunosuppressive effect of MSCs GVHD is highly related with soluble mediators [92,102]. Polchert *et al*. consider that immunosuppressive properties of MSC on GVHD are activated by exposure to inflammatory cytokines, such as interferon gamma (INF-γ) released by T cells [103]. On the other hand, Wang *et al*. 2009 support the idea that MSCs combat GVHD by inducing proliferation of regulatory T cells (Tregs), which are well-characterized as being T cell suppressors [104]. Soluble factors secreted by MSCs that are considered as candidates for

immunoregulation include transforming growth factor beta (TGF-β) [105], indoleamine 2,3-dioxygenase (IDO) [106], hepatocyte growth factor (HGF) [99], inducible nitric oxide synthase (iNOS) [107], prostaglandin E2 (PGE2), human leukocyte antigen G6 (HLA-G6) [108], and interleukin 10 (IL-10) [105]. More recently, Lee *et al*. 2009 identified the protein TSG-6, also known as TNFα-induced protein 6, to be a soluble factor associated with extracellular matrix remodeling and anti-inflammatory functions [109]. Interestingly, TSG-6 is upregulated in response to inflammatory signaling such as IL-1 and TNF-α [110]. Recently, it has been suggested that nanometer scale vesicles (exosomes) released by MSCs may be involved in immunomodulation properties of these cells [111]. Since inflammation plays a fundamental role in GVHD pathogenesis [112], the use of MSCs for clinical trials may lead to the development of future therapies for difficult diseases [113].

1.2.7. MSCs in the Treatment of GVHD

The safety and efficacy of MSC is currently being evaluated for at least 12 pathologic conditions, and several completed studies have shown the effectiveness of MSC to prevent or treat GVHD [114]. In 2004, Le Blank *et al*. reported a case of dramatic reduction in clinical symptomatology in a 9-year old patient suffering grade IV steroid-refractory aGVHD after administration of the first dose of MSCs derived from a haplo-identical donor [115]. This report was followed by a pilot study performed by Ringden *et al.* in 2006 who transferred MSCs in 8 patients with steroid-refractory grade II and IV GVHD and one with cGVHD; aGVHD symptoms were completely abolished in 6 out 8 patients, whose survival rate was significantly improved in comparison with untreated controls [116].

The efficacy of intravenous (IV) infusion of MSCs to control inflammatory responses in immunological disorders has been reported [103, 104, 113]. While MSCs homing and engraftment are considered fundamental requirements for cell therapy [117], the cell kinetics and biodistribution upon IV administration show that the number of cells that home to the target tissues is extremely low and most MSCs remain trapped in capillary beds within the liver, spleen and lung [109, 118, 119]. Rochefort *et al*. found a 50 to 60% of MSCs in rats accumulate in lung microvasculature 1 hour after the infusion with a reduction and stabilization of about 30% at 3 hours post-infusion. However, exosomes (20-200 nm in size) released by MSCs may mediate a

paracrine effect by acting local or at distance establishing an intercellular communication through via membrane receptors, intracellular uptake of exosomes or membrane fusion [111]. Roddy *et al*. used MSCs in a rat corneal model for inflammatory responses, and they suggest that MSCs engraftment is not a requirement since these cells are capable to work at distance from injury sites being activated to release the protein TSG-6 [120]. It is, therefore, suggestive that the therapeutic effects of MSCs are systemic and at a distance from injury sites [110, 120, 121].

Studies determining the effectiveness of MSCs to control aGVHD in murine models have reported contradictory results [122]. Several studies [123, 124, 125] have reported that co-infusion of MSCs with hematopoietic cells might be beneficial for hematopoietic cell engraftment and hematopoietic recovery. Christensen *et al.* evaluated timing of administration and dose-responses of MSCs using a GVHD murine model and showed that MSCs have only a transient immunosuppressive effect on the delay of GVHD progression. However, this study was performed by using cyclophosphamide as a pre-transplant therapy [126]. Nevertheless, since MSC are unable to exert immunosuppression activity when Tregs are depleted [127] and, being that cyclophosphamide targets Treg populations [128], it may be reasonable to conclude that the MSCs may have failed to express their immunosuppressive functions successfully under these conditions. Prigozhina *et al*. also reported that MSCs failed to reduce GVHD-related mortality in a mouse model [129]. In this case, MSCs were administrated at days 0, 7 and 14 after HSCT at tolerated doses of $5x10^5$ or $0.5x10^5$ per mouse. If an inflammatory response is required for MSC activation [130], Prigozina's results may be correlated with inadequate timing of administration of the cells as co-infusion of MSCs with hematopoietic cells at day 0 may not increase the level of inflammatory cytokines enough to activate the MSCs and prevent GVHD progress [103]. Joo and colleagues utilized a mouse model of GVHD and found that MSCs used at dose of $1x10^6$ and $2x10^6$ MSCs per mouse given together with hematopoietic cells after radiation (day 0) via IV improved survival to 40% and 60% respectively until day 50 after hematopoietic reconstitution, while a lower dose of $0.5x10^6$ cells per mouse did not improve survival time [131]. Based upon this data, in addition to timing of administration, cell dose may be another variable that impacts the efficiency of MSCs to induce immune –regulation in GVHD settings. Joo's research by using MSCs which expresses red fluorescent protein (RFP) derived from transgenic mice C57BL/6 RFP, and splenocytes derived from transgenic mice which express enhanced green fluorescent protein (EGFP) established in an *in vivo* fluorescent imaging study that MSCs and splenocytes

show similar kinetic and biodistribution pattern following IV infusion, reaching first lung and remaining there for about 24 hours, then moving to gastrointestinal tract and finally to lymp node and skin. In summary, reports about the efficiency of MSC infusions to prevent or treat GVHD are inconsistent. These inconsistencies could be related to the source of MSCs, donor age, using fresh or cryopreserved-thawed MSC, isolation and culture conditions for expansion and dose [132, 133].

1.2.8. Wharton's Jelly Cells

Wharton's jelly is a specialized, primitive connective tissue which constitutes the functional supportive framework of the umbilical cord [82]. The umbilical cord contains fibroblast-like cells surrounded by an extracellular matrix composed of glycoprotein microfibrils, collagen fibrils and glycosaminoglycans (GAGs) [136]. Hyaluronic acid is the most abundant GAG present in the Wharton's jelly [12]. Disperse mast cells can be found within the Wharton's jelly, most frequently in the proximity of the umbilical blood vessels [137]. Fetal sources of MSCs, such as Wharton's jelly cells (WJCs), retain characteristics that make them an interesting resource for clinical applications and tissue engineering [138]. The fetal MSCs (fMSCs) can be derived from ethically compromised source of aborted material [113] or from derived from discarded perinatal tissue e.g.,WJCs [87], while adult MSCs (aMSCs) isolation involves an invasive procedure[139]. Second, fMSCs proliferate faster than adult MSCs (aMSCs). Third, the immunosuppressive effect of fMSCs *in vitro* is stronger than aMSCs [140]. Finally fMSCs express broader differentiation potential than aMSCs [141]. For clinical applications aMSCs present some drawbacks, such as reduction in both MSC number and differentiation potential with age [142], early senescence in culture [143], reduced proliferation [144]. The umbilical cord is a perinatal tissue collected painlessly at birth and has no ethical controversy associated with its collection. It is also is a rich source of stem-like cells [141]. The WJCs maintain long telomeres in culture which is an indicator of proliferation and lifespan [10], as well as a high frequency of colony-forming unit fibroblasts (CFU-F) which assess clonogenic capacity [142, 143] and secrete soluble factors probably as exosomes [111] implicated in immunomodulation [144, 145].

Little scientific information is available about the effectiveness of WJCs in GVHD prophylaxis. Wu and colleagues show that MSCs derived from umbilical cord had higher suppressive effect on peripheral blood mononuclear cell proliferation compared from the ones

derived from bone marrow, *in vitro* [139]. In addition, they reported that after four infusions of umbilical cord derived MSCs into two patients suffering severe steroid-resistant aGVHD, GVHD associated symptomatology dramatically improved, with no adverse effect observed [139].

In a xenogeneic model of GVHD under a major histocompatibility mismatch setting, Guo e*t al.* show that human WJCs given on day 0 and day 3 post-transplant alleviated clinical symptomatology of GVHD in mice and improved survival time [149]. Guo and colleagues showed that WJC are transplantable across xenogeneic barriers and infusion of them at day zero is effective to delay GVHD occurrence. Xeno transfer of human WJCs in mice alleviated GVHD-symptoms and increased survival. However, questions about WJC's xenoreactivity and persistence after engraftment are not answered by Guo's study.

In the present study, I addressed the hypothesis that allogeneic WJCs would prevent the pathology syndrome associated with GVHD after allogeneic bone marrow transplantation. To accomplish this, I created a clinically relevant model of rat GVHD by transplanting allogeneic bone marrow across minor histocompatibility antigen (HA) barriers. To enhance alloreactive T-cell stimulation, bone marrow (BM) was co-infused with a fraction of $CD8^+$ cells magnetically selected from spleen. Bone marrow tissue was isolated from donor rats Fischer 344 (F344, RT1lv) and transplanted into lethally irradiated (10 Gray) Lewis (LEW, RT1l) rats. MSCs derived from umbilical cord Wharton's jelly (WJCs) were either co-transplanted at day 0 with bone marrow, or administered on day 2 post-BMT.WJCs and bone marrow were collected from haploidentical donors. The prophylactic potential of WJCs in an *in vivo* GVHD model was assessed as survival time, clinical symptomatology occurrence, and histopathological damages in target tissue.

References

[1]. Gratwohl, A., Baldomero, H., Aljurf, M., *et al*. (2010). Hematopoietic stem cell transplantation: a global perspective. *JAMA*, 303: 1617–1624.

[2]. Yu., *et al*. (2001). Allogeneic hematopoietic stem cell transplantation for acute leukemia with Gilbert's syndrome. *Journal of Hematology & Oncology*. 4:9.

[3] .Ribera, J.M. (2011). Allogeneic stem cell transplantation for adult acute lymphoblastic leukemia: when and how. *Haematologica,* 96(8):1083-1086.

[4]. Witherspoon, R.P., Deeg, H.J., Storer, B., *et al*. (2001). Hematopoietic stem-cell transplantation for treatment related leukemia or myelodysplasia. *J Clin. Oncol*, 19: 2134-2141.

[5]. Harousseau, J.L and Moreau, P. (2009). Autologous hematopoietic stem-cell transplantation for multiple myeloma. *N. Engl. J. Med*., 360(25): 2645–2654.

[6]. Gahrton, G., Iacobelli, S., Apperley, J., Bandini, G., Björkstrand, B., Bladé, J., *et al*. (2005).The impact of donor gender on outcome of allogeneic hematopoietic stem cell transplantation for multiple myeloma: reduced relapse risk in female to male transplants. *Bone Marrow Transplant*, 35:609–617.

[7]. Handgretinger, R. (2012). Alternative donor HSCT in refractory acquired aplastic anemia: The time has come. *Pediatr Transplant,* 16: 513-514.

[8].Urban, C., Benesch, M., Sovinz P., *et al.* (2012). Alternative donor HSCT in refractory acquired aplastic anemia - Prevention of graft rejection and graft versus host disease by immunoablative conditioning and graft manipulation. *Pediatr Transplant,* 16: 577-581.

[9]. Maury, S., Balere-Appert, M.L., Chir, Z., *et al*. (2007). French Society of Bone Marrow Transplantation and Cellular Therapy (SFGM-TC). Unrelated stem cell transplantation for severe acquired aplastic anemia: improved outcome in the era of high-resolution HLA matching between donor and recipient. *Haematologica*, 92: 589–596.

[10]. Angelucci, E. (2010).Hematopoietic stem cell transplantation in thalassemia. *Hematology*, 2010, (1): 456–462.

[11]. Fang, J.P and Xu L.H. (2010). Hematopoietic stem cell transplantation for children with thalassemia major in China. *Pediatr. Blood Cancer*, 55:1062–1065.

[12]. Cowan, M.J., Neven, B., Cavazanna-Calvo M., Fischer A., Puck J. (2008). Hematopoietic stem cell transplantation for severe combined immunodeficiency diseases. *Biology of Blood and Marrow Transplantation*, 14(1 Suppl 1):73-75.

[13]. Patel, N.C, Chinen, J., Rosenblatt, H.M., Hanson, I.C., Brown, B.S., Paul, M.E., *et al*. (2008). Long-term outcomes of nonconditioned patients with severe combined immunodeficiency transplanted with HLA-identical or haploidentical bone marrow depleted of T cells with anti-CD6 mAb. *J Allergy Clin Immunol*, 122, 1185–1193.

[14]. Durand, C., Ambinder, R., Blankson, J and Forman, S. (2012). HIV-1 and Hematopoietic Stem Cell Transplantation. *Biology of Blood and Marrow Transplantation*, 18(1):S172-S176.

[15]. Serrano, D., Miralles, P., Balsalobre, P., *et al*. (2010). Hematopoietic stem cell transplantation in patients infected with HIV. *Curr HIV/AIDS Rep*., 175–184. *Curr HIV/AIDS Rep* 2010; 7: 175–184.

[16]. Hausermann, P., Walter, R.B., Halter, J., Biedermann, B.C., Tichelli, A., Itin, P., *et al*. (2008). Cutaneous graft-versus-host disease: a guide for the dermatologist. *Dermatology*, 216*:* 287–304.

[17]. Tyndall, A and Gratwohl, A. (2000). Immune ablation and stem-cell therapy in autoimmune disease. Clinical experience. *Arthritis Res.,* 2(4):276–280.

[18]. Troeger, A., Meisel, R., Moritz, T., Dilloo, D. (2005). Immunotherapy in allogeneic hematopoietic stem cell transplantation-mot just a case for effector cells. *Bone Marrow Transplant.,* 35:S59-S64.

[19]. Mahgerefteh, S.Y, Sosna J., Bogot N., *et al*. (2011). Radiologic imaging and intervention for gastrointestinal and hepatic complications of hematopoietic stem cell transplantation. *Radiology*, 258:660–671.

[20]. Latif, T., Pohlman, B., Kalaycio, M., *et al*. (2003). Syngeneic graft-versus-host disease: a report of two cases and literature review. *Bone Marrow Transplant*., 32:535–539.

[21]. Krishna, S.G., Barlogie, B., Lamps, L.W., Krishna, K., Aduli, F., Anaissie, E. (2010). Recurrent spontaneous gastrointestinal graft-versus-host disease in autologous hematopoietic stem cell transplantation. *Clin Lymphoma Myeloma Leuk.,* 10:E17-21.

[22]. McGuirk, J.P & Weiss, M.L (2011). Promising cellular therapeutics for prevention or management of graft-versus-host disease (a review). *Placenta*, 32(Suppl 4):5304-5310.

[23].Warren, E.H., Zhang, X.C., Li, S., Fan, W., Storer, B.E., *et al*. (2012). Effect of MHC and non-MHC donor/recipient genetic disparity on the outcome of allogeneic HCT. *Blood.,* 120(14):2796-2806.

[24]. Messina, C., Faraci, M., de Fazio, V., Dini, G., Calo, M.P., Calore, E. (2008). Prevention and treatment of acute GVHD. *Bone Marrow Transplant*, 41(Suppl. 2): S65-S70.

[25]. Deeg, H.J., Spitzer, T.R., Cottler-Fox, M., Cahill, R., Pickle, L.W. (1991). Conditioning-related toxicity and acute graft-versus-host disease in patients given methotrexate/cyclosporine prophylaxis. *Bone Marrow Transplant,* 7(3):193-198.

[26]. Ogawa, H., Ikegame, K., Kaida, K., Yoshihara, S., Fujioka, T, Taniguchi, Y., *et al*.(2008.) Unmanipulated HLA 2–3 antigen-haploidentical (haploidentical) bone marrow transplantation using only pharmacological GVHD prophylaxis. *Exp. Hematol*, 36:1–8.

[27]. van Bekkum, DW., Knaan, S., Zurcher, C. (1980). Effects of cyclosporin A on experimental graft-versus-host disease in rodents. *Transplant Proc,* 12(2):278-282.

[28]. Reddy, P and Ferrara, J.L.M. (2008). Mouse models of graft-versus-host disease. In *StemBook*. Lisa Gerard, editor. StemBook, Cambridge, MA. http://www.stembook.org/node/548

[29]. Holler, E., Landfried, K., Meier, J., Hausmann, M., Rogler, G. (2010).The role of bacteria and pattern recognition receptors in GVHD. *Int J Inflam*, 2010; 2010:814326.

[30]. Coghill, J.M., Sarantopoulos, S., Moran, T.P., Murphy, W.J., Blazar, B.R., Serody, J.S. (2011). Effector CD4+ T cells, the cytokines they generate, and GVHD: something old and something new. *Blood*, 117:3268–3276.

[31]. Shlomchik, W.D. (2007). Graft-versus-host disease. Nat. Rev. Immunol, 7:340–352.

[32]. Vigorito, A.C., Campregher, P,V., Storer, B.E., *et al*. (2009). Evaluation of NIH consensus criteria for classification of late acute and chronic GVHD. *Blood*, 114:702–708.

[33]. Filipovich, A.H., Weisdorf, D., Pavletic, S., *et al*. (2005). National Institutes of Health consensus development project on criteria for clinical trials in chronic graft-versus-host disease: I—diagnosis and staging working group report. *Biol Blood Marrow Transpl*, 11: 945–956.

[34]. Toubai, T., Sun, Y., Reddy, P. (2008). GVHD pathophysiology: is acute different from chronic? *Best Pract Res Clin Haematol*., 21:101–117.

[35]. Gilliam, A.C., Whitaker-Menezes ,D., Korngold, R., Murphy, G.F. (1996). Apoptosis is the predominant form of epithelial target cell injury in acute experimental graft-versus-host disease. *J Invest Dermatol*, 107:377-383.

[36]. Washington, K., Gossage, D.L., Gottfried, M.R. (1994). Pathology of the pancreas in severe combined immunodeficiency and DiGeorge syndrome: acute graft-versus-host disease and unusual viral infections. *Hum Pathol*, 25:908–914.

[37]. Khurshid, I and Anderson, LC. (2002). Non-infectious pulmonary complications after bone marrow transplantation. *Postgrad Med J*, 78:257−262.

[38]. Knox, K.S., Behnia, M., Smith, L.R., Vance, G.H., Busk, M., Cummings, O.W., *et al*. (2002). Acute graft-versus-host disease of the lung after liver transplantation. *Liver Transpl,* 8:968–971.

[39]. Niculescu, F., Niculescu, T., Nguyen, P., Puliaev, R., Papadimitriou, J.C., *et al*. (2005). Both apoptosis and complement membrane attack complex deposition are major features of murine acute graft-vs.-host disease. *Exp Mol Pathol,* 79:136–145.

[40]. Tichelli, A., Rovo, A., Gratwohl, A. (2008) Late pulmonary, cardiovascular, and renal complications after hematopoietic stem cell transplantation and recommended screening practices. *Hematology Am Soc Hematol Educ Program,* 2008:125–133.

[41]. Kuzmina, L.A., Petinati, N.A.,Parovichnikova, E.N., *et al*. (2012). Clinical Study Multipotent Mesenchymal Stromal Cells for the Prophylaxis of Acute Graft-versus-Host Disease—A Phase II Study. *Stem Cells International.,*2012, Article ID 968213.

[42]. Billingham, R.E. (1966). The biology of graft-versus-host reactions. *Harvey Lect*., 62: 21-78.

[43]. Shlomchik, W.D., Couzens, M.S., Tang, C.B., *et al*. (1999). Prevention of graft versus host disease by inactivation of host antigen-presenting cells. *Science,* 285 (5426):412-415.

[44]. Hanash, A,M.(2012). Mata Hari reveals secrets of GVHD. *Blood,* 119:3656-3657.

[45]. Chakraverty, R and Sykes M. (2007). The role of antigen-presenting cells in triggering graft-versus-host disease and graft-versus-leukemia. *Blood,* 110: 9-17.

[46]. Kosco-Vilbois, M.H., Gray, D., Scheidegger, D., Julius M. (1993). Follicular dendritic cells help resting B cells to become effective antigen-presenting cells induction of B7/BB1 and upregulation of major histocompatibility complex class II molecule. *J. Exp. Med.*, 178: 2055–2066.

[47]. Koyama, M., Kuns, R. D., Olver, S. D., Raffelt, N. C., Wilson, Y. A., Don, A. L. J., Lineburg, K. E., *et al.* (2012). Recipient nonhematopoietic antigen-presenting cells are sufficient to induce lethal acute graft-versus-host disease. *Nature Medicine,* 18(1):135–142.

[48]. Toubai, T., Tawara, I., Sun, Y., *et al.* (2012). Induction of acute GVHD by sex-mismatched H-Y antigens in the absence of functional radiosensitive host hematopoietic–derived antigen-presenting cells. *Blood,* 119(16):3844-3853.

[49]. Inoue, M., Okamura, T., Yasui, M., Sawada, A., Sakata, N., Koyama, M., *et al.* (2006). Increased intensity of acute graft-versus-host disease after reduced-intensity bone marrow transplantation compared to conventional transplantation from an HLA-matched sibling in children. *Bone Marrow Transplant*, 37: 601–605.

[50]. Jacobsohn, D.A. (2008). Acute graft-versus-host disease in children. *Bone Marrow Transplan.*, 41: 215–221.

[51]. Matsuda, Y., Hara, J., Osugi, Y., *et al*. (2001).Serum levels of soluble adhesion molecules in stem cell transplantation-related complications. *Bone Marrow Transplant*, 27: 977–982.

[52]. Zeiser, R., Penack, O., Holler, E., Idzko, M. (2011). Danger signals activating innate immunity in graft-versus-host disease. *J. Mol. Med*. (Berl.), 89:833–845.

[53]. Cooke, K.R., Olkiewicz, K., Erickson, N., Ferrara, J.L. (2002).The role of endotoxin and the innate immune response in the pathophysiology of acute graft versus host disease. *J. Endotoxin Res*, 8: 441–448.

[54]. Koltun, W.A., Bloomer, M.M., Colony, P., Kauffman, G.L. (1996). Increased intestinal permeability in rats with graft versus host disease. *Gut*, 39:291–298.

[55]. Abreu, M.T. (2010).Toll-like receptor signalling in the intestinal epithelium: how bacterial recognition shapes intestinal function. *Nature Rev. Immunol*, 10:131–144.

[56]. Zhang, J.L., Hou. C.M., Wei, Y.L., Li, X.Y., Sun, D.J., *et al*. (2010). Influence of excessive complement activation on pathological process of acute graft versus host disease in mice. *Zhongguo Shi Yan Xue Ye Xue Za Zhi*, 18(6):1585-1589.

[57]. Daneshpouy, M., Socié, G., Lemann, M., Rivet, J., Gluckman, E., Janin, A. (2002). Activated eosinophils in upper gastrointestinal tract of patients with graft-versus-host disease. *Blood*, 99(8):3033-3040.

[58]. Murphy, G.F., Sueki, H., Teuscher, C., Whitaker, D., Korngold, R. (1994). Role of mast cells in early epithelial target cell injury in experimental acute graft-versus-host disease. *J Invest Dermatol*, 102(4):451-461.

[59]. Claman, H.N. (1985). Mast cell depletion in murine chronic graft-versus-host disease. *J Invest Dermatol*, 84: 246-248.

[60]. Claman H.N., *et al*. (1986). Mast cell 'disappearance' in chronic murine graft-vs-host disease (GVHD)-ultrastructural demonstration of 'phantom mast cells'. *J. Immunol*, 137:2009–2013.

[61]. Socié, G., Mary, J.Y., Lemann, M., *et al*. (2004). Prognostic value of apoptotic cells and infiltrating neutrophils in graft-versus-host disease of the gastrointestinal tract in humans: TNF and Fas expression. *Blood,* 103: 50–57.

[62]. Nishiwaki S, Terakura S, Ito M., *et al*. (2009). Impact of macrophage infiltration of skin lesions on survival after allogeneic stem cell transplantation: a clue to refractory graft-versus-host disease. *Blood*, 114: 3113–3316.

[63]. Fukushi N, Arase H, Wang B., *et al*. (1990). Thymus: a direct target tissue in graft-versus-host reaction after allogeneic bone marrow transplantation that results in abrogation of induction of self-tolerance. *Proc Natl Acad Sci USA*, 87, 6301-6305.

[64]. Lee, Y.J., Min, H.S., Kang, E.H., Park, H.J., Jeon, Y.K., Kim, J.H., *et al*. (2012). Sclerodermatous chronic graft-versus-host disease induced by host T-cell-mediated autoimmunity. *Immunol Cell Biol,* 90:358–367.

[65]. Ceredig, R. (2012). Graft-versus-host disease: who's responsible? *Immunol Cell Biol,* 2011:1–2

[66]. Zhao, D., Young, J.S., Chen, Y.H., Shen, E., *et al*. (2011). Alloimmune response results in expansion of autoreactive donor $CD4^+$ T cells in transplants that can mediate chronic graft-versus-host disease. *J. Immunol,* 186:856–868.

[67]. Levine, J.E; Logan, B.R; Wu, J; Alousi, A.M; Bolaños-Meade, J., *et al*. (2012).Acute graft-versus-host disease biomarkers measured during therapy can predict treatment outcomes: A blood and marrow transplant clinical trials network study. *Blood*, 119 (16): 3854-3860.

[68]. Paczesny, S., Krijanovski, O.I., Braun, T.M., *et al*. (2009). A biomarker panel for acute graft-versus-host disease. *Blood,* 113: 273–278.

[69]. Paczesny, S., *et al*. (2010). Elafin is a biomarker of graft-versus-host disease of the skin. *Sci Transl Med, 2, 13ra2*.

[70]. Ram, R., *et al*. (2009). Prophylaxis regimens for GVHD: systematic review and meta-analysis. *Bone Marrow Transplant*, 43: 643–653

[71]. Bozulic, L.D., Breidenbach, W.C., Ildstad, S.T. (2007). Past, present, and future prospects for inducing donor-specific transplantation tolerance for composite tissue allotransplantation. *Semin Plast Surg*, 4: 213-225.

[72]. Wysocki, C.A., Panoskaltsis-Mortar,i A., Blazar, B.R., Serody, J.S. (2005). Leukocyte migration and graft-versus-host disease. *Blood*, 105: 4191–4199.

[73]. Deeg, H.J. (2007). How I treat refractory acute GVHD. *Blood*, 109: 4119–4126.

[74]. Weisdorf, D. (2007). GVHD—the nuts and bolts. *Hematology Am Soc Hematol Educ Program 2007*: 62–67.

[75]. Lee, S.J., Zahrieh, D., Agura, E., MacMillan, M.L., Maziarz, R.T., *et al*. (2004). Effect of up-front daclizumab when combined with steroids for the treatment of acute graft-versus-host disease: results of a randomized trial. *Blood*, 104: 1559–1564.

[76]. Basić-Jukić, N., Labar, B. (2003). Immunosuppressive drugs in the prevention and treatment of GVHD after allogenic bone marrow transplantation (Review). *Acta Med Croatica*, 57(2): 131-139.

[77]. Fung, J.J., Todo, S., Jain, A., *et al*. (1990). Conversion from cyclosporine to FK 506 in liver allograft recipients with cyclosporine-related complications. *Transplant Proc*, 22(1): 6–12

[78]. Mir, M.A., & Battiwalla, M. (2009). Immune deficits in allogeneic hematopoietic stem cell transplant (HSCT) recipients. *Mycopathologia*, 168:271–282.

[79]. Van Der Straaten, H.M., Fijnheer, R., Dekker, A.W., Nieuwenhuis, H.K., Verdonck, L.F. (2001). Relationship between graft-versus-host disease and graft-versus-leukaemia in partial T cell-depleted bone marrow transplantation. *Br. J. Haematol*, 114: 31–35.

[80]. Brunstein, C. G., Miller, J. S., Cao, Q., McKenna, D. H., Hippen, K. L., Curtsinger, J., Defor, T., *et al*. (2011). Infusion of ex vivo expanded T regulatory cells in adults transplanted with umbilical cord blood: safety profile and detection kinetics. *Blood*, 117:1061–70.

[81]. Komanduri, K.V., & Champlin, R.E. (2011). Can Treg therapy prevent GVHD? *Blood*, 117: 751–752.

[82]. Troyer, D.L & Weiss, M.L. (2008). Concise review: Wharton's jelly-derived cells are a primitive stromal cell population. *Stem Cells*, 26(3):591–599.

[83]. Dominici, M., Le Blanc, K., Mueller, I., Slaper-Cortenbach, I., Marini, F., Krause, D., Deans, R., *et al*. (2006). Minimal criteria for defining multipotent mesenchymal stromal cells. The International Society for Cellular Therapy position statement. *Cytotherapy*, 8(4): 315–317.

[84]. Chao, K.C., Chao. K.F., Fu, Y.S., Liu, S.H. (2008). Islet-Like Clusters Derived from Mesenchymal Stem Cells in Wharton's Jelly of the Human Umbilical Cord for Transplantation to Control Type 1 Diabetes. *PloS One*, 1, e1451.

[85]. Mitchell, K. E., Weiss, M. L., Mitchell, B. M., Martin, P., Davis, D., Morales, L., Helwig, B., *et al*. (2003). Matrix cells from Wharton's jelly form neurons and glia. *Stem Cells*, 21(1):50–60.

[86]. Nayan, M., Paul, A., Chen, G., *et al*. (2011) Superior therapeutic potential of young bone marrow mesenchymal stem cells by direct intramyocardia l delivery in aged recipients with acute myocardial infarction: in vitro and in vivo investigation. *Journal of Tissue Engineering*, 2011;2011:741213

[87]. López, Y., Lutjemeier, B., Seshareddy, K., Trevino, E. M., Sue, K., Musch, T. I., Borgarelli, M., *et al*. (2013). Wharton's Jelly or Bone Marrow Mesenchymal Stromal Cells Improve Cardiac Function Following Myocardial Infarction for More Than 32 Weeks in a Rat Model : A Preliminary Report. *Current Stem Cell Research & Therapy*, (8), 1:46-59.

[88]. Valtieri, M., & Sorrentino, A. (2008). The mesenchymal stromal cell contribution to homeostasis. *J. Cell. Physiol*, 217:296–300.

[89]. Zinöcker, S., Wang, M.Y., Rolstad, B., Vaage, J.T. (2012). Mesenchymal Stromal Cells Fail to Alleviate Experimental Graft-Versus-Host Disease in Rats Transplanted with Major Histocompatibility Complex-Mismatched Bone Marrow. *Scand. J. Immunol*, 76(5): 464-470.

[90]. Rasmusson, I. (2006). Immune modulation by mesenchymal stem cells. *Exp Cell Res*, 312: 2169-2179.

[91]. Bassi, E.J., *et al*. (2011). Immune regulatory properties of multipotent mesenchymal stromal cells: Where do we stand? *World J Stem Cells*, 3: 1–8.

[92]. Sato, K., Ozaki, K., Mori, M., Muroi, K., Ozawa, K. (2010). Mesenchymal stromal cells for graft-versus-host disease: basic aspects and clinical outcomes. *J Clin Exp Hematol*, 50(2):79-89.

[93]. Meirelles, L.S., Chagastelles, P.C., Nardi N.B. (2006). Mesenchymal stem cells reside in virtually all post-natal organs and tissues. *J Cell Sci*, 119:2204–2213.

[94]. Baksh, D., Yao, R., Tuan, R.S. (2007). Comparison of proliferative and multilineage differentiation potential of human mesenchymal stem cells derived from umbilical cord and bone marrow. *Stem Cells*, 25:1384-1392.

[95]. Panepucci, R.A., Siufi, J,L., Silva, W,A, Jr., *et al*. (2004). Comparison of gene expression of umbilical cord vein and bone marrow-derived mesenchymal stem cells. *Stem Cells*, 22: 1263–1278.

[96]. Gotherstrom, C., West, A., Liden, J., *et al*. (2005). Difference in gene expression between human fetal liver and adult bone marrow mesenchymal stem cells. *Haematologica*, 90(8): 1017–1026.

[97]. Lu, L.L., Liu, Y.J., Yang, S.G., *et al*. (2006). Isolation and characterization of human umbilical cord mesenchymal stem cells with hematopoiesis-supportive function and other potentials. *Haematologica*, 91(8):1017-1026.

[98]. Prasanna, Y.S., & Jahnavi, V.S. (2011). Wharton's Jelly mesenchymal stem cells as off-the -shelf cellular therapeutics: A closer look into their regenerative and immunomodulatory properties. *Open Tissue Eng Regen Med J*., 4:28-38.

[99]. Ryan, J.M., Barry, F.P., Murphy, J.M., Mahon, B.P. (2005). Mesenchymal stem cells avoid allogeneic rejection. *J Inflamm*. (Lond),:2, 8.

[100]. Jones, B.J., & McTaggart, S.J. (2008).Immunosuppression by mesenchymal stromal cells: from culture to clinic. *Exp Hematol*, 36:733–741.

[101]. Ben-Ami, E., Berrih-Aknin, S., Miller, A. (2011). Mesenchymal stem cells as an immunomodulatory therapeutic strategy for autoimmune diseases. *Autoimmun Rev*, 10, 410–415.

[102]. Tyndall, A.,& Houssiau, F.A. (2010). Mesenchymal stem cells in the treatment of autoimmune diseases. *Ann Rheum Dis*, 69(8):1413-1414.

[103]. Polchert, D., Sobinsky, J., Douglas, G., Kidd, M., Moadsiri, A., *et al*., (2008). IFN-γ activation of mesenchymal stem cells for treatment and prevention of graft versus host disease. *Eur. J. Immunol*, 38: 1745–1755.

[104]. Wang, L., & Zhao, R. (2009). Mesenchymal stem cells targeting the GVHD. *Sci. China C. Life Sci*, 52(7):603–609.

[105]. Newman, R.E., Yoo, D., LeRoux, M.A., Danilkovitch-Miagkova, A. (2009).Treatment of inflammatory diseases with mesenchymal stem cells. *Inflamm. Allergy Drug Targets*, 8: 110–123.

[106]. Ge, W., Jiang, J., Baroja, M.L., *et al*. (2009). Infusion of mesenchymal stem cells and rapamycin synergize to attenuate alloimmune responses and promote cardiac allograft tolerance. *Am. J. Transplant*, 9:1760–1772.

[107]. Uccelli, A., Moretta, L., Pistoia, V. (2008). Mesenchymal stem cells in health and disease. *Nat Rev Immunol*., 8(9):726–736.

[108]. Weiss, M.L., Anderson, C., *et al.,* (2008). Immune properties of human umbilical cord Wharton's jelly-derived cells. *Stem Cells*, 26:2865–2874.

[109]. Lee, R.H., Pulin, A.A., Seo, M.J., Kota, DJ., Ylostalo, J., Larson, B.L. *et al.,* (2009). Intravenous hMSCs improve myocardial infarction in mice because cells embolized in lung are activated to secrete the anti-inflammatory protein TSG-6. *Cell Stem Cell*, 5:54–63.

[110]. Maina, V., Cotena, A., Doni, A., Nebuloni, M., Pasqualini, F., *et al*. (2009). Coregulation in human leukocytes of the long pentraxin PTX3 and TSG-6. *J. Leukoc. Biol*, 86:123–132.

[111]. Lai, R. C., Chen, T. S., & Lim, S. K. (2011). Mesenchymal stem cell exosome: a novel stem cell-based therapy for cardiovascular disease. *Regen. Med*, 6(4):481–492.

[112]. Sinha, M.L., Fry, T.J., Fowler, D.H., Miller, G., Mackall, C.L. (2002). Interleukin 7 worsens graft-versus-host disease. *Blood*, 100: 2642-2649.

[113]. Choi, H., Lee, R.H., Bazhanov, N., Oh, J., Prockop, D. (2011). Anti-inflammatory protein TSG-6 secreted by activated MSCs attenuates zymosan-induced mouse peritonitis by decreasing TLR2/NF-κB signaling in resident macrophages. *Blood*, 118:330–338.

[114]. Wang, S., Qu, X., and R. C. Zhao, R.C. (2012). Clinical applications of mesenchymal stem cells. *J. Hematol Oncol*, 5:19.

[115]. Le Blanc, K., Rasmusson, I., Sundberg, B., *et al*. (2004).Treatment of severe acute graft-versus-host disease with third party haploidentical mesenchymal stem cells. *Lancet*, 363:1439–1441.

[116]. Ringden, O., Uzune,l M., Rasmusson, L., *et al*. (2006). Mesenchymal stem cells for the treatment of therapy-resistant graft-versus-host disease. *Transplantation*, 81*:* 1390–1397.

[117]. Chavakis, E., Urbich, C., Dimmeler, S. (2008). Homing and engraftment of progenitor cells: A prerequisite for cell therapy. *J. Mol. Cell. Cardiol*, 45:514–522.

[118]. Fischer, U.M, Harting, M.T, Jimenez. F., *et al*. (2009). Pulmonary passage is a major obstacle for intravenous stem cell delivery: The pulmonary first-pass effect. *Stem Cells Dev*, 18,: 683–692.

[119]. Rochefort, G.Y., Vaudin. P., Bonnet, N., Pages, J.C., Domenech, J., Charbord, P., Eder, V. (2005). Influence of hypoxia on the domiciliation of mesenchymal stem cells after infusion into rats: possibilities of targeting pulmonary artery remodeling via cells therapies? *Respir Res*, 6, 125

[120]. Roddy, G. W., Oh, J. Y., Lee, R. H., Bartosh, T. J., Ylostalo, J., Coble, K., Rosa, R. H., *et al*. (2011). Action at a distance: systemically administered adult stem/progenitor cells (MSCs) reduce inflammatory damage to the cornea without engraftment and primarily by secretion of TNF-α stimulated gene/protein 6. *Stem Cells*, 29(10):1572–1579.

[121]. Shabbir, A., Zisa, D., Lin, H., Mastri, M., Roloff, G., Suzuki, G. *et al*., (2010). Activation of host tissue trophic factors through JAK-STAT3 signaling: a mechanism of mesenchymal stem cell-mediated cardiac repair. *Am J Physiol Heart Circ Physiol*, 299: H1428-H1438.

[122]. Caimi P.F., Reese J., Lee Z., Lazarus H.M. (2010). Emerging therapeutic approaches for multipotent mesenchymal stromal cells. *Current Op. Hematol*, 17(6):505–513.

[123]. Koc, O.N., Gerson, S.L., Cooper, B.W., Dyhouse, S.M., Haynesworth, S.E., Caplan, A.I. & Lazarus, H.M. (2000). Rapid hematopoietic recovery after co-infusion of autologous-blood stem cells and culture-expanded marrow mesenchymal stem cells in advanced breast cancer patients receiving high-dose chemotherapy. *J. Clin. Oncol*, 18:307–316.

[124]. Meuleman, N., Tondreau, T., Ahmad, I., Kwan, J., *et al*., (2009). Infusion of mesenchymal stromal cells can aid hematopoietic recovery following allogeneic hematopoietic stem cell myeloablative transplant: A pilot study. *Stem Cells and Development*, 18(9):1247-1252.

[125]. Ghannam, S., Bouffi, C., Djouad, F., Jorgensen, C., Noël, D. (2010). Immunosuppression by mesenchymal stem cells: mechanisms and clinical applications. *Stem Cell Res. Ther*, 1:2.

[126]. Christensen, M.E., Turner, B.E., Sinfield, L.J., *et al.* (2010). Mesenchymal stromal cells transiently alter the inflammatory milieu post-transplant to delay graft-versus-host disease. *Haematologica*, 95:2102–2110.

[127]. Kavanagh, H., Mahon, B.P. (2011). Allogeneic mesenchymal stem cells prevent allergic airway inflammation by inducing murine regulatory T cells. *Allergy,* 66: 523–531.

[128]. Ikezawa, Y., Nakazawa, M., Tamura, C., Takahashi, K., Minami, M., Ikezawa, Z. (2005). Cyclophosphamide decrease the number, percentage and the function of CD25+CD4+ regulatory T cells, which suppress the induction of contact hypersensivity. *J Dermatol Sci*, 39:105–112.

[129]. Prigozhina, T. B., Khitrin, S., Elkin, G., Eizik, O., Morecki, S., & Slavin, S. (2008). Mesenchymal stromal cells lose their immunosuppressive potential after allotransplantation. *Exp. Hematol*, 36:370–1376.

[130]. Auletta, J.J, Deans. R.J, Bartholomew, A.M. (2012). Emerging roles for multipotent, bone marrow-derived stromal cells in host defense. *Blood*, 119:1801-1809

[131]. Joo, S,Y., Cho, K.A., Jung, Y.J., Kim, H.S., Park, S.Y., *et al*. (2011). Bioimaging for the monitoring of the in vivo distribution of infused mesenchymal stem cells in a mouse model of the graft-versus-host reaction. *Cell Biol. Int*, 35: 417–421.

[132]. Naaldijk, Y., Staude, M., Fedorova, V., & Stolzing, A. (2012). Effect of different freezing rates during cryopreservation of rat mesenchymal stem cells using combinations of hydroxyethyl starch and dimethylsulfoxide. *BMC Biotechnology*, 12: 49

[133]. Stolzing, A., Jones E., McGonagle, D., Scutt, A. (2008). Age-related changes in human bone marrow-derived mesenchymal stem cells: consequences for cell therapies. *Mech. Ageing Dev*, 129:163–173.

[134]. Meyer, F,A., Laver-Rudich, Z., Tanenbaum, R. (1983). Evidence for a mechanical coupling of glycoprotein microfibrils with collagen fibrils in Wharton's jelly. *Biochim Biophys Acta*, 755:376–387.

[135]. Engberg Damsgaard ,T.M., Windelborg Nielsen, B., Sorensen, F.B., *et al*. (1992). Estimation of the total number of mast cells in the human umbilical cord. A methodological study. *APMIS*, 100:845–850.

[136]. Chan, C.K., Wu, K.H., Lee, Y.S., *et al*.(2012).The comparison of interleukin 6-associated immunosuppressive effects of human ESCs, fetal-type MSCs, and adult-type MSCs. *Transplantation*, 94(2):132-138.

[137]. Chen, M., Lie, P., Li, Z., Wei, X. (2009). Endothelial differentiation of Wharton's jelly-derived mesenchymal stem cells in comparison with bone marrow-derived mesenchymal stem cells. *Exp Hematol*, 37:629–640.

[138]. Wagner, W., Bork, S., Horn, P., *et al*. (2009). Aging and replicative senescence have related effects on human stem and progenitor cells. *PLoS One, 4, e5846.*

[139]. Dalous, J., Larghero, J., Baud, O. (2012). Transplantation of umbilical cord–derived mesenchymal stem cells as a novel strategy to protect the central nervous system: technical aspects, preclinical studies, and clinical perspectives. *Pediatr Res*, 71:482–490.

[140]. D'ippolito, G., Schiller, P.C., Ricordi, C., Roos, B.A., Howard, G.A. (1999). Age-related osteogenic potential of mesenchymal stromal stem cells from human vertebral bone marrow. *J Bone Miner Res*, 14:1115–1122.

[141]. Forraz, N., & Mcguckin, C. P. (2011). The umbilical cord : a rich and ethical stem cell source to advance regenerative medicine. *Cell Prolif*, 2011(44) Suppl 1:60-69.

[142]. Sarugaser, R., Lickorish, D., Baksh, D., *et al*.(2005). Human umbilical cord perivascular (HUCPV) cells: A source of mesenchymal progenitors. *Stem Cells,* 23:220–229.

[143]. Ennis, J., Gotherstrom, C., Le Blanc, K., Davies, J.E. (2008). In vitro immunologic properties of human umbilical cord perivascular cells. *Cytotherapy,* 10:174–181.

[144]. Wu, K.H., Chan, C.K., Tsai, C., Chang, Y.H., *et al.* (2011). Effective Treatment of Severe Steroid-Resistant Acute Graft-Versus-Host Disease with Umbilical Cord-Derived Mesenchymal Stem Cells. *Transplantation*, 91:1412-1416.

[145]. Guo, J., Yang, J., Cao, G., *et al*.(2011).Xenogeneic immunosuppression of human umbilical cord mesenchymal stem cells in a major histocompatibility complex-mismatched allogeneic acute graft-versus-host disease murine model. *Eur J Haematol*, 87(3):235-243.

Chapter 2

RAT UMBILICAL CORD WHARTON'S JELLY CELLS ISOLATION AND PRELIMINARY CHARACTERIZATION

Abstract

Mesenchymal stromal cells derived from umbilical cord, called Wharton's jelly cells (WJCs), are a promising source of undifferentiated cells with stem-like properties. WJCs are harvested painlessly after birth, can be expanded rapidly to clinically relevant numbers and banked for autologous or allogeneic transplantations. The most attractive characteristic of WJC for cellular therapy is their ability to modulate immune reactions and to be immunotolerated. In addition, these cells are suitable for tissue engineering, regenerative medicine and gene therapy. WJCs have been used as a cell therapy for immunological disorders including graft versus host disease (GVHD). Here, I isolated, expanded and characterized rat WJCs and used them for treatment of GVHD in a rat model after allogeneic bone marrow transplantation (BMT). An explant method to isolate rat WJCs is described here. Briefly, timed-pregnant female rats were humanely euthanized and the uterus was removed aseptically to a sterile 150 mm culture dish. Inside a biosafety cabinet (BSC), the uterus was opened and the umbilical cords from each pup collected. The cord was moved to a single well of a six well dish (8.7 cm2) and torn into many small pieces (1 mm or smaller) using Dumont #5 forceps. The pieces were allowed to dry in the well for about 10 minutes before DMEM with 20% fetal bovine serum (FBS) culture medium was added. Over the next week, cells were seen migrating out from the cord explants onto the culture dish. Cells were passed when they reached 85% confluence. WJCs were used at passage 4 for transplantation studies. Surface maker expression was used to characterize WJCs population and multipotency was confirmed via tri-lineage differentiation assays. In summary, rat WJCs express mesenchymal stem cell-like characteristics, they can be easily harvested and expanded and represent a novel allogeneic source of MSCs to be tested as a cell therapy in rat disease models.

Key words: Wharton's jelly cells, mesenchymal stromal cells, rat umbilical cord.

Chapter 2- RAT UMBILICAL CORD WHARTON'S JELLY CELLS ISOLATION AND PRELIMINARY CHARACTERIZATION

2.1. Isolation and Characterization of rat WJCs

2.1.1. Design and Methods Isolation and Cell Culture

All protocols were reviewed and approved by the Institutional Animal Care and Use Committee (IACUC). Rat WJCs were isolated from four pregnant rats Fischer 344 (F344) at between 19 to 21 days post coitus (DPC). Timed-pregnant female rats were humanely euthanized: anesthesia was induced by exposing the rat to a 5% isofluorane -oxygen mixture in a closed chamber until death. The uterus was removed aseptically to a sterile 150 mm culture dish. Inside a biosafety cabinet (BSC), the uterus was opened and the umbilical cord from each pup collected**.** The umbilical cord was rinsed with Dulbecco's Phosphate Buffered Saline (DPBS, Invitrogen, cat # 14190-250) to remove as much blood as possible, and blotted. Two umbilical cords were dissected into 2-3 mm pieces and were placed in a single well (9.6 cm^2/ well), and after attachment, 500 µl of growth medium was added. Isolation and expansion of rat Wharton's jelly-derived MSCs (WJCs) was achieved by using an explant method. The pieces were allowed to dry in the well for about 10 minutes before culture medium containing low glucose Dulbecco's Modified Eagle Medium (DMEM GIBCO cat# 11885-092), 20% fetal bovine serum (FBS, Hyclone Thermo Scientific cat# SH3008803), 1% glutamine (GlutaMAX™ Gibco cat# 35050-079**)** and 1% Penicillin Streptomycin (Pen Strep GIBCO cat# 15140-122) was added. Cell were incubated at 37 ˚C, saturating humidity in a 5% CO_2 atmosphere. Over the next 2 days, cells migrated out from the cord explants onto the culture dish. At passage 0, about 5-7 days after plating, the cells had grown to 85% confluence and then were passaged. To pass, the cells were rinsed twice with DPBS followed by 0.05% Trypsin/ Ethylene diamine tetraacetic acid (EDTA) (Gibco ca# 15050-065) for 5 minutes at 37°C. The trypsin was inactivated by adding 3 times volumes of growth medium then the cells were pelleted by 200x*g* centrifugation for 5 min at room temperature. Cells were plated at 10000 cells/cm^2 after passage 0. WJCs were used at

passage 3 for immunophenotyping, and passage 4 for differentiation potential and transplantation studies.

2.1.2. Cell yield

The cell yield from 2 cords was calculated at passage 1. After trypsinization, cells were suspended in 1000 µl of DPBS and cell counts were performed by using a hemocytometer and viability was assessed by trypan blue exclusion test. Data was analyzed by descriptive statistics using GraphPad Software. Data was expressed as mean± SD and 95 % confidence interval (CI) of the mean.2.1.3. Immunophenotype analysis using flow cytometry

To detect rat WJCs' surface marker expression, cells were characterized by flow cytometry after passage 3. A total of $6x10^6$ cells were used for flow cytometry analysis; aliquots of $1x10^6$ cells were suspended in 12 x75 mm Falcon polystyrene tubes in 500 µl of DBPS and incubated with the specific antibody conjugated with fluorescein isothiocyanate (FITC). Expression of mesenchymal markers CD44 (Millipore cat# CBL1508F), CD73 (BD Pharmingen ™ cat# 551123), CD90 (BD Pharmingen ™ cat# 554897) and hematopoietic marker CD45 (BD Pharmingen ™ cat# 554877) and CD34 (Santa Cruz Biotechnology cat# sc-7324) were analyzed. FITC conjugated mouse IgG1 (BD Pharmingen ™ cat# 550616) was used as the isotype control. Antibodies were used at 1:100 dilution. Tubes were incubated at 4˚C in the dark for 20 min. After the incubation, the cells were washed with DPBS and the results were obtained by reading the output of a FACS Calibur flow cytometer (Becton Dickinson). For each tube, 10000 events were collected and the data was analyzed using Cell Quest software and the forward and side scatter profile gated out debris and dead cells. Data are expressed as percent of positive cells based on the mean fluorescence intensity of antibody compared with control.

2.1.4. Differentiation potential of rat WJCs

Rat WJCs derived from rat F344 and expanded till passage 4 were differentiated into adipogenic, osteogenic, and chondrogenic lineages following a described protocol [1]. A non-quantitative differentiation assay was performed. Briefly, for differentiation 10×10^3 cells/cm^2

was cultured in 6 well Falcon plates. Cells were incubated at 37 ˚C, saturating humidity in a 5% CO_2 atmosphere. WJCs obtained from the same litter were pooled together and induced into the tri-lineage differentiation separately. Once they reached 85% confluence, growth medium was replaced by adipogenic induction medium containing DMEM high glucose (Gibco cat# 11965-092) supplemented with 10% FBS (Hyclone Thermo Scientific cat# SH3008803), 0.5 mM isobutyl-methylxantine (Sigma I5879-100MG), 200 µM indomethacin (Sigma cat#17378), 1 µM dexamethasone (Sigma cat# D4902) and 10 µg/ml insulin (Sigma cat#12643). The growth medium was replaced every 3 days. At 21 days of culture, cells were fixed in 4% paraformaldehyde and stained with oil red-O solution (Sigma cat# O06525). For osteogenic differentiation, once cells reached 85% confluence, growth medium was replaced by osteogenic induction medium containing low glucose DMEM (Gibco cat#11885-092) supplemented with 10% FBS (Hyclone Thermo Scientific cat# SH3008803), 10 mM β-glycerophosphate (Sigma cat# G9422-10G), 0.2 mM ascorbic acid (Sigma cat# A5960-25G), and 10 nM dexamethasone (Sigma Cat#D4902), and cultured for 21 days, replacing the medium every 3 days. Cells were fixed in 4% paraformaldehyde for 10 minutes and osteogenic differentiation was detected by Von Kossa staining. For chondrogenic differentiation, medium was replaced by chondrogenic induction medium containing DMEM high glucose (Gibco cat# 11965-092), 6.25 µg/ml insulin (Sigma cat#12643), 6.25 µg/ml insulin transferrin selenium (GIBCO cat# 41400), 6.25 µg/ml selenous acid (Sigma cat# 211176-10G), 5.33 µg/ml linolenic acid (Sigma cat# L2376), 1.25 mg/ml bovine serum albumin (BSA), 0.35 mM proline (Sigma cat#P5607), 1 mM sodium pyruvate (Sigma cat#P2256), 100 nM dexamethasone (Sigma cat# D4902), 0.1 mM L-ascorbic acid-2-phosphate (Sigma cat# A8960), supplemented with 10 ng/ml transforming growth factor-beta 3 (TGF-β3) (R&D Systems,cat#243-B3/CF). The cells in culture plates were fixed with 4% paraformaldehyde for 10 minutes and stained with Masson's trichrome stain. Cells cultured in regular growth medium were used as negative control.

2.3 Results

2.3.1 Primary explant culture of WJCs

In the present study, fragments of umbilical cord adhered onto the surface of the culture dish about 10 min after plating. After 24 hour, adherent cells with fibroblast –like morphology

started to migrate from explants reaching 90% confluence between 7 and 10 days. The average cell yield at passaged 1 obtained from 2 cords plated together (n=24 , 6 cords from each litter) was 237430± 36480 cells, the 95% confidence interval of the mean was (222020 to 2528300).

Migrating adherent cells from rat umbilical cord (UC) explants were identified 24 hours after culture. Primary cell cultures reached a confluence of 80%-90% at days 7-8. WJCs displayed a fibroblast-like or stellate morphology. In most cells a prominent nucleus with oval shape and disperse chromatin was observed (fig. 2.1).

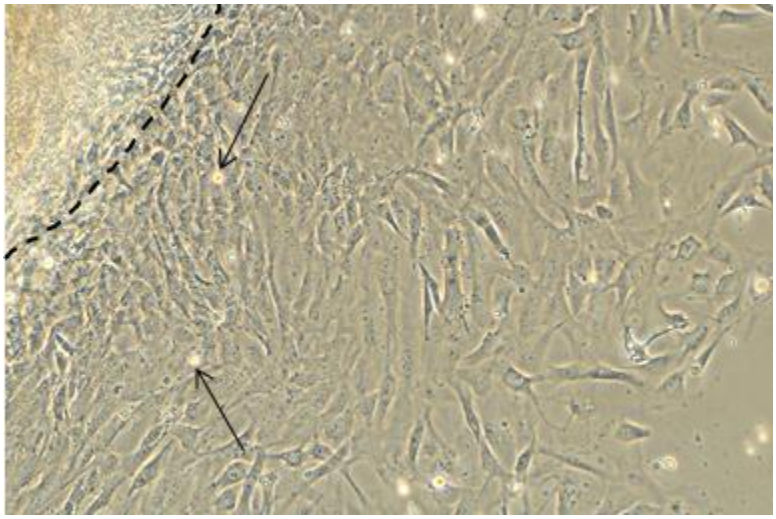

Figure 2.1. Morphological characterization of rat Wharton's jelly cells (WJCs) passage 0. Objective magnification 10X. After culture of rat umbilical cord (UC) explants, adherent cells with fibroblast-like and spindle-shaped morphology were observed migrating from rat UC explants 24 hours after plating. Spindle-shaped and fibroblast-like cells, as well as phase-bright cells (arrows) with rounded morphology, were seen growing out of the explants. Dashed line (---) indicates the UC explant's margin. WJCs were sub-cultured for more than 8 passages without showing morphologic changes associated with senescence.

2.3.2. Immunophenotyping

Surface marker expression of WJCs at passage 3 revealed expression of MSCs defined markers, such as CD44 (47.7%), CD73 (68.02%) and CD90 (90.33%) and negative expression of hematopoietic-specific markers CD34 (0.04%) and CD45 (0.05%) (fig.2.2).

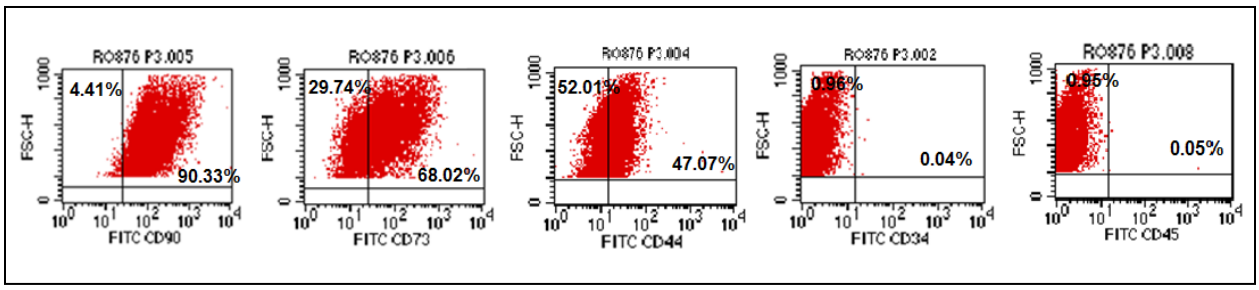

Figure 2.2. Flow cytometry was performed on rat Wharton's jelly cells (WJCs) at passage 3. Dot plot representation shows percentage of Wharton's jelly cells expressing specific marker in upper right quadrant, percentage of cells not expressing specific markers are represented in upper left quadrant. Wharton's jelly cells express CD44, CD73, CD90 and do not express CD34 or CD45. The FITC isotype control (negative staining) was set at 1% (data not shown).

2.3.3. Differentiation potential of rat WJCs

Another defining characteristic of MSCs is their ability to differentiate in cells of the adipocytic, osteocytic and chondrocytic lineages. Differentiation of WJCs at passage 4 into fat, bone and cartilage lineage is showed in figure 2.3 When WJCs were cultured in adipogenic medium, they accumulated intracytoplasmic lipid drops which is associated with differentiation into adipocyte lineage cells. When WJCs were cultured in osteogenic medium, extracellular mineralization related to osteocyte differentiation was detected. Finally, when WJCs were cultured in chondrogenic medium, I noticed interstitial accumulation of collagen fibers. Taken together, these results provide support the mesenchymal differentiation potential of rat WJCs.

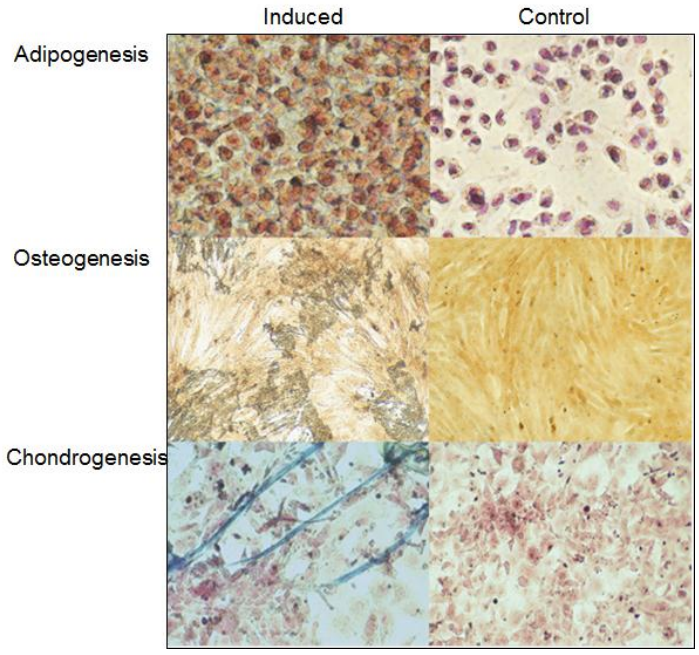

Figure 2.3. Multilineage differentiation potential of rat Wharton's jelly-derived mesenchymal stromal cells (WJCs) at passage 4. Differentiation induced by incubation in adipogenic differentiation medium (top panel), in osteogenic differentiation medium (middle panel), or in chondrogenic differentiation medium (bottom panel). Adipogenic differentiation conditions (induced) or standard culture conditions (control) for 21 days is shown in top panels. Oil Red-O was used to stain lipids and hematoxylin for staining nuclei. Differentiation to adipogenic lineage induced small lipid droplets which stained positive with oil red-O to accumulate in the cytoplasm. WJCs maintained in osteogenic differentiation medium (left) or control (undifferentiated) conditions (right) is shown in middle panels Cells were differentiated for 21 days prior to being fixed and stained using von Kossa's stain Note the dark crystalline staining in the differentiated cells indicating deposition of calcium. WJCs maintained in chondrogenic differentiation medium (left) or control (undifferentiated) conditions (right) is shown in the bottom panels. Cells were differentiated for 21 days prior to being fixed and stained using Mason's Trichromic staining for collagen detection. Note that WJCs maintained in chondrogenic medium (left) displayed fascicules of fibrillar material staining positive for collagen.

2. 4 Discussion

Mesenchymal stromal cells (MSCs) are classically defined by three properties: their adherence to plastic in regular conditions, their expression of select surface marker antigens and their ability to differentiate along mesenchymal lineage such as fat, bone and cartilage [2]. However, some investigators consider this definition as unspecific, since these proposed typical characteristics to define MSC are based exclusively on culture conditions [3]. The standard definition of MSCs proposed by Dominici *et al*. states that ≥95% of MSC population must

express CD73, CD90 and CD105 [2]. In the present study I found that 68 and 90 percent of rat WJCs expressed CD73 and CD90 respectively. The lower mesenchymal-associated marker expression of CD73 and CD44 may be correlated with species-specific differences, isolation procedure, culture conditions and passage. Mitchell *et al*. reported that human WJCs show heterogeneity in cell morphology after primary culture by explant method [4]. Most protocols to obtain WJCs from human UC include removing of blood vessels to potentially reduced heterogeneity of the cell population [5]. In the present study, removing blood vessels from rat UC was not feasible due to UC's size. This is a variable which may impact rat WJCs surface markers expression.

Due to their differentiation potential and immune properties, MSCs have been used as cell therapy for immunologic disorders including GVHD [6]. Results from transplantation studies showed that a subpopulation of WJCs can promote tissue repair by maintaining multilineage differentiation *in vivo* [7]. Although the mechanism underlying MSCs differentiation is not completely elucidated, it is thought that cell determination and differentiation into completely differentiated specific cell types might be connected with epigenetic changes [8], cell fusion [9], soluble factors [10] and cell-to cell contacts [11], extracellular matrix components and mechanical forces [12]. According to our literature review, we are describing for the first time a protocol to isolate and expand rat WJCs. The three minimum criteria defining MSCs, such as plastic-adherence, specific surface antigen expression, and MSCs *in vitro* differentiation potential into adipocytes, osteoblasts and chondroblasts [2], is reached for rat WJCs. Similar to bone marrow-derived MSCs, rat WJCs expressed fibroblastic morphology, immunophenotyping and *in vitro* differentiation capacity. The rat has been used as a clinical model for GVHD [13, 14, 15], however until now non-availability of rat WJCs was a limitation to use them in allogeneic and syngeneic settings to prevent or treat GVHD in rat models.

REFERENCES

[1]. Angelucci, S., Marchisio, M., Di Giuseppe, F., *et al*. (2010). Proteome analysis of human Wharton's jelly cells during in

[2]. Dominici, M., Le Blanc, K., Mueller, I., *et al*. (2006). Minimal criteria for defining multipotent mesenchymal stromal cells. The International Society for Cellular Therapy position statement. *Cytotherapy,* 8(4): 315–317.

[3]. Augello, A., Kurth, T. B., & De Bari, C. (2010). Mesenchymal stem cells: a perspective from in vitro cultures to in vivo migration and niches. *European Cells & Materials*, 20: 121–133.

[4]. Mitchell, K. E., Weiss, M. L., Mitchell, B. M., Martin, P., Davis, D., Morales, L., Helwig, B., *et al*. (2003). Matrix cells from Wharton's jelly form neurons and glia. *Stem Cells*, 21(1):50–60.

[5]. Jeschke, M. G., Gauglitz, G. G., Phan, T. T., Herndon, D. N., & Kita, K. (2011). Umbilical cord lining membrane and Wharton's mesenchymal stem cells : The similarities and differences. *Open Tissue Eng Reg Med J*, 2011;4 : 21–27.

[6]. Ra, J. C., Kang, S. K., Shin, I. S., Park, H. G., *et al*. (2011). Stem cell treatment for patients with autoimmune disease by systemic infusion of culture-expanded autologous adipose tissue derived mesenchymal stem cells. *Journal of Translational Medicine*, 2011, 9:181.

[7]. Sarugaser, R., Hanoun, L., Keating, A., Stanford, W. L., & Davies, J. E. (2009). Human mesenchymal stem cells self-renew and differentiate according to a deterministic hierarchy. *PloS One*, *4*(8), e6498.

[8]. Teven, C. M., Liu, X., Hu, N., Tang, N., *et al*. (2011). Epigenetic regulation of mesenchymal stem cells: a focus on osteogenic and adipogenic differentiation. *Stem Cells Int*. 2011;2011:201371

[9]. Kode, J. A, Mukherjee, S., Joglekar, M. V., & Hardikar, A. A. (2009). Mesenchymal stem cells: immunobiology and role in immunomodulation and tissue regeneration. *Cytotherapy*, 11(4): 377–391.

[10]. Schittini, A. V., Celedon, P. F., Stimamiglio, M. A., *et al*. (2010). Human cardiac explant-conditioned medium: soluble factors and cardiomyogenic effect on mesenchymal stem cells. *Experimental Biology and Medicine,* 235(8):1015–1024.

[11]. Vallabhaneni, K, C., Haller, H., Dumler, I. (2012). Vascular Smooth Muscle Cells Initiate Proliferation of Mesenchymal Stem Cells by Mitochondrial Transfer via Tunneling Nanotubes. *Stem Cells Dev,* 21(17):3104-3113.

[12]. Reilly, G. C., & Engler, A. J. (2009). Intrinsic extracellular matrix properties regulate stem cell differentiation. *Journal of Biomechanics*, 1: 1–8.

[13]. Beschorner, W.E., Tutschka, P.J., Santos, G.W. (1983). Chronic graft-versus-host disease in the rat radiation chimera. III. Immunology and immunopathology in rapidly induced models. *Transplantation*, 35(3): 224–230.

[14]. Glazier, A., Tutschka, P.J., Farmer, E.R., Santos, G. (1983). Graft-versus-host disease in cyclosporin A-treated rats after syngeneic and autologous bone marrow reconstitution. *J Exp Med*, 158: 1–8.

[15]. Zinöcker, S., Sviland, L., Dressel, R., & Rolstad, B. (2011). Kinetics of lymphocyte reconstitution after allogeneic bone marrow transplantation: markers of graft-versus-host disease. *J Leuk Biol*, 90(1): 177–187.

Chapter 3-EXPERIMENTAL MODEL OF GVHD TO MINOR HISTOCOMPATIBILITY ANTIGENS IN A RAT MODEL

Abstract

A clinically relevant model of GVHD across minor mismatch histocompatibility setting in rats was developed by allogeneic bone marrow (BM) cells and $CD8^+$ splenocytes transplantation 24 hours after lethal total body irradiation (TBI). Donor cells from 40 Fischer 344 rats (F344) (RT1lv) were transplanted through the dorsal vein of the penis into recipient Lewis rats (RT1l).

Recipient rats were divided in 4 groups categorized as1) positive control (receiving T cell-depleted BM only), 2) GVHD-induced (rats receiving BM plus $CD8^+$ splenocytes without Wharton's jelly cells (WJCs)), 3) GVHD-induced receiving WJCs on day 0, and 4) GVHD-induced receiving WJCs on day 2 post-transplantation. GVHD was assessed daily by clinical signs such as food intake, weight loss, posture, diarrhea, skin integrity, hair coat, body temperature and survival. GVHD was confirmed using histopathological study of damaged tissues and immunohistochemistry expression of the GVHD biomarker Elafin in tissue sections. Other biomarkers of GVHD, such as complement activation, and collagen deposition, were also evaluated in affected tissues. Clinical data was scored from 0 to 3 using a previously described GVHD grading scale. Co-administration of WJCs with hematopoietic cells on day 0 failed to alleviate GVHD-associated symptomatology and mortality. WJCs administered on day 2 post-induction ameliorated GVHD-associated symptomatology, hematopoietic niche reconstitution, survival time and enhanced hematopoietic recovery.
Keyword: graft versus host disease, Wharton's jelly, mesenchymal stromal cells, immunosuppression

Chapter 3- EXPERIMENTAL MODEL OF GVHD TO MINOR HISTOCOMPATIBILITY ANTIGENS IN A RAT MODEL

3.1 Background

Graft versus host disease (GVHD) is defined by the concurrence of clinical symptoms and pathological manifestations in an immunocompromised host receiving hematological stem cell transplantation (HSCT) [1]. Although the most important risk factor for the development of GVHD is genetic disparity at loci within the major histocompatibility complex (MHC), disparity at loci outside the MHC which encode minor histocompatibility antigens (MiHAs) can trigger donor T-cell activation and GVHD [2]. Therefore, in humans, even after transplantation of matched MHC tissues, incidence of acute GVHD can reach 30% [3, 4]. After autologous HSCT,

even though there is no genetic disparity, a GVHD-like syndrome has been reported to occur [5,6]. This auto-immune syndrome or autologous GVHD (auto-GVHD) has been described in patients receiving preparative conditioning regimen before HCT, immunosuppressive therapy, depletion of Tregs [5], suffering underlying malignant disease or receiving a second HCT [7]. After transplantation the initial donor T-cell recognition is amplified by proinflammatory cytokines released by the myeloablative conditioning regimen [8, 9]. Since in most clinical models of bone marrow transplantation (BMT) donor and recipient are MHC matched and disparate only for MiHAs, the experimental model of BMT needs to focus on clinically relevant MiHAs mismatch models [10]. GVHD pathophysiology has been largely dissected in mouse models [10,11]. However, rat models for GVHD are also suitable since they have been proved to mimic dermatologic manifestations of GVHD in human [12]. Studies of BMT in rats have revealed the role of autoreactive T cells in the development of GVHD after autologous [13] and syngeneic BMT [14].

3.1.2. The Histocompatibility Antigens of the Rat

The laboratory rat (*Rattus norvegicus*) is an important model for studying transplantation [15,16,17] and for studying experimentally induced auto-immune diseases [15, 19]. The rat is an outstanding experimental model which combines the advantages of being an intermediate-size rodent [16] and it is well-characterized immunologically and immunogenetically [19]. The major histocompatibility complex (MHC) in the rat, known as the RT1 complex, is located in chromosome 20 [15, 20]. RT1 plays a fundamental role controlling immune responses [15, 18] and graft rejection [17]. RT1 complex has been characterized based on serological [16, 21], molecular [16], and transplantation studies [21]. The RT1 complex displays a similar organization to the MHC in human and mice [16, 17, 21]. Thus, the rat RT1 complex gene family contains classical class Ia genes and non-classical class Ib genes, class II and class III regions [15]. However, a distinctive characteristic of rat MHC is the presence of supplementary class I genes (Class Ia) centromeric to the class II region [15, 17, 22]. Class Ia loci encode proteins expressed on all nucleated somatic cells [23], which achieve antigen-presenting function to $CD8^+$ T cells [18, 22, 24]. The function of the non-classical class Ib loci is mostly unidentified

[18, 22, 24]. The class II locus encodes molecules which present antigens to CD4+ T helper cells [18]. The class II antigens are expressed on a number of cells such as dendritic cells, macrophages and B cells [25]. Since these cells are specialized to initiate or stimulate T cell activation, they are known as professional antigen presenting cells (APCs) [26]. Due to their hematopoietic ontogeny, these cells are also known as hematopoietic APCs [27]. Nonetheless, a wider spectrum of cells derived from non-hematopoietic tissues, which do not constitutively express class II antigens necessary for recognition of naïve T cells [28], such as epithelial, stromal [29] and vascular endothelial cells [30], can acquire APC functions once they are stimulated by inflammatory conditions [31]. While class I and class II loci are responsible for adaptive immune responses [32], the class III loci expressed on a variety of cell types [33] encode secreted proteins, including some elements of the complement cascade and cytokines [18] such as tumor necrosis factor alpha and beta (TNF-α and -β) [34], and heat shock proteins [35],and are involved in innate immune responses [18].

3.2. Establishment of a GVHD model following bone marrow transplantation in a minor histocompatibility complex matching rats

The model of GVHD in rats was established using allogeneic BMT plus donor-derived $CD8^+$ from spleen with or without additional haploidentical MSC co-transplantation. I used male rat Lewis $RT1^l$ as recipients and female Fischer 344 (F-334) $RT1^{lv}$ as donor of hematopoietic cells from bone marrow and spleen, and WJCs from the umbilical cord of pups obtained from the female Fischer 344 rat. The establishment of this model was based upon studies of Schulak *et al*. and Nakao *et al*. who performed experiments of transplantation across minor histocompatibility in rats [36, 37]

MHC complex from rat Lewis and F344 express similar haplotypes which vary at a single RT1-linked locus [38]. This model mimics clinical allogeneic hematopoietic cell transplantation (HCT), where donor and recipient are MHC-matched [10]. These studies were carried out with permission of Institutional Animal Use and Care Committee (IACUC) of Kansas State University dated 21.17.11.

GVHD model was created by BMT across minor histocompatibility barriers after lethal 10 Gy total body irradiation (TBI). Male Lewis (RT1l) rat recipients (10-12 weeks old, 200-250g) were given 10 Gy TBI by using a linear accelerator (Varian Clinac 2100C/D) in Kansas State University, College of Veterinary Medicine, Clinical Sciences department. Radiation was given a dose of 600 cGy/min to un-anesthetized, restrained rats. Animals were injected 24 hours later with 30 x 10^6 unfractionated bone marrow cells and 2 x10^6 immuno-magnetically selected splenocytes ($CD8^+$) female from F344 ($Rt1^{lv}$) donor rats intravenously via the dorsal penis vein. Donor cells were suspended in 1000 µl of DPBS and infused using a scalp vein infusion set (27-gauge). Once the cells were injected, an additional 500 µl of DPBS was infused to flush the infusion line and assure each animal received the complete amount of cells.

3.2.1. Experimental design of the *in vivo* GVHD model

Fifty five Lewis (RT1l) rats were divided in 6 groups: 3 experimental and 3 control groups. The experimental groups were composed of recipients Lewis rats randomly assigned (see Table 3.1) and were induced to develop GVHD following TBI and allogeneic hematopoietic cell transplantation (allo-HCT) with cells derived from F344 ($Rt1^{lv}$) rat BM and spleen. Group 1 (n=10) was composed of $RT1^l$ rats Lewis that were induced to develop GVHD by co-transplantation of 30x10^6 bone marrow cells and 2 x10^6 immuno-magnetically selected splenocytes ($CD8^+$) from F344 ($Rt1^{lv1}$), this group was identified as GVHD-induced. Group 2 (n=10) was formed by recipient Lewis rats which were induced to develop GVHD as in group 1, and received 2 x 10^6 WJCs simultaneously with the allo-HCT (day 0) identified as WJCs day 0 (WJC0).Group 3 (n=10) was composed of recipient Lewis rats which were induced to develop GVHD as in group 1, and received 2 x 10^6 WJCs 2 days after allo-HCT (day 2), this group was identified as WJC day 2 (WJC2). Control groups were formed by recipient rat Lewis which were randomly assigned to the group but were induced to develop GVHD. Control group 4 (negative control) (n=10) was formed by rats which received TBI without allo-HCT or WJCs; control group 5 (positive control) (n=10) was made up of rats that received TBI followed by bone marrow cells immunomagnetically depleted of $CD4^+$ and $CD8^+$ cells (positive control), and group 6 (normal healthy control) (n=5) was comprised of untreated Lewis rats used to compile histopathological evaluation parameters. In a pilot study, by using the same combination of rat strains male Lewis (RT1l) as recipients and female F344 ($Rt1^{lv}$) as donors, I established that

using bone marrow cells at dose of 30 x 10^6 cells per rat together with 2 x 10^6 splenocytes was enough to induce GVHD. At the same time by using WJCs at dose of 2 x 10^6 cell/rats attenuation in GVHD-associated symptomatology was observed (data not shown).

Table 3.1
Experimental groups

Group	TBI 10 Gy	Transplantation	Bone marrow (BM) $30x10^6$ cells	$CD8^+$ Splenocytes $2x10^6$ cells	WJCs $2x10^6$ cells/rat	N
1 GVHD-induced (GVHD)	yes	yes	yes	yes	no	10
2 GVHD-induced Plus WJCs day 0 (WJC0)	yes	yes	yes	yes	no	10
3 GVHD-induced Plus WJCs day 2 (WJC2)	yes	yes	yes	yes	no	10
4 Negative control	yes	no	no	no	no	10
5 Positive control	yes	yes	yes BM $CD8^+$ and $CD4^+$ depleted	no	no	10
6 Untreated (normal control)	no	no	no	no	no	5

Abbreviations: TBI: total body irradiation; WJCs: Wharton's jelly cells; BM: bone marrow; GVHD: graft versus host disease

3.2.2. Total Body Irradiation

Allogeneic hematopoietic cell transplantation (HCT) is the standard treatment for patients suffering hematological disorders of malignant or non-malignant cause [39]. The efficacy of HCT in cancer treatment depends on myeloablative conditioning regimens, such as radiation, which eradicates circulating and bone marrow resident neoplastic cells, thus allowing the engraftment and repopulation of bone marrow with healthy donor hematopoietic cells. Ionizing radiation causes rupture of DNA by overproduction of activated radicals such as hydrogen peroxide, hydrogen radicals, OH radicals, and superoxide anions [40]. Since ionizing radiation causes rupture in the DNA double-strand, mitotically active cells including hematopoietic and gastrointestinal lining cells are mostly affected. DNA damage occurs in multiple sites and the cellular repair system is unable to fix them and resulting in cell death in target tissues which progress to either necrosis or apoptosis [41]. TBI induces systemic inflammatory responses, activation of innate immune responses and triggers release of inflammatory cytokines in different organs [42]. While DNA damage caused by low-dose exposure to radiation may be repaired, a high enough dose of total body radiation (TBI) exposure affects all stem cell compartments making autologous regeneration and repair no longer possible [40]. After TBI the only treatment to restore the hematological system is hematopoietic stem cell transplantation (HSCT) [42]. Lange and colleagues showed in a mouse model of acute radiation syndrome that infusion of BM derived MSCs were able to modulate toxic and inflammatory effects of radiation, reduce fibrosis, increase survival and even promote hematopoietic recovery in the absence of hematopoietic stem cell transplantation [42].

3.2.3. Bone Marrow Hematopoietic Cells Harvesting

Forty female rats F344 ($RT1^{lv}$, 10-12 weeks old, weighing 150-200 g obtained from Charles Rivers breeding laboratories, Wilmington, MA) were anesthetized by inhalation of isofluorane at 5% (Baxter Forane® Deerfield, IL cat# 1001936060) dissolved in oxygen using a V-10 Anesthesia system (VetEquip, Inc., Pleasanton, CA) and then were euthanized by cervical dislocation. The hind legs were shaved and betadine antiseptic solution was applied with gauze. Skin and muscle were removed and femur and tibia were excised and placed in a sterile specimen cup containing pre-warmed sterile DPBS (GIBCO cat#14190) at 37˚C. Inside a

biosafety cabinet (BSC) under aseptic conditions, bone epiphysis were removed using a bone cutter Rongeur and bone marrow was flushed from femur and tibia using a 10 ml syringe with a 19 gauge needle filled with pre-warmed DPBS at 37 °C. Marrow plugs were transferred into 50 ml conical tube and broken up by aspirating the suspension in and out of the needle at least three times. Cells were passed through a 40 micrometer filter and centrifuged at 200 x*g* for 5 minutes at room temperature. The supernatant was discarded and red blood cells (RBCs) were lysed by adding 1 ml of lysing buffer (ACK lysing buffer GIBCO cat# A10492-01). After 1 minute exposure to lysing buffer, the cells were centrifuged at 600 x*g* for 6 minutes, the supernatant was discarded and the cells were washed twice with DPBS. Bone marrow cells harvested from one donor were transfused in one recipient at a dose of $30x10^6$ cells per recipient.

3.2.4. Magnetic Cell Sorting

Bone marrow T cell depletion was achieved by using a Magnetic Cell Sorting (MACS) isolation kit containing depletion buffer and CD4 MicroBeads conjugated to monoclonal mouse anti-rat CD4 antibodies (isotype: mouse IgG2a, κ; clone: OX-38, Miltenyi Biotech cat# 130-090-319); and MicroBeads conjugated to monoclonal mouse anti-rat CD8a antibodies (isotype: mouse IgG2a, Miltenyi Biotech cat# 130-090-318). Single cell suspension from bone marrow were obtained and cell number was determined and $10x10^7$ cells were suspended in 80 µl of buffer at 4˚C in an Eppendorf tube, then 20 µl of CD8 microbeads was added to each fraction and cells were incubated for 20 minutes at 4 ˚C. After incubation, cells were washed in 1 ml of buffer and centrifuged at 300 x*g* for 10 minutes and the supernatant was discarded. This procedure was repeating using CD4 microbeads. After the incubation with microbeads, the cell suspension was applied onto the magnetic column separator and $CD8^+$ and $CD4^+$ depleted cells were collected in the flow-through fraction.

In order to evaluate depletion efficiency, bone marrow aspirates were labeled separately with FITC Mouse Anti-Rat CD8a (BD Pharmingen™ cat# 554856) and FITC Mouse Anti-Rat CD4 (BD Pharmingen™ cat# 554837). Antibodies were used at 1:100 dilution and incubation was done for 20 minutes in the dark, then cells were washed in DPBS to remove unbound antibody. CD4 and CD8 cell numbers were determined by flow cytometry and data was acquired using a BD FACS Calibur and CellQuest software. Depletion efficiency was calculated

by comparing the percentage of $CD8^+$ and $CD4^+$ before- and after- magnetic microbeads depletion.

3.2.5. Splenocytes Isolation

The spleen from donor female F344 ($Rt1^{lv}$) rats was excised and placed in a petri dish (100 x10 mm). The spleen was cut into longitudinal thin strips using a scalpel, and each strip was cut into smaller pieces. All the pieces were further diced using a small scissor. Spleen pieces were placed in 50 ml centrifuge tubes and treated with 0.25% trypsin at 37 ˚C for 5 minutes. Then, the tubes were centrifuged at 200 x*g* for 5 minutes, the supernatant was discarded and tissue was homogenized by using a pestle glass homogenizer (15 ml capacity) in an isolation buffer containing DPBS, 2% bovine albumin, and 0.5% EDTA at 37°C. The suspension was collected, mixed and passed through a 100 micrometer filter, and then through a 40 micrometer filter. Cells were centrifuge at 200 x*g* for 5 min at room temperature, and the supernatant was discarded, and RBCs were lysed by adding 1 ml of lysing buffer (ACK lysing buffer, GIBCO, cat # A10492-01). After 1 minute of lysing buffer exposure, the cell pellet was centrifuged at 600 x*g* during 6 minutes, the supernatant was discarded and cells were washed twice with DPBS, and resuspended in depletion buffer (Miltenyi Biotech, cat# 130-091-376). A fraction of spleen $CD8^+$ cells was obtained by positive selection by using a Magnetic Cell Sorting (MACS) isolation kit containing MicroBeads conjugated to monoclonal mouse anti-rat CD8a antibodies (isotype: mouse IgG2a, κ; clone: G28, Miltenyi Biotech, cat# 130-090-318). After incubation with microbeads, unlabeled cells which passed though the column were discarded, and the column holding $CD8^+$ cells was washed twice using the depletion buffer.

Efficiency of spleen $CD8^+$ cells selection was assessed by flow cytometry. Selected $CD8^+$ cells were labeled with FITC Mouse Anti-Rat CD8a (BD Pharmingen™, cat# 554856). The percentage of $CD8^+$ cells present in splenocytes cell suspension before- and after- magnetic selection was used to calculate $CD8^+$ purification efficiency. Cell suspensions from bone marrow and spleen were combined and injected in the dorsal vein of the penis into rats 24 hours after TBI on day 0 (e.g., the day of BM transplantation).

3.2.6. Adoptive Transfer of Rat WJCs

For WJCs adoptive transfer, recipient Lewis rats received $2x10^6$ donor WJCs from F344 rat (WJCs isolated from F344 rat pups) ($Rt1^{lv}$) via the dorsal penis vein either 24 hours after lethal TBI together with the hematopoietic cells on day 0, or 48 hours after hematopoietic transplantation on day 2. WJCs were infused at passage 4 and had never been subjected to a freeze/thaw cycle.

WJCs from each litter were combined and suspended in 1000 µl of DPBS warmed at 37^0C. For dorsal penis vein injection, recipient rats were anesthetized by inhalation of isofluorane at 2% (Baxter Forane® Deerfield, IL cat#1001936060) dissolved in oxygen using a V-10 Anesthesia system (VetEquip, Inc., Pleasanton, CA). After the rat became insensitive to pain (e.g., loss of flexion reflex), the penis was extruded by descending the prepuce to the penis base, then the gland penis is held at the tip to visualize the dorsal penis vein for injection [43]. Injection was done using a 1 ml syringe with 25-gauge needle. The syringe was filled, air bubbles removed and cell injection was performed slowly.

.

3.2.7. Assessment of GVHD

The indicators of systemic GVHD in murine models, such as those reported by Polchert *et al*. and Taylor *et al*. [44, 45] include survival, percentage of weight lost, posture, behavior, and ruffled fur and skin integrity and erythema, and were evaluated daily. Rats were monitored for clinical symptomatology of GVHD including hair loss, skin rash, scleroderma, diarrhea, hunched posture and fur texture. Hematocrit was measured weekly by using standard microhematocrit technique; for hematology and serum biochemistry, samples were processed in the Clinical Pathological Laboratory at College of Veterinary Medicine in Kansas State University. Hematological parameter including serum biochemistry analysis were performed at 3 time points; first before radiation, second at day 35, which was considered as the midterm survival time, and finally at the end point defined as day 77 or at the time of euthanasia as indicated by advanced degree of GVHD (loss of 25% of initial body weight or hematocrit dropping to 20% or less). Individual values of creatinine, Alanine aminotransferase (ALT), Aspartate aminotransferase (AST) and bilirubin total were compared with the specie-specific reference values, as well as with the pretreatment normal values. Liver functionality was measured through

ALT, AST and total bilirubin, while renal function was measured by creatinine serum values. Animals dying before 15 days after TBI and showing aplastic anemia were considered to be suffered from acute radiation toxicity instead of GVHD. Recipient rats were considered as long-term survivors if their survival time exceeded 60 days after hematopoietic cell transplantation. The degree of each GVHD associated symptom was semi-quantitatively scored from 0 to 3 (Table 3.2). Negative control group formed by rats which received TBI without allo-HST or WJCs and normal healthy control group untreated control were not included in the GVHD score analysis.

TABLE 3.2
Semi-quantitative score of GVHD-associated clinical symptomatology

CRITERIA	SCORE			
	0	1	2	3
Alopecia	Not observed	Hair loss without skin damage	Hair loss with skin damage	Hair loss and skin rash
Erythema	Not observed	Ear skin erythema	Ear and pad skin erythema	Ear and pad skin erythema and exudate
Weight loss	Not observed	Less than 10%	10-20%	More than 20%
Diarrhea	Not observed	One period	Two period	Bleeding
Hunched posture and ruffled fur	Not observed	Moderate one time	Moderate more than 2 times	Severe

The average for all symptoms daily observed in each rat was used to grade the severity of GVHD. The scores obtained from rats in transplanted with bone marrow cells and $CD8^+$ splenocytes untreated with WJCs(GVHD group), were compared to those in rat transplanted

with bone marrow cells and $CD8^+$ splenocytes treated with WJCs at day 0 and day 2 to determine if the WJCs treatment had an effect in the prevention of GVHD.

3.2.8 GVHD Grading and Staging score

Clinical symptomatology in rats were monitored and recorded daily. Blood analysis was evaluated weekly. GVHD incidence in each target tissue was graded and staged using the Glucksberg and International Bone Marrow Transplant Registry (IBMTR) criteria (Table 3.3). The overall grading based on the individual stages of the organs involved was assigned using Glucksberg criteria (Table 3.4). A combination of both criteria was used to categorize GVHD as stage/grade.

TABLE 3.3
Glucksberg and IBMTR criteria target organ staging

Organ	STAGE 1	2	3	4
Skin Maculopapular rash extent, % of body surface area	<25%	25-50%	>50% or generalized erythroderma	Generalized erythroderma with bullous formation or desquamation
Liver Bilirubin total mg/dL	(2-3) or AST 150-750 U/L	(3-6)	(6-15)	(>15)
Gut Daily diarrhea volume	3mL/100g	6mL/100g	9mL/100g	>9 mL

Graft versus host disease staging per International Bone Marrow Transplant Registry criteria [46, 47, 48].

TABLE 3.4
GVHD overall grade Glucksberg criteria

Overall Grade Glucksberg	Criteria
I	Skin stage 1 or 2 only (no liver or gut aGVHD)
II	Up to stage 1 liver or gut, up to stage 3 skin
III	Up to stage 4 liver, up to stage 3 in any other organ
IV	Stage 4 skin or gut

Graft versus host disease grading per Gluckberg and criteria [46, 47, 48].

3.2.9 Supportive Care

After TBI the animals were manipulated inside a High Efficiency Particulates Air (HEPA)-filtered isolation laminar flow unit (LABCONCO® PuriCare laminar flow cabinet). Rats were housed in an isolation room and had sterilized cages, food and water provided. Clinical observation, body weight and body temperature were recorded daily. Animals showing dehydration (indicated by a dorsal skin fold that was slow to return to normal position when gently pulled up), diarrhea or suddenly weight loss were given 0.2% glucose in their drinking water, as well as with intraperitoneal or subcutaneous administration of an ionic balance solution (Veterinary 0.9% sodium USP cat# 012007), ionic balance solution was pre-warmed at 37˚C and administered at 10 ml/kg. In addition, a high energy diet (Nutrical) and cereal (a highly preferred diet) were given to animals showing dehydration, diarrhea and weight loss. For intraperitoneal rehydration, animals were restrained using a sterile towel, the abdominal area was disinfected using betadine antiseptic solution. A 3 ml syringe with a 25 gauge needle was used to inject the solution. Solution was injected at a rate of 1 ml per minute.

3.2.10 Neutrophil Recovery

After myeloablative conditioning regimen followed by hematopoietic cell transplantation, neutropenia is a common event which increases susceptibility to infectious diseases until neutrophil number is recovered [49]. To determine the kinetics of peripheral blood neutrophil

recovery, manual differential cell count by blood smear was performed every 7 days for 5 weeks after hematopoietic cell transplantation. Neutrophil differential were determined by counting 100 nucleated cells on Giemsa stained blood smear [50].

3.2.11. Engraftment and Chimerism

Hematopoietic engraftment was evaluated by three criteria. First, hematological evaluation of hematocrit (microhematocrit) and neutrophil recovery (blood smear differential count) every week while alive. Second, histopathological evidence of hematopoietic compartments reconstitution (after euthanasia), and thirdly by donor-recipient chimerism assessed by PCR using strain-specific DNA microsatellites from a spleen, a tail snip or bone marrow tissue sample (after euthanasia).

3.2.12. Rat gDNA polymerase chain reaction (PCR) using Microsatellite

Genomic DNA was isolated from rat tissue samples using a DNeasy blood and tissue kit Qiagen cat# 69581. For each rat gDNA was isolated from three tissues, the spleen, bone marrow and from a tail snip. The genomic DNA was analyzed using PCR amplification with the microsatellite primer pair manufactured by IDT primer and obtained from the rat genome database [51]. PCR amplification conditions were 95˚C for 3 min, 94˚C for 15 s, 55˚C for 15 s, 72˚C for 30 s for 40 cycles and 72˚C for 10 min for final extension. The microsatellite was D5mgh20 (Forward-5'-GAAGACACCCAGTGCAACCT, Reverse 5'-CTCTTTGCTTGAAAGACTTTTGC). Expected product size was 252bp for Lewis and 219bp for F344. The amplification products were visualized by electrophoresis on a 2% agarose gel, stained with ethidium bromide and imaged using a gel imaging system (Fotodyne Inc., Hartland, WI).

3.2.13. Survival

Survival and/or relapse-free survival of GVHD after hematopoietic cell transplantation was calculated using the Kaplan–Meier method, and the log-rank test was used for comparison of curves. Statistical analyses were done using GraphPad Prism® software.

3.3 Histopathological Evaluation

3.3.1 Hematoxylin and Eosin stain for morphological study

Necropsy was performed in the Animal Resource Facility laboratory at Kansas State University. Animals were euthanized by CO_2 overdose, then 500 µl of heparin was injected into the heart and blood perfusion was performed with a neutral pH phosphate buffer saline solution and then 10% neutral buffered formalin by using perfusion pump (Masterflex, Cole-Parmer instrument company, Vernon Hill, IL). Gross characteristics and occurrence of lesions in organs were recorded by photography (Nikon D70). Representative samples of target organs included: thin skin (forehead region), thick skin (pads), liver, lungs, pancreas, bone marrow (femur), spleen, thymus, small intestine (jejunum) and stomach were collected. The tissue samples were fixed by immersion in 10% neutral buffered formalin for 48 hours. Samples for healthy, untreated animals (n=5), lethally irradiated rats without BMT (negative control, n=10) and positive controls (rats receiving T-cell depleted BMT, n=10) were used as controls. For histopathological study using the routine stain hematoxylin and eosin (H&E), 1 cm^2 samples were collected and processed by using the paraffin technique by the Kansas State University histopathology laboratory. Four 4 µm transverse sections were cut on a rotary microtome and the sections were stained by hematoxylin and eosin (H&E) and observed microscopically. Tissue samples were analyzed by a Board-Certified Veterinary Pathologist, Dr. Bhupinder Bawa, who was blinded to experimental conditions of the slides that were reviewed. The histopathological parameters evaluated and scored include epithelial cells degeneration, necrosis or loss; atrophy, inflammation, hemorrhage, histiocytosis, edema and fibrosis.

3.3.2 Special stains

3.3.2.1 Mast cells, eosinophils and collagen deposition

Mast cell distribution was studied using two different staining methods. First, mast cells were identified by their metachromatic properties using Toluidine blue staining [52]. Second, a simultaneous demonstration of mast cells and eosinophils was performed using a combined eosinophil/mast cells staining kit (American Master Tech, Lodi, CA, cat# KTCEM). Collagen

deposition was studied using Masson's trichrome stain [53]. Histopathological processing was carried out at the clinical histopathology laboratory at Kansas State University College of Veterinary Medicine.

3.3.1. Immunohistochemistry Evaluation

3.3.1.2 Complement, eosinophil major basic protein, and Elafin

Immunohistochemistry was performed on 4 micrometer paraffin embedded sections. Antigen retrieval was performed by incubation of microscopic preparations in preheated (95˚C) 10mM Sodium Citrate Buffer for 20 minutes. After 20 min of cooling, the sections were rinsed twice in DPBS with 0.05% Tween 20 for 2 min. After antigen retrieval procedures, tissue samples were blocked with 5% normal goat serum for 5 minutes to prevent the nonspecific binding of the antibodies. Sections were evaluated for complement (C3d) and anti-eosinophil major basic protein (MBP), and Elafin.

Deposition of complement factor C3 was evaluated by using a immunoperoxidase staining kit (ImmunoCruz™ mouse ABC Staining System, Santa Cruz Biotechnology, cat# sc-2017) following the manufacturer's instructions. Briefly, tissue sections were first incubated with mouse anti-goat primary antibody at 2.5 µg/ml overnight at 4°C. Tissues were washed with three changes of DPBS for 5 minutes each. Incubation was done with biotinylated secondary antibody goat anti-mouse for 30 minutes at room temperature. After washing three times with DPBS for 5 minutes each, tissues were incubated for 30 minutes with ABC reagents. Finally, the target protein was visualized by incubation in peroxidase substrate.

Immunofluorescence staining was performed to assess presence of major basic protein (MBP). After antigen retrieval and nonspecific antibodies binding blocking, tissue sections were incubated with mouse IgG anti- eosinophil MBP primary antibody (Millipore, cat# CBL419) at dilution of 1:500 overnight at 4 °C. Incubation was done with secondary antibody FITC goat anti-mouse IgG (Millipore, cat# AP181F) at dilution 1:500 for 4 hours at room temperature. Cell nuclei were counterstained with 1 µg/ml 4'-6-Diamidino-2-phenylindole (DAPI) for 20 minutes and tissue sections were rinsed with DPBS. The fluorescence emission of FITC was obtained using an excitation wavelength of 490 nm and the emission was acquired using a 515 nm

longpass filter. The fluorescence emission of DAPI was obtained using an excitation wavelength of 358 nm and the emission was acquired using a 435-470 nanometers bandpass filter. Fluorescence was examined using a Nikon Eclipse TE2000-S microscope equipped with Semrock high-Q epifluorescence filters and micrographs taken with a Roper CoolSnap ES black and white camera using Metamorph software.

Elafin was detected by rabbit polyclonal anti-Elafin antibody conjugated to biotin (Bioss, cat# bs-6531R-Biotin) for amplification of signal, a two-step biotin-avidin-enzyme system (ABC) was used following the manufacturer's instructions.

3.4 Statistical analysis

For all outcome variables normality was assessed by Shapiro-Wilk normality test. Variables that did not meet the assumption of homogeneity of variance or normal distribution were analyzed by Kruskal–Wallis one-way analysis of variance by ranks. Growth curves were calculated by using Excel and GraphPad prism software. Results are expressed as the means± standard deviation (mean± SD). For analysis of more than 2 data sets Kruskal-Wallis test with Dunn's post-hoc test were used (non-parametric). Significance was set at $p<0.05$. The variables studied were survival time, body weight, body temperature, hematocrit, blood analysis, serum biochemistry and histopathological and immunohistochemistry study. Survival time was evaluated by the Kaplan-Meier curve, a method of estimating time-to-event models in the presence of censored cases. Comparison between groups for: body weight, body temperature and hematocrit were conducted using Kruskal –Wallis one-way analysis of variance by ranks. Comparison within groups was conducted using a paired two-tailed *t*-test. Blood analysis and serum biochemistry between groups was compared using an unpaired two-tailed *t*-test. Data was analysed using GraphPad prism software.

3. 5. Results

3.5.1. Bone Marrow T-cell Depletion

By using magnetic activated cell sorting (MACS), T-cell depletion efficiency was 96.1 %. Total T cell recorded by flow cytometry in bone marrow cells suspension before depletion was 55% as detected by expression of $CD4^+$ and $CD8^+$ conjugated FITC antibodies. After magnetic depletion using Magnetic Cell Sorting (MACS) isolation kit containing Microbeads conjugated to $CD4^+$ and $CD8^+$ T cell population dropped to 1.9%. After depletion the percentage of individual fractions of $CD4^+$ and $CD8^+$ were 0.6% and 0.6% respectively (fig.3.1).

Before depletion total T cells	**After depletion**	**After depletion**	**After depletion**
$CD4^+$ + $CD8^+$ conjugated FITC antibody	**$CD4^+$ $CD8^+$ conjugated FITC antibody**	**$CD4^+$ fraction**	**$CD8^+$ fraction**
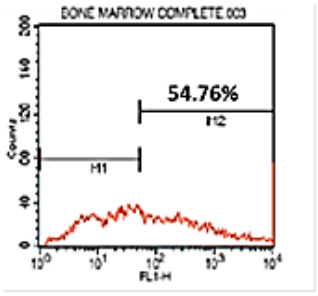	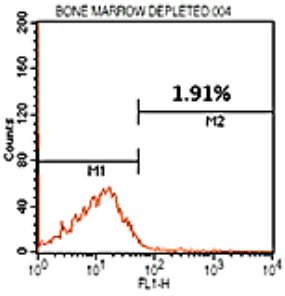	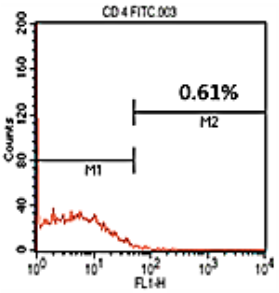	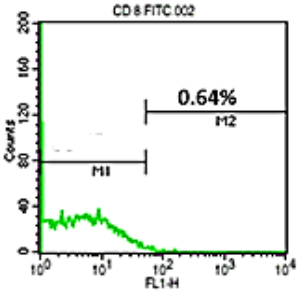

Figure 3.1. Flow cytometry analysis of bone marrow T cell content before and after $CD4^+$ and $CD8^+$ depletion by magnetic activated cells sorting (MACS). Bone marrow cells were obtained by flushing BM from the femur and tibia of donor F344 rats.

3.5.2. Effect of Total Body Irradiation

3.5.2.1. Lethally irradiated, not transplanted rats (negative control group)

Control animals which received the TBI-based conditioning regimen without hematopoietic cell transplantation did not survive longer than 12 days. Hematopoietic and gastrointestinal manifestations of acute radiation syndrome were observed as early as day 4 after TBI. Hematological analysis revealed aplastic anemia measured as pancytopenia (dramatic reduction in white and red blood cells counts) (Table 3.10). Histopathology study showed marked depletion of parenchymal components (hypoplasia) of hematopoietic organs spleen and bone marrow (fig. 3.6).

3.5.2.2. Acute Radiation Syndrome Pathogenesis

Pathogenesis observed in negative control rats is summarized in figure 3.2. Rats exposed to 10 Gy TBI without hematopoietic cells transplantation had body weight loss of 20.8 % at day 7 post-irradiation with a reduction from the initial weight average of 265 g to 210g (fig.3.3); also they presented anemia (defined as a hematocrit less than 42 percent or a hemoglobin level less than 13g/dL) and diarrhea (defined as having three or more loose or liquid and frequent bowel movements) less than 7 days after TBI. Respiratory symptoms such as dyspnea, breathing resistance were observed in all rats.

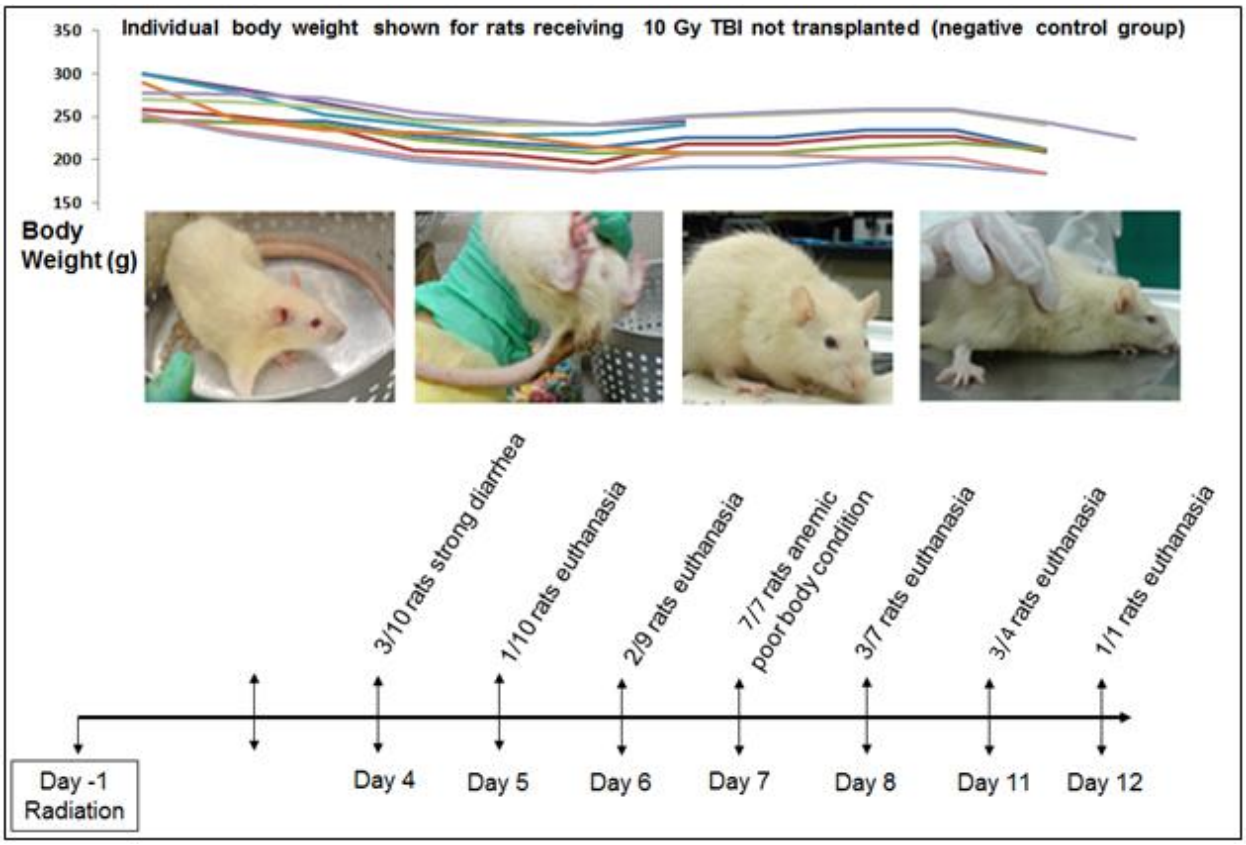

Figure 3.2. Acute radiation syndrome pathogenesis. Rats exposed to10 Gy total body irradiation (TBI) without hematopoietic cells transplantation (negative control) showed at 7 days post-irradiation anemia symptomatology such as paleness of gums, ears and feet, reduction in hematocrit, pancytopenia and poor body condition. No alopecia was observed for negative control group.

3.5.2.3 Body weight

The growth curve of rats during the 12 days study of negative control group is shown in figure 3.3.

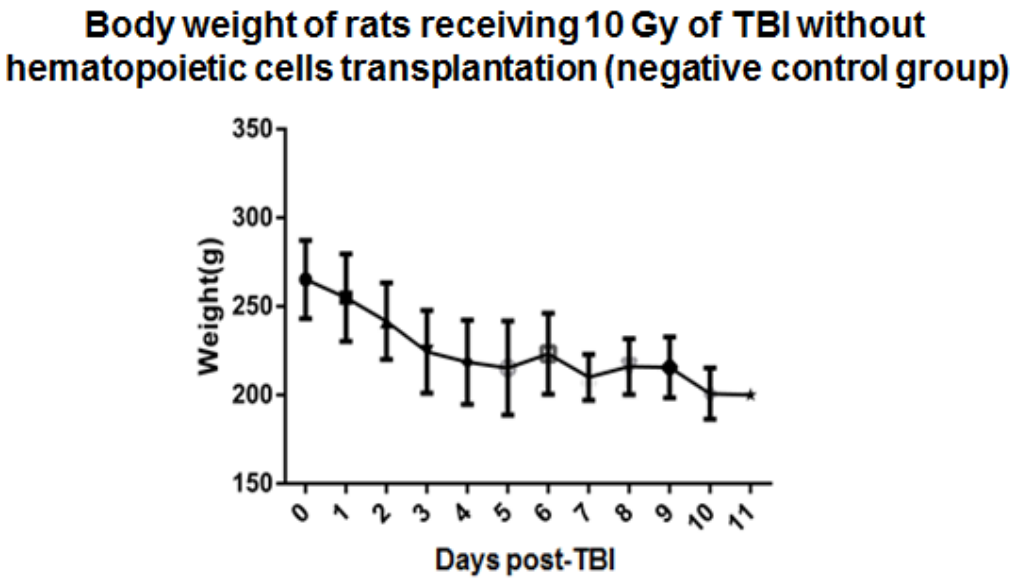

Figure 3.3. Growth curve of rats receiving lethal 10 Gy total body irradiation (TBI) without hematopoietic cells transplantation (negative control group). Growth curve declined from day 1 post-irradiation until day 12. Data is expressed as mean± SD.

3.5.2.4 Hematocrit

The negative control group rats' hematocrit was measured before TBI (day 0), and 7 days post-TBI and at the end point (7-12 days) by microhematocrit. The group values are presented in figure 3.4. The negative control group hematocrit measured before radiation was 50±2%, at seven days was 30±4%, which represents a decrease of 40%, and at the end point 9-11 days was 12±4%, which denotes the hematocrit dropped to 76 % of the pre-radiation value (fig.3.4)

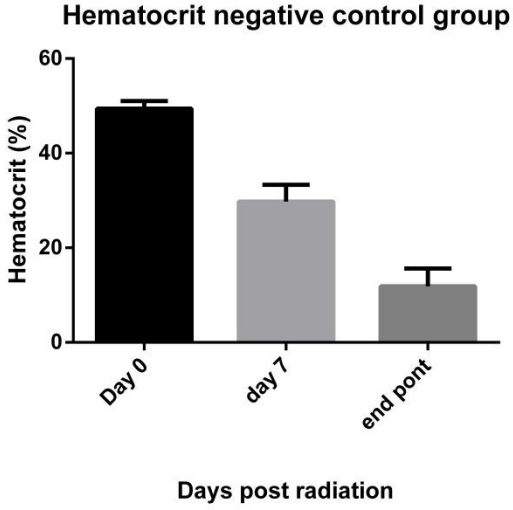

Figure 3.4. Hematocrit values in Lewis rats irradiated with 10 Gy total body irradiation(TBI) and not transplanted with bone marrow (negative control). Values represent the hematocrit (percentage of the volume blood sample occupied by red blood cells). Data are expressed as mean±SD.

3.5.2.5. Gross anatomy observations

Gross anatomy observation of organs at necropsy of negative group rats revealed pulmonary hemorrhage, petechial hemorrhage in gastrointestinal tract and splenic atrophy (fig. 3.5)

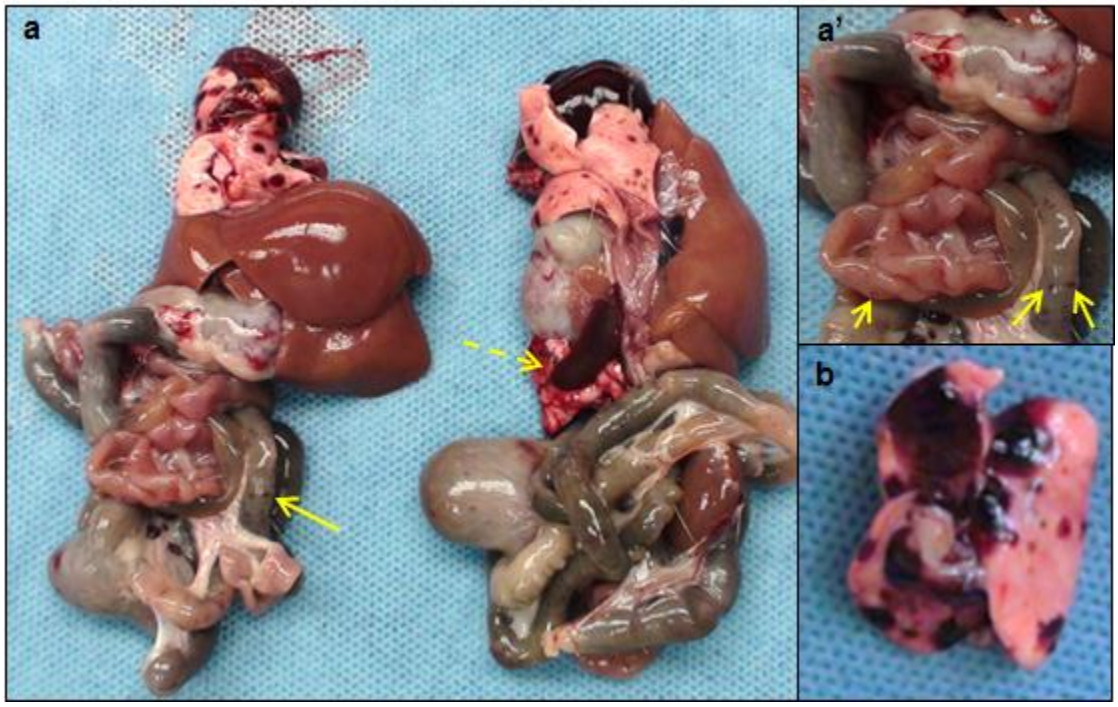

Figure 3.5. Gross anatomy appearance of Lewis rats irradiated with 10 Gy total body irradiation (TBI) and not transplanted with bone marrow (negative control group)**.** Macroscopic aspect of gastrointestinal tract and lungs from negative control group at day 10 post-irradiation. (a) Viscera of 2 rats showing similar pathological injuries, petechial hemorrhages disperse around intestine (solid yellow arrow) and pancreatic hemorrhage (dashed yellow arrow) was observed. (a') At higher magnification, petechial hemorrhage were easily distinguished (arrows). (b) Dramatic focal hemorrhage was present in all pulmonary lobes.

3.5.2.6. Histopathology

Histopathological evaluation was performed at the end point (euthanasia) of negative control group rats. Tissue injuries observed were mucosal and sub-mucosal hemorrhage at intestinal level, hemorrhage and focal edema in lungs, and reduction in epidermis cell layers.

Deposition of collagen was observed by Masson's trichrome staining. Qualitative observation of collagen deposition showed a reduction in loose connective conforming papillary dermis in skin in specimens taken from negative control group animals (fig. 3.39)

3.5.2.7 Hematopoietic organs depletion

Histopathological evaluation of hematopoietic compartments was performed at the end point (euthanasia) of negative control rats. Representative results are shown in figure 3.6

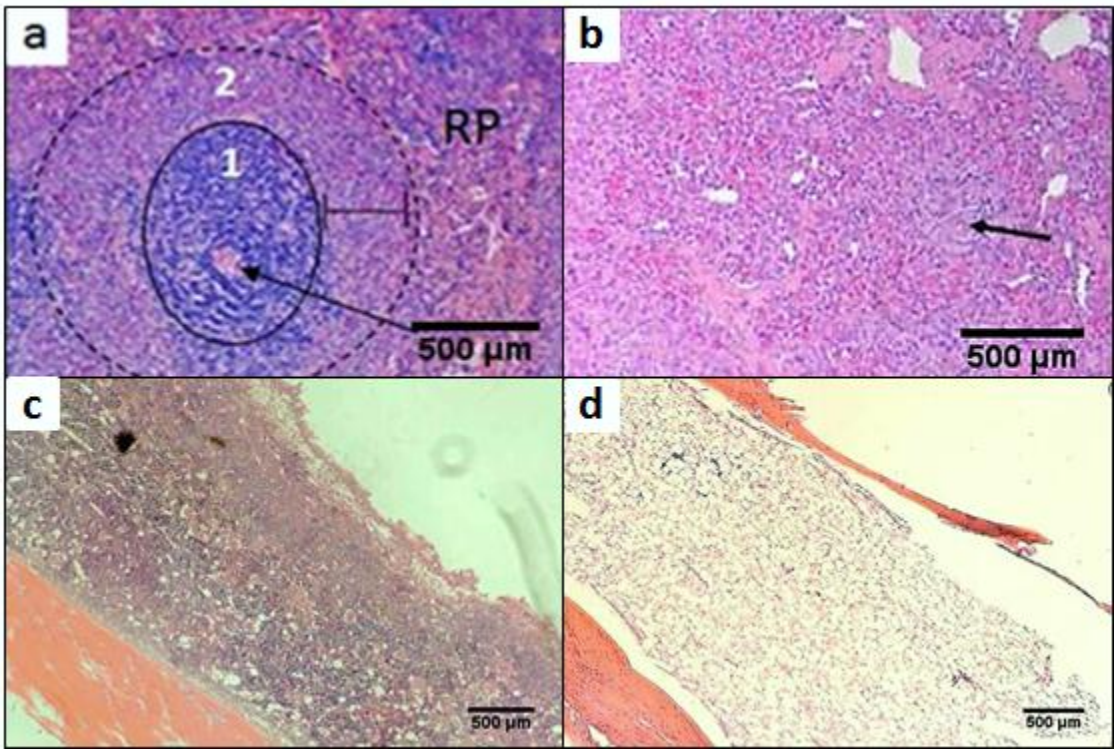

Figure 3.6. Hematoxylin and eosin photomicrograph of sections from hematopoietic organs (spleen and bone marrow). (a) Healthy normal control spleen. Note the parenchymal components white pulp represented by primary lymph nodules spherical cluster of tightly packed small lymphocytes (solid ring), arrow indicates the central arteriole (1), surrounded by the mantle zone (2), red pulp (RP) surrounding white pulp is indicated. (b) Representative section from Negative control group spleen showing hypoplasia of parenchymal components white pulp (indicated by ring and arrow) and RP (area adjacent to solid ring). (c) Bone marrow cavity from healthy normal rat, occupied by hematopoietic cells. (d) Bone marrow from representative section from the negative control group. Note the reduction in bone marrow parenchymal components (hypoplasia) observed in negative control group rat's bone marrow cavity (c). This cavity is

mostly filled with fat stromal cells. (panels a and b objective magnification 10X, panels c and objective magnification 4X.Calibration bar is 500 micrometers.

3.5.2.8 TBI induced lung innate immunity activation.

Histopathological evaluation of lung samples revealed extracellular deposition of eosinophil granule major basic protein (MBP) crystals close to hemorrhagic areas of lung parenchyma (fig 3.7). Definitive identification of MBP crystals was done by immunohistochemistry (fig 3.8). Intra-alveolar MBP crystals were observed in all negative control rats, and not in healthy animals (data not shown).

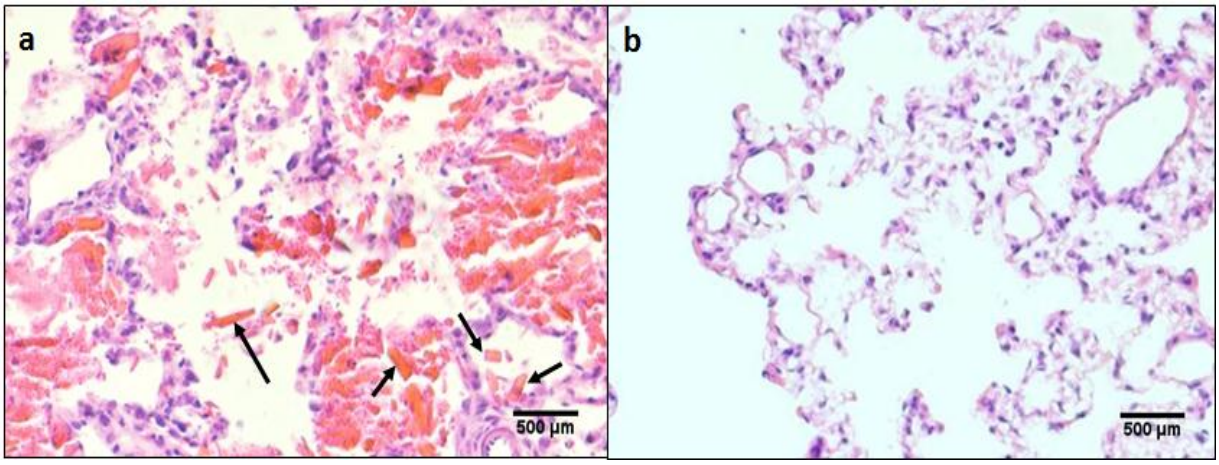

Figure 3.7. Irradiation induced lung injury. (a) Lung parenchyma of rat irradiated with 10 Gy of total body irradiation (TBI) that was not transplanted with bone marrow (negative control group) showing lung injury indicated by extracellular acidophilic crystals (arrows). These crystals were observed close to focal hemorrhage areas. (b) Lung parenchyma of healthy normal rat, alveolar clear airways are observed, magnification 20X. H&E stain. Calibration bar is 500 micrometers.

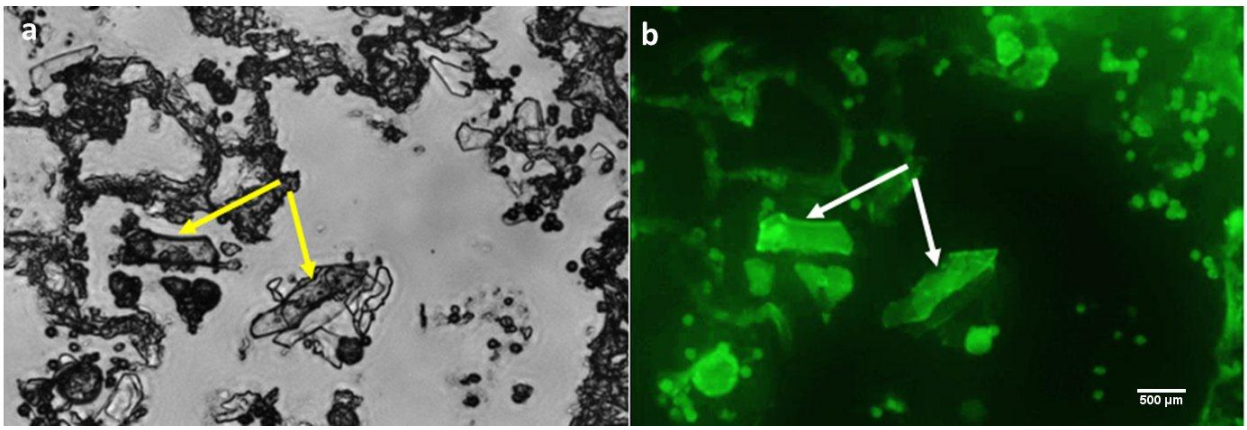

Figure 3.8. Major basic protein (MBP) immunohistochemical staining of lung tissues from irradiated rats (negative control group). a) Bright field micrograph of lung section arrows indicates crystalloid structures into lung airways. b) Immunofluorescence micrograph of same field as in a) indicating MBP staining associated with crystalloid structures (arrows). Objective magnification 40X. Calibration bar is 500 micrometers.

3.5.2.9. Mast cells distribution.

Following total body irradiation, stainable mast cells were almost undetectable in small intestine lamina propia (fig.3.9), and at lung sub-pleural zone and in liver periportal areas.

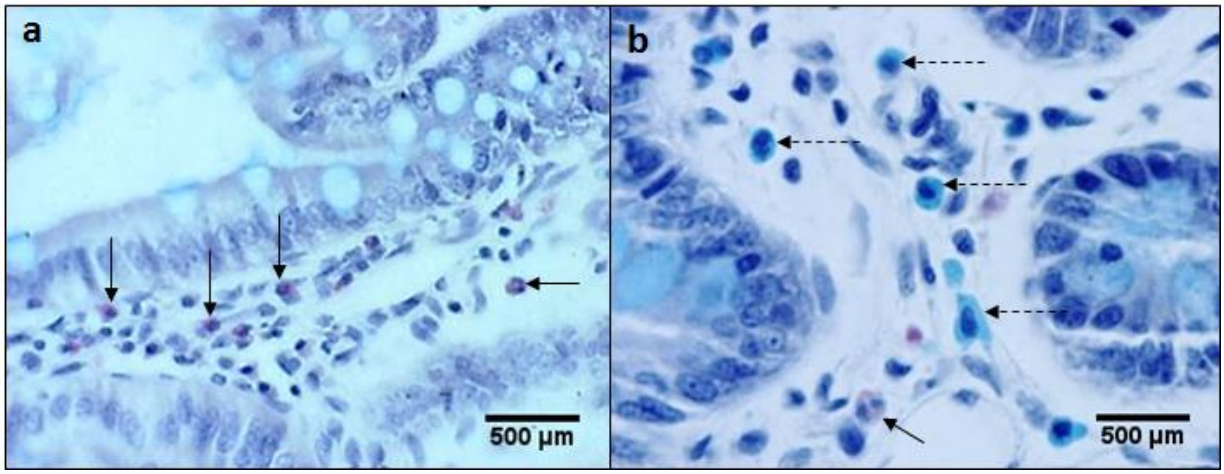

Figure 3.9. Eosinophil/mast cells staining of paraffin embedded tissues of rat irradiated with 10 Gy of total body irradiation and not transplanted with bone marrow (negative control group). Representative small intestine section showing the epithelial surface lining and the subjacent lamina propia loose connective tissue. Sections were stained with vital new red stain to visualize eosinophils, astra blue stain to show mast cells, and nuclei were counterstained with modified Mayer's hematoxylin. (a) No stained mast cell were observed in small intestine lamina propia of negative control group (arrows indicate eosinophils, objective magnification 10X). (b) Mast cells

(stained cells indicated by dashed arrows) and eosinophils (arrows) were found in small intestine lamina propia of healthy normal control rats (40X). Eosinophils were identified by their typical morphology of rounded cells with bilobed nucleus and affinity for vital new red dyes (arrows). Mast cells were identified by their oval morphology and intracytoplasmic granules with affinity for astra blue dye (dashed arrows).Calibration bar is 500 micrometers.

3.6. Positive control group receiving bone marrow magnetically depleted of $CD8^+$ and $CD4^+$ 24 hours after TBI

3.6.1 Pathogenesis

Rats that received 10 Gy of total body irradiation follow by bone marrow depleted of $CD4^+$ and $CD8^+$ T cells was called the positive control group. These animals survived until the 77 days end point following bone marrow transplantation. The growth curve (fig 3.10) indicates a drop in body weight around day 7 post-transplantation, then body weight constantly increased until around day 45 when some rats (n=3) reached a second drop in body weight. At day 10 all rats presented facial alopecia, more pronounced at the nasal area. Starting at day 20 hair was seen to be re-growing in all rats and by the mid-term of the study (day 35), alopecia was almost unnoticeable (fig 3.10). At midterm study (day 35) hematological parameter and serum levels of creatinine, alanine transaminase (ALT), aspartate transaminase (AST) and total bilirubin were within the healthy normal control reference values (Table 3.10). However, at the end point (day 77) 5 of out 8 rats showed a significant elevation of hepatic enzymes ALT, t= 2.69, p value <0.03 and AST, t=1.68, p value <0.02. The mean values were ALT 81±52 U/L, and AST 219±166 U/L (references values ALT=18-45 U/L; AST=74-143 U/L) [54].

Clinical manifestations of positive control rats receiving allogeneic hematopoietic cell transplantation (T-cell depleted bone marrow 24 hours after lethal TBI exposure) are summarized in figure 3.10. Growth curves of daily mean body weight is presented figure 3.11

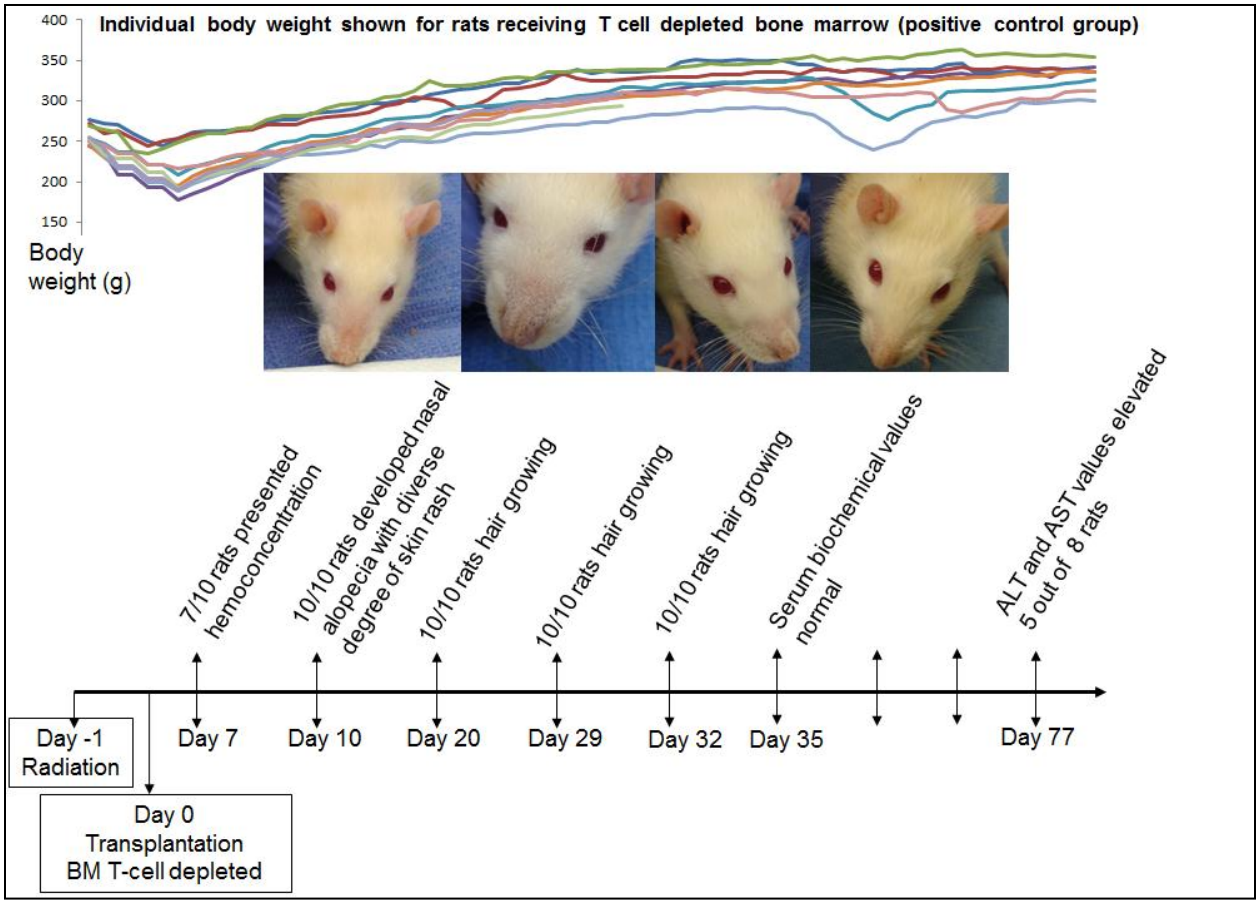

Figure 3.10. Pathogenesis observed in the positive control group (rats which received 10 Gy total body irradiation followed twenty four hours later by bone marrow transplant of CD4 and CD8 depleted bone marrow). This group showed very slight alopecia from day 4-10 post BMT and hair regrowth by day 20.

3.6.2 Body weight

The growth curve of positive control group rats (rats which received 10 Gy total body irradiation followed twenty four hours later by bone marrow transplant of CD4 and CD8 depleted bone marrow) during the 77 days after transplantation is shown in figure 3.11, data is expressed as mean±SD.

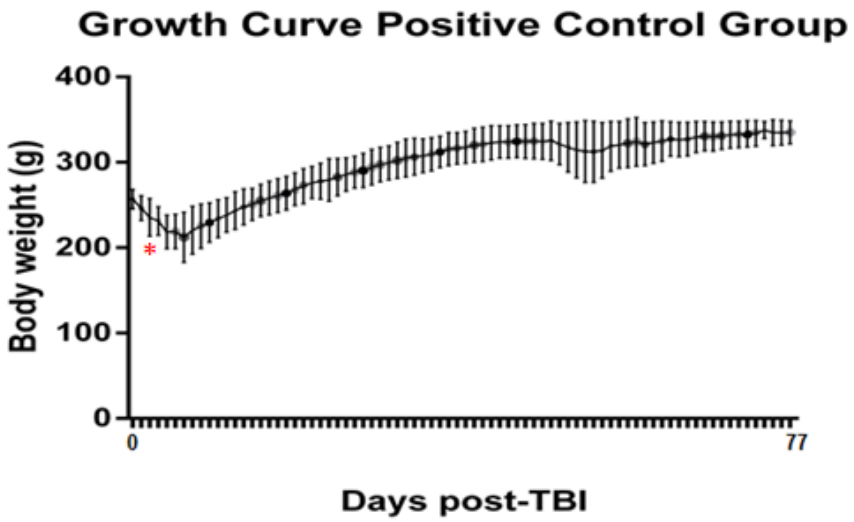

Figure 3.11. Body weight positive control group (rats which received 10 Gy total body irradiation followed twenty four hours later by bone marrow transplant of CD4 and CD8 depleted bone marrow). Rats in the positive control group showed a significant body weight lost at day 3 post-TBI asterisk (indicated by *, t=2.72, df=18, p value=0.0140). Body weight continued falling until day 7 reaching the first nadir in body weight. A second drop in growth curve was observed around day 50. However, this was not significant differences in body weight lost t= 1.428, df=16, p value=0.1689. Data is expressed as mean ± SD.

3.6.3 Hematocrit

Mean values of hematocrit of the positive control group (rats which received 10 Gy total body irradiation followed twenty four hours later by bone marrow transplant of CD4 and CD8 depleted bone marrow), was measured weekly by microhematocrit. These data are presented in figure 3.12.

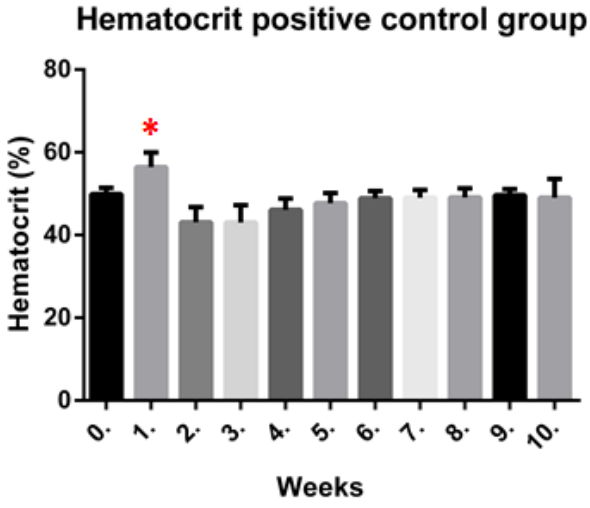

Figure 3.12 Hematocrit measured weekly during 77 days of study for rats that were irradiated with 10 Gy total body irradiation on day-1, and received T-cell depleted bone marrow on day 0.

Asterisk (*****) indicates hemoconcentration. At week 1, 7 out 10 rats presented hemoconcentration. At week 2, hematocrit dropped and showed statistical difference with initial pre-treatment value (49.9%) until week 4, when hematocrit reached no significant differences with the pre-treatment value. (paired t test P value <0.03 α=0.05).

3.6.4. Gross anatomy observations

Macroscopic observations of positive control group viscera were recorded at day35 and day 77, when rats in the positive control group were euthanized. At day 35 after bone marrow transplantation, no noticeable damage was observed macroscopically (data not shown). At the end point (day 77), focal hyperemia and edema was observed in lung in 4 out of 8 rats (fig.3.13)

Figure 3.13. Macroscopic aspect of gastrointestinal tract and lungs of transplanted rats with bone marrow T-cell-depleted at day 77 after bone marrow transplantation with T-cell depleted bone marrow . Notice the hyperemia in the lungs and liver.

3.6.5. Histopathology

Tissue samples were taken and processed for histopathology from rats that were irradiated with 10 Gy total body irradiation on day-1, and received T-cell depleted bone marrow on day 0 (positive control group) at day 35 (n=2) and day 77 end point (n=8). Deposition of collagen was observed by Masson's trichrome staining. Qualitative observation of collagen deposition showed a normal collagen network in target tissues as compared with healthy normal rat samples (fig 3.39). Representative histopathology results from skin, small intestine and liver are presented in figure 3.29. Mast cells distribution and in positive control groups are presented in figure 3.14.

At day 35 post-transplantation, small intestine samples of rats receiving T-cell depleted bone marrow and untreated with WJCs (positive control), by using metachromatic stains the characteristics metachromatic granules of mast cells were not observed. However mast cells were localized exclusively in connective tissue of intestine lamina propia (fig3.14 (a)and (a')). At day 77, mast cells which exhibit a positive metachromatic reactive reaction were observed in lymph node, lungs (fig.3.14 (b) and (c)) as well as in most tissues.

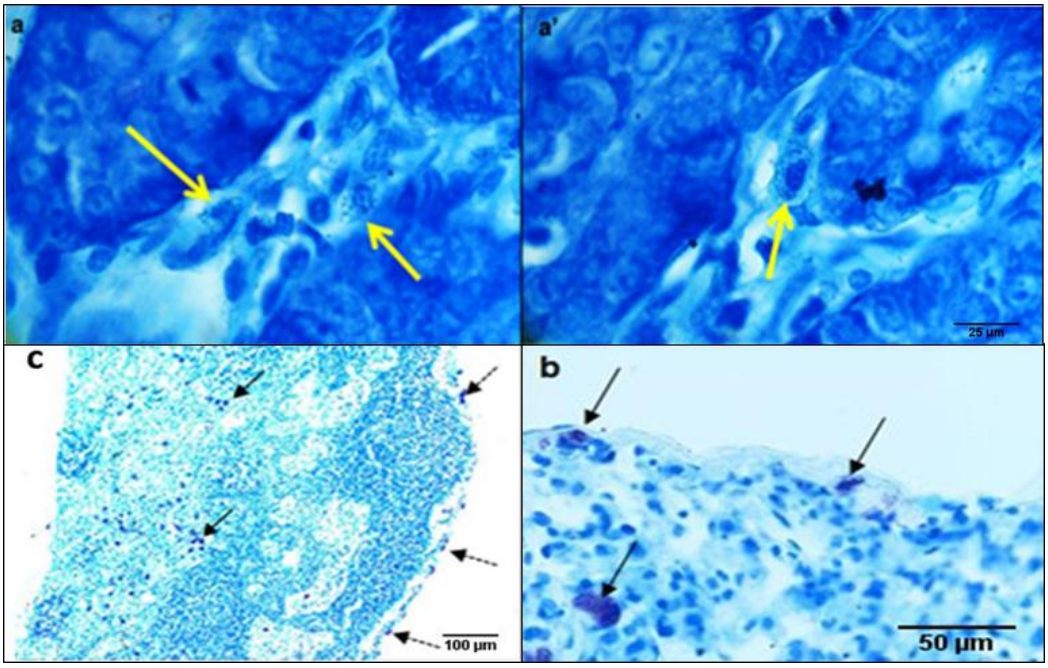

Figure 3.14. Mast cells distribution in positive control rats, e.g., rats that were irradiated with 10 Gy total body irradiation on day-1, and received T-cell depleted bone marrow on day 0. Toluidine blue stain at 77 days post-transplantation. (a) and (a') Small intestine interstitial mast

cells (yellow arrows) containing fine intracytoplasmic orthochromatic granules were observed, objective magnification 100X. (b) Mast cells were detected in lung sub-pleural zone (indicated by arrows). (c) Lymph node showing mast cell distribution in outer capsule (dashed arrows) and medullar zone (solid arrow). Note that mast cells stain purple and contain no metachromatic structures that stain blue. Calibration bar is 100 micrometers in a and a'; 50 micrometers in b and 100 micrometers in c.

3.7. Establishment of rat model of GVHD

3.7.1. GVHD-induced rat with hematopoietic cells transplantation not receiving WJCs.

GVHD induction was assessed by several criteria. The most prominent signal of GVHD in our model was alopecia. All GVHD-induced animal developed mild alopecia on their forehead. In addition to forehead, alopecia 4 out of 10 rats presented alopecia on their posterior legs, or on their anterior and posterior legs, as well as dorsal area. As we observed in the positive control group, alopecia was observed at day 10 post-transplantation in the GVHD group, too. Two rats in the GVHD group presented a cyclic episode of diarrhea starting on day 10 and the second one at day 50 post-transplantation. At 35 day after transplantation in the GVHD group, serum chemistry revealed an increase in bilirubin total in 5 out of 10 rats, with a mean of 0.3±0.25 U/L (reference value 0.05-0.15 U/L) (Table 3.10). Other serum biochemical values were within normal reference values. However, at the end point (day 77) an elevation of creatinine, ALT and AST was recorded in 5 out 5 rats. The mean values of creatinine, ALT and AST were 0.58±0.15, 54±17 and 153±51 U/L respectively (Table 3.11). The pathogenesis of GVHD in a rat minor histocompatibility mismatch model is summarized in figure 3.15.

3.7.2 GVHD Pathogenesis

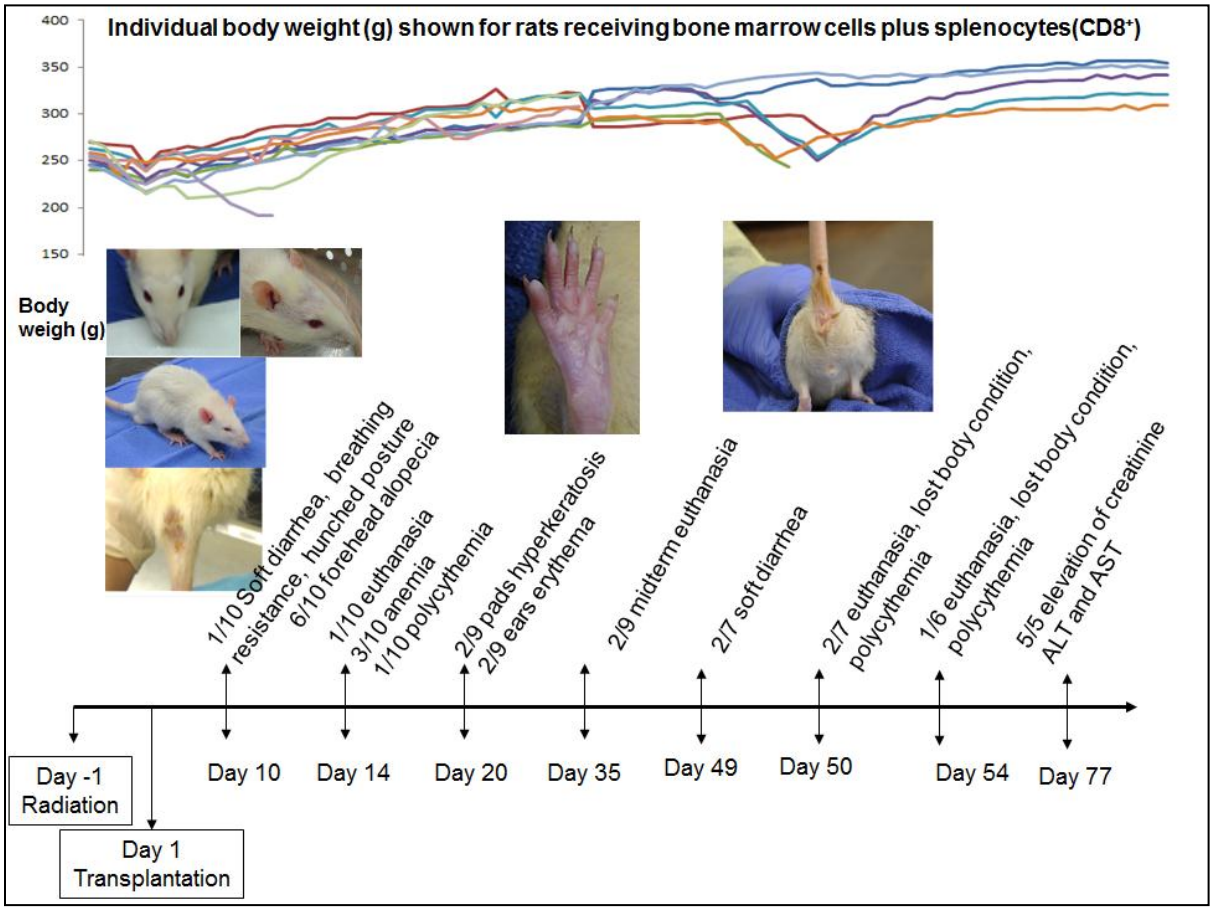

Figure 3.15. Graft versus host disease pathogenesis observed in rats receiving bone marrow cells plus splenocytes ($CD8^+$) after 10 Gy total body irradiation (GVHD group).

Clinical manifestations of GVHD began at day 10 post-transplantation with 2 out of 10 rats showing mild diarrhea at day 10 post-transplantation, and 6 out of 10 showing forehead alopecia.

3.7.3. Body weight

The growth curve of rats during the 77 days study of GVHD group, e.g., rats receiving bone marrow cells plus splenocytes ($CD8^+$) after 10 Gy total body irradiation, is showed in figure 3.16.

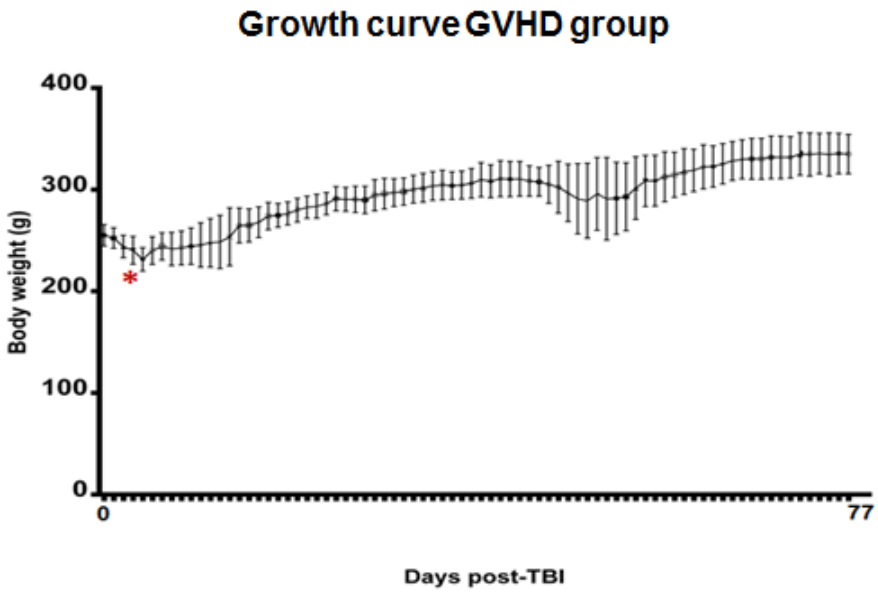

Figure 3.16. Growth of the graft versus host (GVHD) group, e.g., rats receiving bone marrow cells plus splenocytes ($CD8^+$) after 10 Gy total body irradiation. GVHD rats showed a drop in body weight at day 3 post-TBI, paired t-test showed significant differences, asterisk (*) t=2.719, df=18, p value<0.05. A second drop in body weight was observed at day 50, however this drop was not significant, paired t-test t= 1.394, df=12, p value<0.02. Data is expressed as mean ± SD.

3.7.4 Hematocrit

Mean values of hematocrit of the graft versus host (GVHD) group , e.g., rats receiving bone marrow cells plus splenocytes ($CD8^+$) after 10 Gy total body irradiation. GVHD rats are presented in figure 3.17.

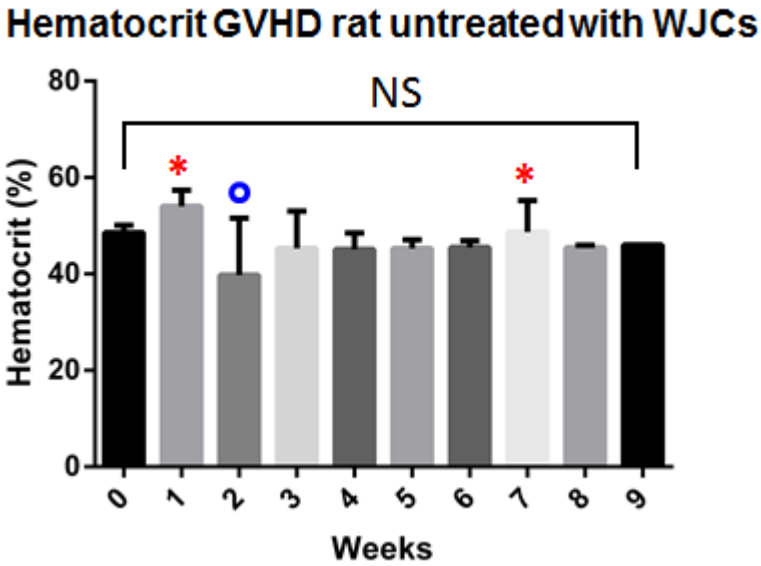

Figure 3.17. Hematocrit measured weekly during 77 days of study of the graft versus host (GVHD) group , e.g., rats receiving bone marrow cells plus splenocytes ($CD8^+$) after 10 Gy total body irradiation. GVHD rats showed. Asterisk (*****) indicates hemoconcentration. At week 1, 5 out 10 rats showed hemoconcentration. At week 2, co-existence of hemoconcentration in 2 rats and anemia in 2 more rats (**o**) was recorded. A third occurrence of hemoconcentration was observed in 1 out of 6 rats at week 7. At week 7, hematocrit was not significantly different from the initial pre-treatment value, paired t test t=0.05, p value>0.90

3.7.5. Survival

Estimates of survival of in the graft versus host disease (GVHD) only group (e.g., rats receiving bone marrow cells plus splenocytes ($CD8^+$) one day after lethal irradiation) were calculated by Kaplan-Meier method. Rats that develop GVHD and which died of transplant-related toxicities within 77 days were recorded and rats which were euthanized to evaluate GVHD histopathology at day 35 . Statistical comparison of these data was performed using the log-rank test. Results were considered statistically significant when p was ≤ 0.05.

Total mortality was observed in rats receiving lethal TBI only (e.g., 10 Gy irradiation only, the negative control group).. This was followed by rat receiving bone marrow cells and splenocytes $CD8^+$ together with WJCs 24 hours after lethal TBI (WJC day 0 group) which had 70% death. Rats receiving bone marrow cells and splenocytes $CD8^+$ 24 hours after lethal TBI and who were untreated with WJCs (e.g., the GHVD only group) had a mortality rate of 38% (see Table 3.5). Survival curve was produced using the Kaplan-Meier method is shown in fig. 3.18.

TABLE 3.5

Summary of the Number of Censored and Uncensored Values

Stratum TRT	Total	Died	Censored	Percent Censored	Mortality
1 GVHD only	10	3	2*	62.50	38%
2 Negative control	10	10	0	0.00	100%
3 Positive control	10	0	2*	100.00	0%
4 WJC day 2	10	0	2*	100.00	0%
5 WJC day 0	10	7	2*	30.00	77%
Total	44	20	24	54.24	

*2 rats from each group were euthanized at middle term study (day 35) to evaluate histopathological status (these animals were censored from the survival curve).

Kaplan Meier survival curve

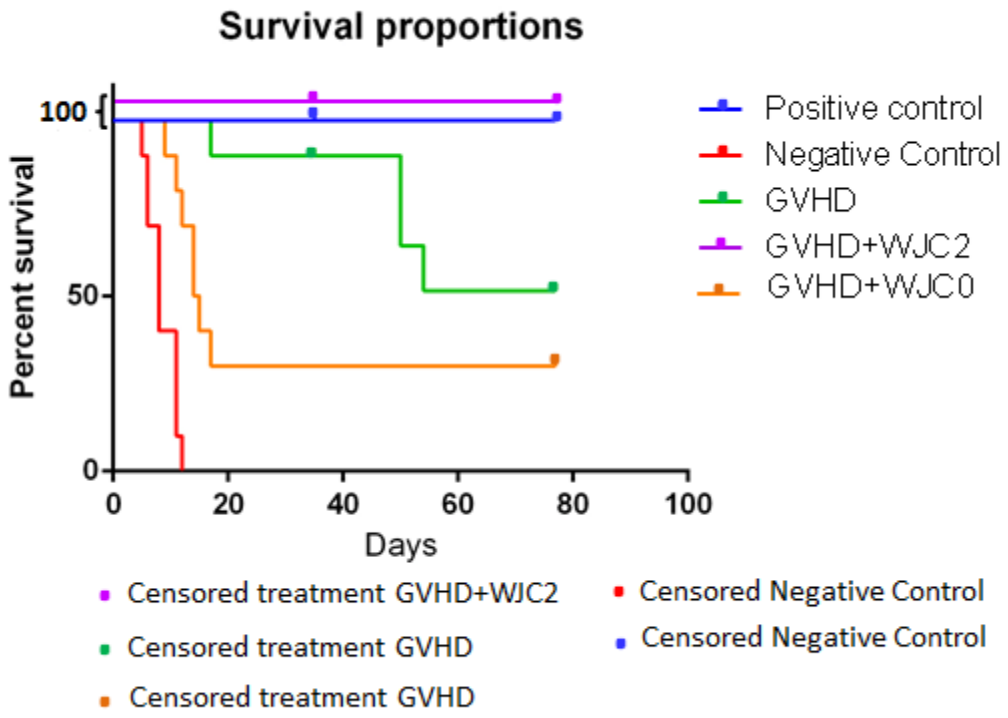

Figure 3.18. Kaplan Meier survival curve. Rats (n = 50) receiving lethal 10 Gy total of body irradiation without hematopoietic cell (e.g., the negative control group, n=10) all died by day 12 (red line). The graft versus host disease (GVHD) only group (e.g., rats receiving bone marrow

cells plus splenocytes ($CD8^+$) one day after lethal irradiation). (GVHD only group, n=10) had a 62% survival by the end of the study (green line). Rats which were lethally irradiation on day -1, and transplanted with bone marrow and splenocytes $CD8^+$ together 2×10^6 Wharton's jelly cells on day 0 (the WJC day 0 group, n=10) had a 38% survival rate by the end of the study (orange line). Rats which were lethal irradiation on day -1, transplanted with bone marrow and splenocytes $CD8^+$ day 0 and received 2×10^6 Wharton's jelly cells on day 2 (the WJC 2 group, n=10) had a 100% survival by the end of the study (purple line). Rats in the positive control group, (e.g., rats transplanted with T-cell depleted bone marrow one day after lethal irradiation (n=10) also had a 100% survival rate by the end of the study (blue line).Log-Rank (Mantel-Cox test) indicates the survival curves are significantly different (Chi square: 68.56; P value <0.0001).

3.7.6. Gross anatomy observations

Periosteal petechiae was observed in the frontal and temporal bones subjacent to skin alopecia after removing of skin in the GVHD only group rats after they were euthanized at different time post- transplantation (figure 3.18). At day 77 after bone marrow transplantation, I observed cecum vascular dilation and serosa thickening in large intestines as well as in peritoneum vascular dilation, and atelectasis in lungs (fig. 3.20).

Figure 3.19 Periosteal petechiae in the graft versus host disease (GVHD) only group (e.g., rats receiving bone marrow cells plus splenocytes ($CD8^+$) one day after lethal irradiation).Note, this rat was euthanized at day 35 post-transplantation.

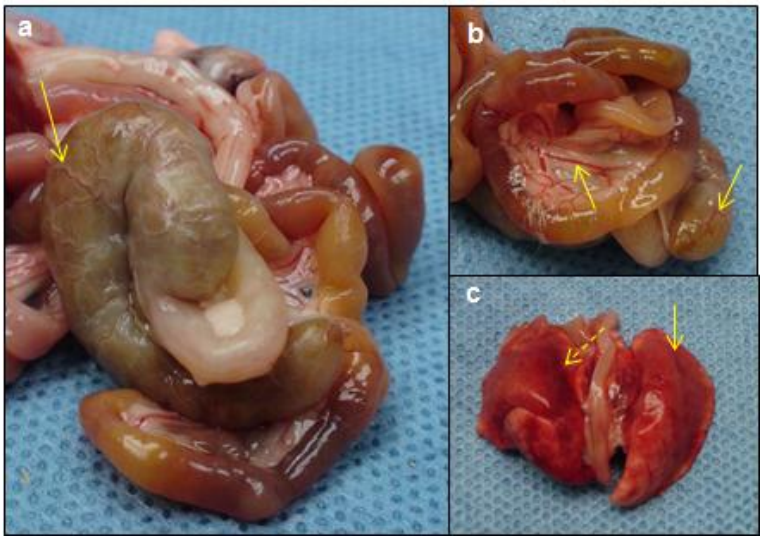

Figure 3.20 Macroscopic aspect of gastrointestinal tract and lung of the graft versus host disease (GVHD) only group (e.g., rats receiving bone marrow cells plus splenocytes ($CD8^+$) one day after lethal irradiation). The GVHD only group was not treated with WJCs. Tissue collected at the end of the survival period on day 77 post-transplantation is shown here. (a) Vascular dilation (yellow arrow) and serosa thickness was observed at cecum level. (b) Large intestine vascular dilation in observed in peritoneum and large intestine wall (yellow arrows). (c) Lungs show atelectasis left lobe (arrow) and in the cranial right lobe (dashed arrow).

3.7.7. Histopathology

The graft versus host disease (GVHD) only group (e.g., rats receiving bone marrow cells plus splenocytes ($CD8^+$) one day after lethal irradiation) was not treated with Wharton's jelly cells. In this group, mild to moderate tissue injuries was noted. In thin skin a reduction in epidermal cell layers (epidermis atrophy) and follicular drop-out were mostly observed. Hepatic centrolobulillar necropsy and periportal fibrosis was noted. In the intestines diffuse hemorrhage, histiocytosis and diffuse lymphocytic infiltration was observed. Abundant connective tissue was observed in samples taken from GVHD only group from target tissues skin, liver, small intestine, as well as from lung, and spleen (fig 3.39). Histopathological study revealed moderate pulmonary damage including peribronchiolar lymphocytic aggregation and mild interstitial mononuclear cells infiltration from tissues collected on day 77 (at the end of the study).

3.7.8. Mast cell distribution

In the GVHD only group at day 35 after transplantation, I observed a pattern similar that in the negative control group rats: masts cell were not detected in lung or small intestine mucosa.

However at day 77, mast cells were detected in the small intestine mucosa, in both loose connective tissue (lamina propia) and epithelial lining (see figure 3.21). Mast cells containing prominent granules were observed with H&E and Astra blue staining. Stains performed in serial sections from formalin-fixed and paraffin-embedded cut at 4 micrometers thicknesses are shown figure 3.21.

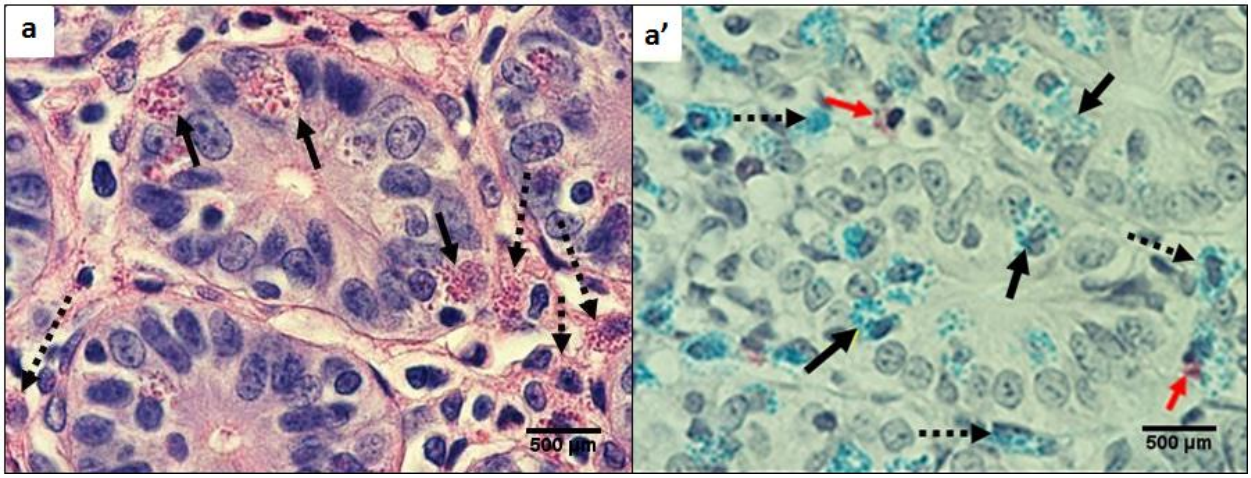

Figure 3.21. Mast cell staining in the graft versus host disease (GVHD) only group (e.g., rats receiving bone marrow cells plus splenocytes ($CD8^+$) one day after lethal irradiation). (a) At day 77 after transplantation, mast cells (which are present within the small intestine lamina propia connective tissue of normal healthy animals) were observed inside the small intestine glandular epithelium in the GVHD only group. Mast cells with globular morphology and acidophilic intracytoplasmic granules were observed in both interstitial connective tissue (dashed arrows) and intraepithelial tissue (solid arrow). H&E staining of small intestine. (a') In an adjacent serial section, combined staining of eosinophils and mast cells confirmed the identification of mast cells (black arrow). Note that mast cells showed affinity by Astra blue dye (black arrows), while eosinophils showed affinity for Vital red dye (red arrows).Objective magnification 100X. Calibration bar is 500 micrometers in both figures.

Mast cell distribution in lung and lymph nodes at day 77 post-transplantation in the GVHD group is presented in figure 3.22.

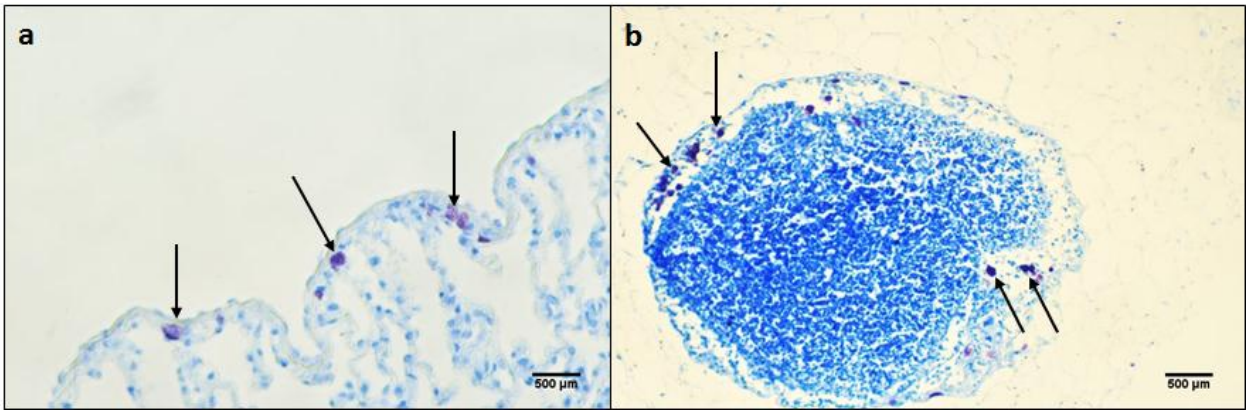

Figure 3.22. Mast cell detection by Toluidine blue in lung (a) and lymph node (b) at day 77 post-transplantation in the graft versus host disease (GVHD) only group (e.g., rats receiving bone marrow cells plus splenocytes ($CD8^+$) one day after lethal irradiation). Mast cells were identified by metachromatic stain of granular content (arrows) in (a) sub-pleural lung zone, objective magnification 20X or (b) lymph node, objective magnification 4X. Note the scare number of mast cells within sub-capsular lymphatic sinus. Mast cells stain purple and non-metachromatic tissues stain blue. Calibration bar is 500 micrometers.

3.7.9. Immunohistochemistry complement system cascade activation

Complement deposition was observed in the GVHD group in a rat that died on day 17 post-transplantation. Complement c3a was observed in the proximal and distal tubule of the kidney, and in Henley's loop (e.g., the thin segment of nephron) (fig.3.23). Complement deposition was also detected in around small intestine glands, and in stomach mucosa (epithelium).

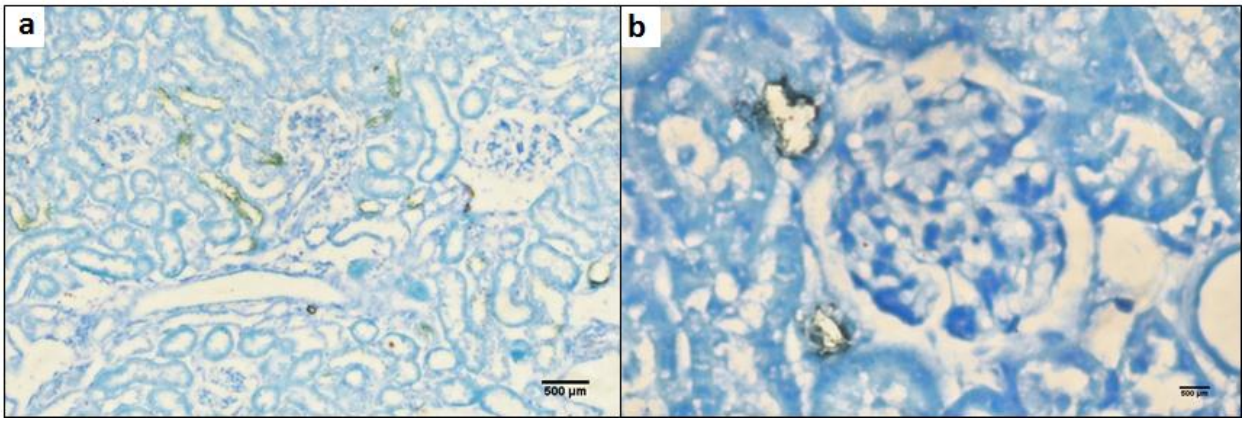

Figure 3.23. Activated complement deposition in the kidney in the graft versus host disease (GVHD) only group (e.g., rats receiving bone marrow cells plus splenocytes ($CD8^+$) after lethal irradiation). Deposition of complement (C3a) in tubular components of nephrons was observed in tissue samples from the GVHD group rat in tissues collected on day 17 post-transplantation.

Positive stain for C3a complement is brown and hematoxylin counterstain is blue.a) Kidney cortex complement C3a deposition was observed in tubular components of nephron, objective magnification 10.b) Complement C3a deposits were found along the luminal side of distal tubule Calibration bars is 500 micrometers.

3.7.10 Elafin: Biomarker of skin GVHD

Elafin, also known as peptidase inhibitor-3, skin-derived anti-leukoproteinase or trappin-2, is a protein overexpressed in patients suffering skin GVHD [55]. I found Elafin in GVHD target organs skin, liver and intestine in the graft versus host disease (GVHD) only group (e.g., rats receiving bone marrow cells plus splenocytes ($CD8^+$) after lethal irradiation). Representative results are presented in figure 3.24

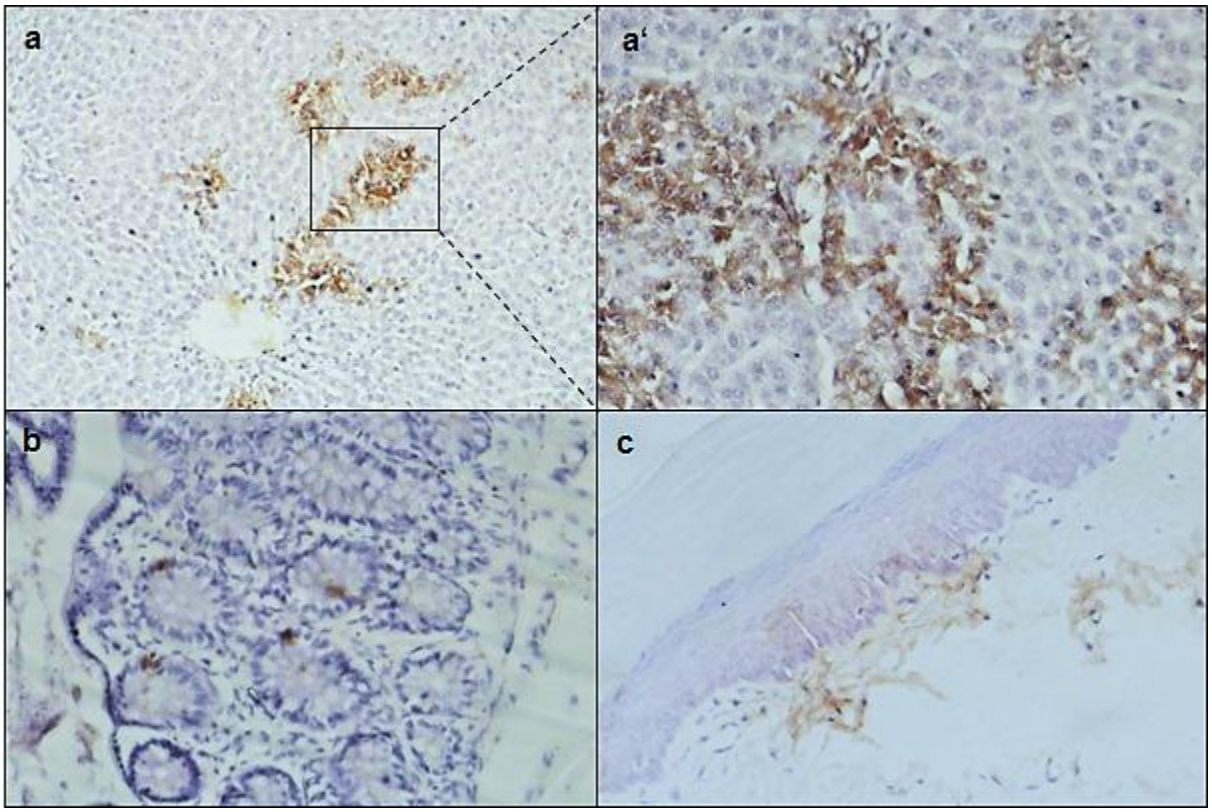

Figure 3.24. Elafin staining in the graft versus host disease (GVHD) only group (e.g., rats receiving bone marrow cells plus splenocytes ($CD8^+$) one day after lethal irradiation) at day 77 post-transplantation. (a+a') Elafin immunoreactivity was observed in liver. b) Few positively stained cells were observed inside large intestine epithelial glandular cells. c) In contrast, no Elafin deposition was found in thin skin samples. Positively stained Elafin is brown and Mayer modified hematoxylin counterstain is purple.

3.8. Adoptive transfer of rat WJCs to prevent GVHD

3.8.1. Allogeneic hematopoietic cell and $CD8^+$ splenocytes transplantation together with WJCs given at day 0 (WJC0).

A summary of the pathogenesis observed in GVHD rats treated with WJCs on day 0 (WJC 0) is presented in figure 3.25. Clinical evaluation and histopathologic study of 7 out of 10 rats dying before day 17 post-transplantation indicated that these animals had engraftment failure (defined as failure to restore the blood cell production after hematopoietic cell transplantation) as a complication after hematopoietic cells transplantation. Histopathological evaluation showed bacterial sepsis in 3 out of these 7 rats in heart, liver and kidneys (fig.3.29).

Five out of 10 the WJC0 group showed symptomatology of acute radiation syndrome including aplastic anemia and weight lost after day 17 post-transplantation. Aplastic anemia was defined as reduction of microhematocrit to less than 30%. A post-mortem validation was done by evaluating the cellularity of bone marrow and spleen parenchyma. WJC 0 group rats (the three rats which survived to day 77) showed mild nose alopecia at day 31 (fig.3.25). Although initially their hematocrit dropped at week 2, by week 6 it reached the pretreatment value (fig.3.27).

WJC0 rats that survived to day 77 may have had lower hepatic and renal damage compared to the GHVD only group as indicated by normal values of serum levels of ALT 38±6 U/L, AST 89±20U/L, creatinine 0.37±0.06 U/L and bilirubin total 0.13±0.06 UL (Table 3.1).

3.5.2. GVHD Pathogenesis.

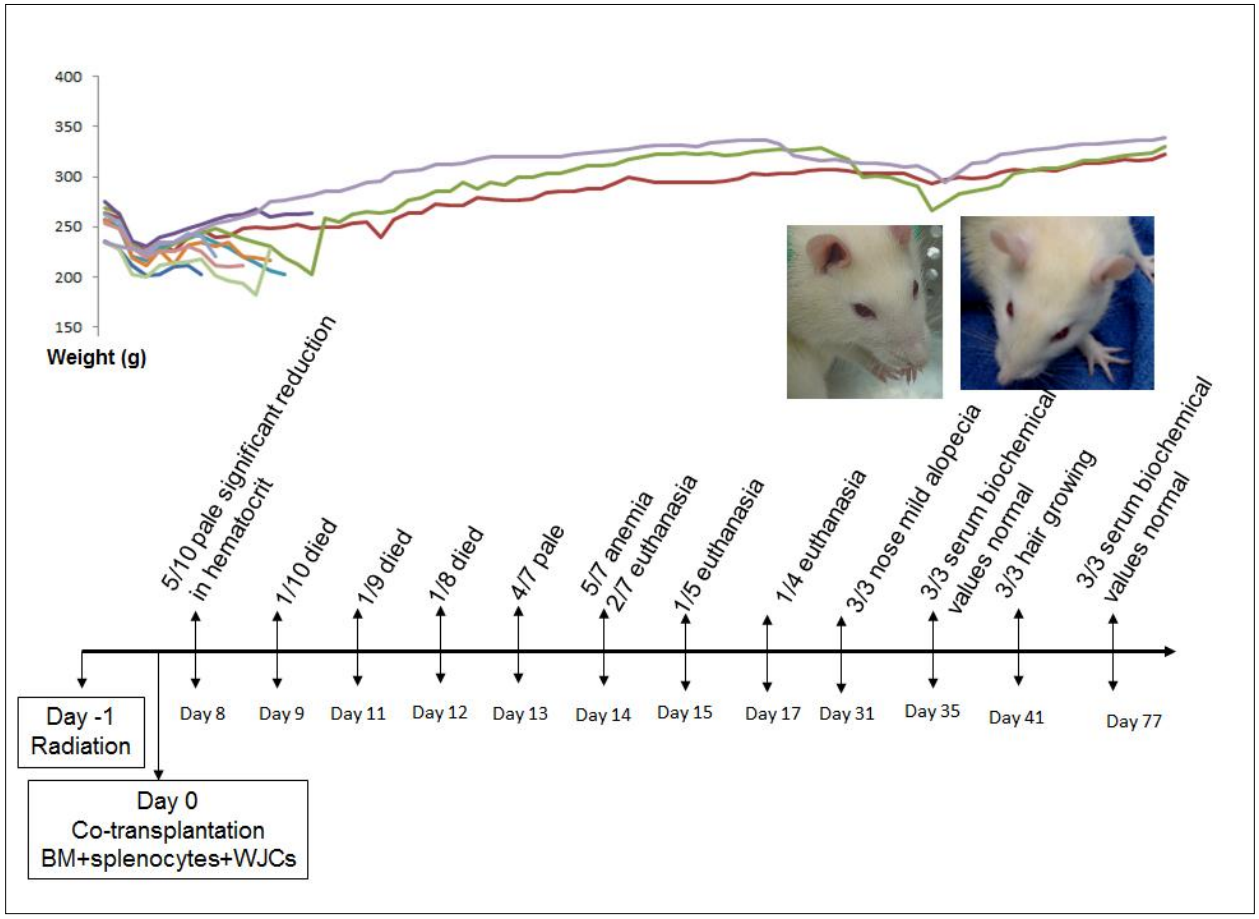

Figure 3.25. Clinical manifestations of graft versus host disease rats which were treated with Wharton's jelly cells, bone marrow and splenocytes 24 hour after lethal 10 Gy TBI (WJC day 0 group).

3.8.3. Body weight

The growth curve of GVHD rats treated with WJCs on day 0 is presented in figure 3.26. A drop in body weight was noted at day 3. At day 4, rats resumed a positive growth curve and they continued to gain weight until the end of the study (day 77) (fig.3.26)

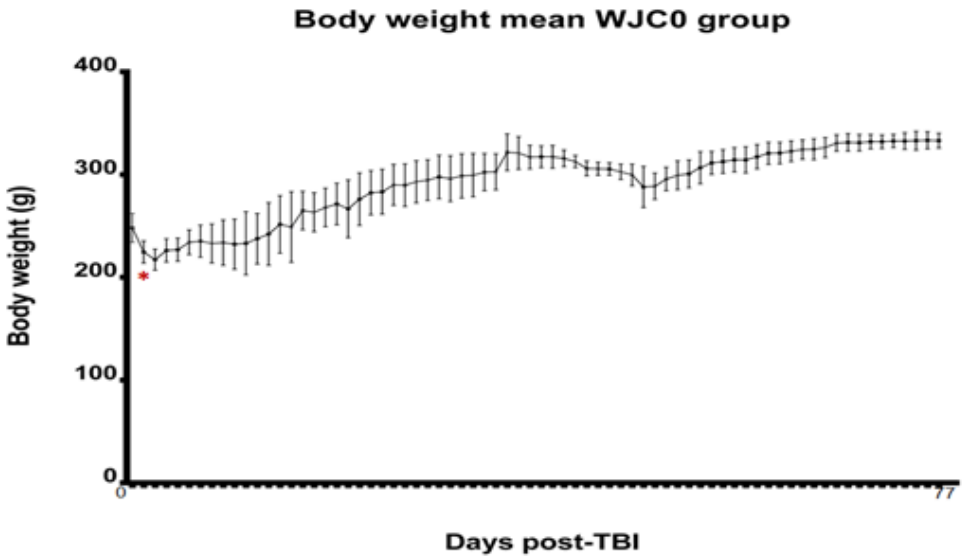

Figure 3.26. Body weight in the Wharton's jelly cells on day 0 (WJC 0) group (e.g., rats which received bone marrow cells plus splenocytes ($CD8^+$) 24 hrs after 10 Gy total body irradiation to induce graft versus host disease and were treated by Wharton's jelly cells on day 0). Rats from WJC 0 group showed a significant body weight loss on day 3 post-TBI asterisk (*). t=5.098, df=18, p value<0.01.

3.8.4 Hematocrit.

The hematocrit of the WJC 0 group is presented in figure 3.27

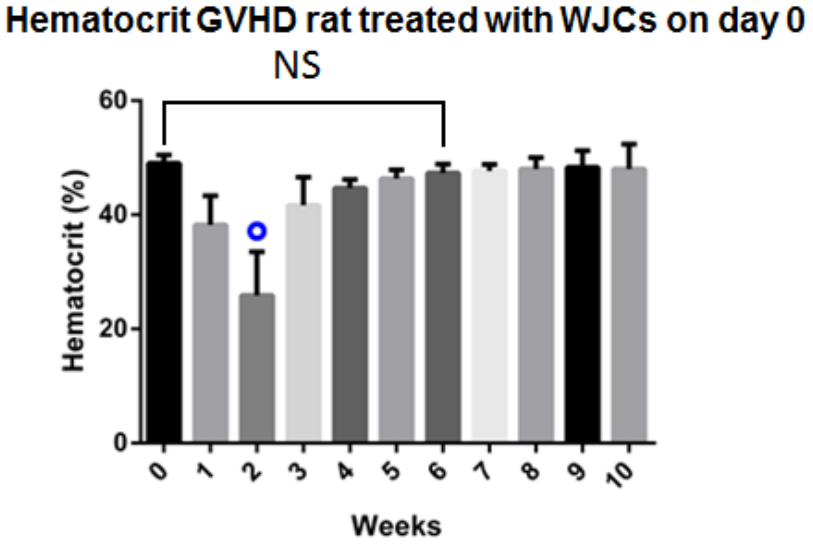

Figure 3.27. Effect of Wharton's jelly cells given on day 0 (WJC day 0 group) on graft versus host disease (GVHD) on weekly hematocrit. In the second week, the hematocrit was 26 ±8%

which indicated anemia (O). After the third week, the hematocrit of surviving rats (n=3) had increased and was reaching the pre-treatment value at week 6.

3.8.5. Gross anatomy observations

Five rats in the WJCs day 0 group died before day 17. These animals showed edema and focal hemorrhage in lungs. In addition, kidney abscesses (fig.3.28), pericarditis, pneumonia and pleural effusion were observed in 3 out 7 rats. Splenic hypoplasia was observed in all rats in the WJC day 0 group after euthanasia.

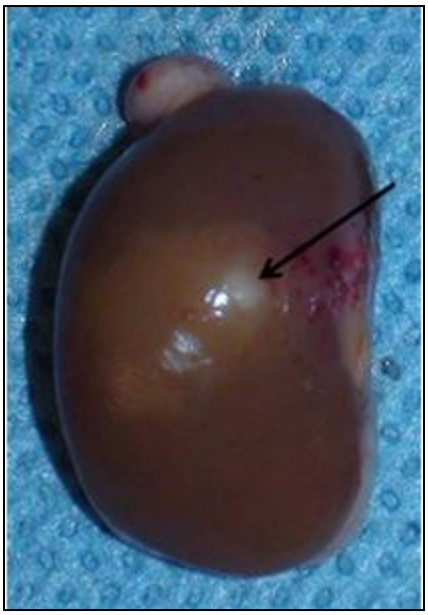

Figure 3.28 Kidney abscesses was observed in 3 out of 7 surviving rats who died before da 17.Arrow indicates gross anatomy appearance of kidney sub-capsular abscesses.

Two GVHD rats treated on day 0 with WJCs and surviving until day 77 showed lung edema when they were euthanized (fig. 3.29). This was similar to what was observed in the lungs of the GVHD only group (see figure 3.20).

Figure 3.29. Effect of Wharton's jelly cells given on day 0 on graft versus host disease gross pathology. Gross aspects of gastrointestinal tract, kidneys and lungs of WJC day 0 rats at day 77 post-transplantation. (a) No gross pathologies were observed in gastrointestinal tract, arrow indicates follicular hyperplasia in spleen. (b) Higher magnification of area indicated by arrow in (a) is shown in (b). Spleen showing reactive follicular hyperplasia (arrow). (c) Lung edema was observed in 1 out 3 WJC day 0 rats which survived 77 days.

3.8.6. Histopathology

The effect of Wharton's jelly cells given on day zero on GVHD (WJC day 0 group) on histopathology was evaluated in the 3 out of the 10 rats which survived till day 77 after transplantation. These rats showed a normal histology in most target tissues. In two rats, mild pulmonary intra-alveolar histiocytosis and mild peribronchiolar lymphocytic inflammation were found. In contrast, 3 out of the 7 rats that died at or before day 17 after bone marrow transplantation, presented with bacterial sepsis in lung, liver (fig. 3.30), heart, intestine and kidney. The same rats showed mild centrolobulillar necrosis in liver. A normal collagen network in tissues from the WJC day 0 group was noted from animals which died before day 17 after transplantation and from animals which died at the end point (day 77 after transplantation). Collagen deposition is shown in figure 3.39.

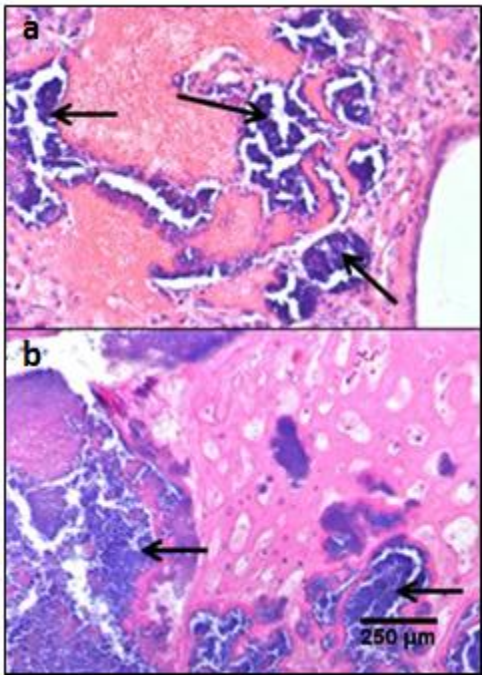

Figure 3.30. Bacterial sepsis was observed in WJC day 0 group rats that died on or before day 17 after transplantation. Bacteria accumulation (arrows) and abscess were observed in lung (a) and liver (b). Hematoxylin and eosin stain. Calibration bar is 250 micrometers.

3.8.6.1 Mast cells distribution

Mast cell distribution in lung and lymph nodes of WJC day 0 group (e.g., rats transplanted with bone marrow cells and $CD8^+$ splenocytes and treated with WJCs on day 0) at day 77 post-transplantation is presented in figure 3.31. Before day 17, mast cells were not detected with metachromatic or Astra blue stains (data not shown). In contrast, at day 77 post-transplantation, mast cells were detected in lung sub-pleural and interstitial zones, dermis, small intestine lamina propia and lymph nodes in the WJC day 0 group (fig 3.31).

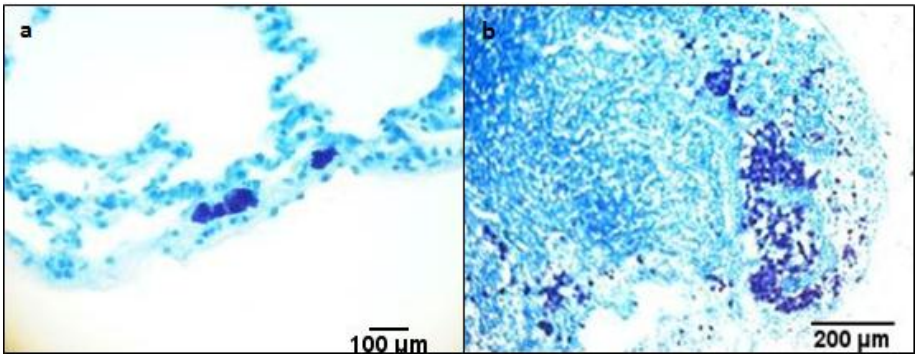

Figure 3.31. Mast cell detection by Toluidine blue in lung and lymph node at day 77 post-transplantation in rats transplanted with bone marrow cells and $CD8^+$ splenocytes and treated with WJCs on day 0 (WJC day 0 group). Mast cells were identified by metachromatic stain of granular content. (a) Sub-pleural lung zone and (b) Lymph node showing mast cells located mainly in outer parenchyma or cortex. Mast cells stain purple and non-metachromatic tissues stain blue. Calibration bar is 100 micrometers in panel (a) and 200 micrometers in panel (b).

3.9. WJCs administered at day 2 post-transplantation attenuated acute radiation toxicity symptomatology

Rats transplanted with bone marrow cells and $CD8^+$ splenocytes to induce graft versus host disease (GVHD) and treated with WJCs on day 2 are called the WJC day 2 group below. In contrast to all other experimental groups, the WJC day 2 group increased their body weight after lethal 10 Gy TBI followed by hematopoietic cell transplantation (fig.3.33). Hematocrit was measured weekly in the WJC day 2 group. As shown in figure 3.34, in week 2 after transplantation, there was a significant reduction in hematocrit, which fell from the pretreatment mean of 51 ±2 % to 48 ±2%. Despite this slight and significant decrease in hematocrit, the hematocrit value remained within the normal reference range (table 3.10).

In the WJC day 2 group, dermatologic and gastrointestinal GVHD-associated symptomatology was observed in 1 out 10 rats (see fig.3.32). On day 35 after transplantation, two rats were randomly selected for euthanasia to evaluate GVHD via histopathology and serum biochemistry. Serum biochemistry measured at day 35 after transplantation revealed normal biochemistry values in all 10 rats (Table 3.10).

3.9.1. Pathogenesis observed in the WJC day 2 group.

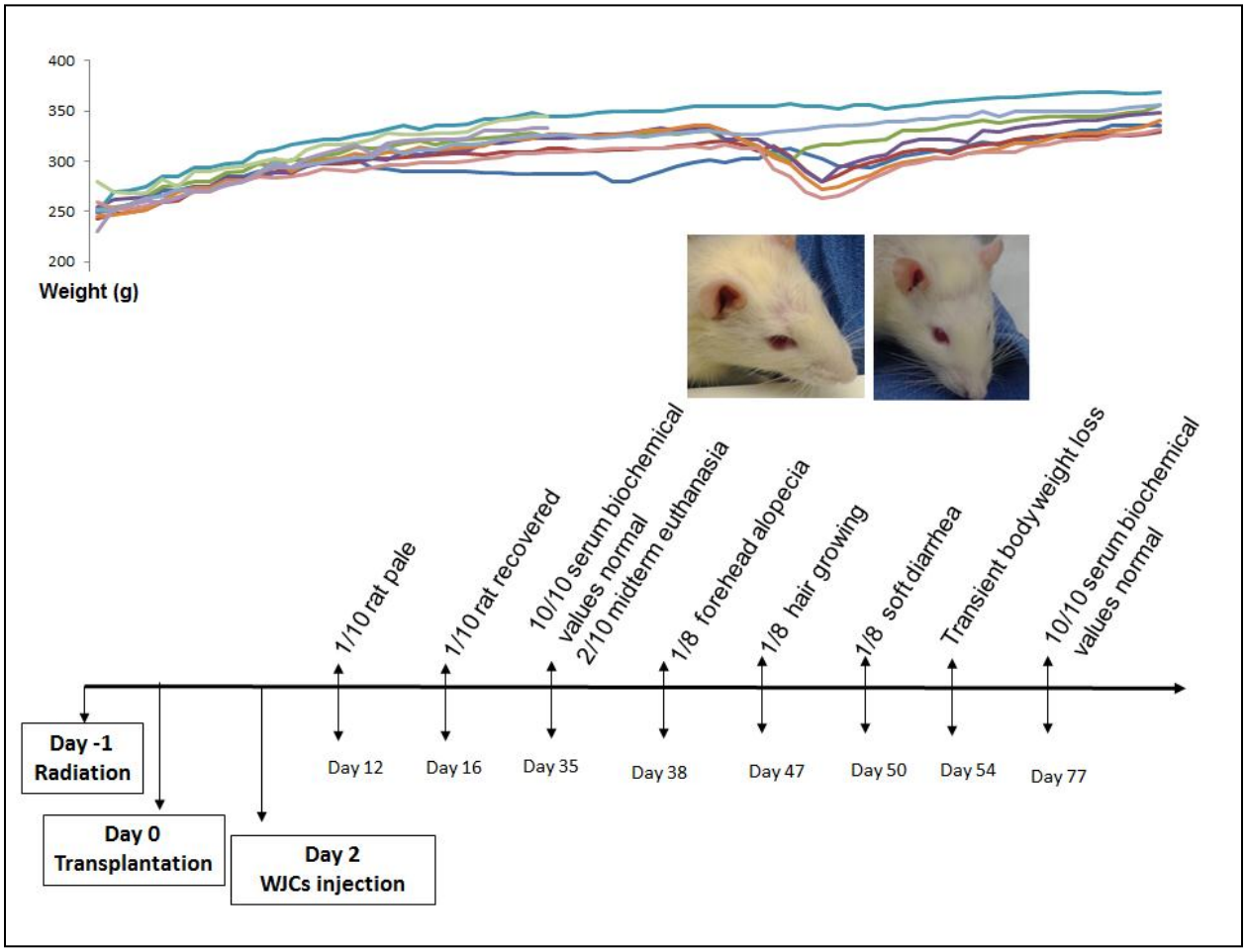

Figure 3.32 Clinical manifestations of graft versus host disease rats which were treated with Wharton's jelly cells, bone marrow and splenocytes 48 hour after lethal 10 Gy TBI (WJC day 2 group).Clinical manifestation of GVHD was observed in 1 out of 10 rats on days 12-16 after transplantation. Alopecia was detected at day 38 after transplantation in 1 out of 8 rats. By day 47 after transplantation, hair growth was observed and by 50 day after transplantation alopecia was almost undetectable. At day 50 after transplantation, diarrhea was detected in the same rat suffering alopecia. Four rats also showed transient body weight loss around days 47-50 after transplantation.

3.9.2. Body weight

The growth curve of the WJCs on day 2 group is presented in figure 3.33. These rats showed a positive growth curve following TBI. Around days 47-50, body average body weight dropped because 4 rats showed a transient weight loss. On day 77 only 8 rats were surviving since 2 were euthanized on day 35.

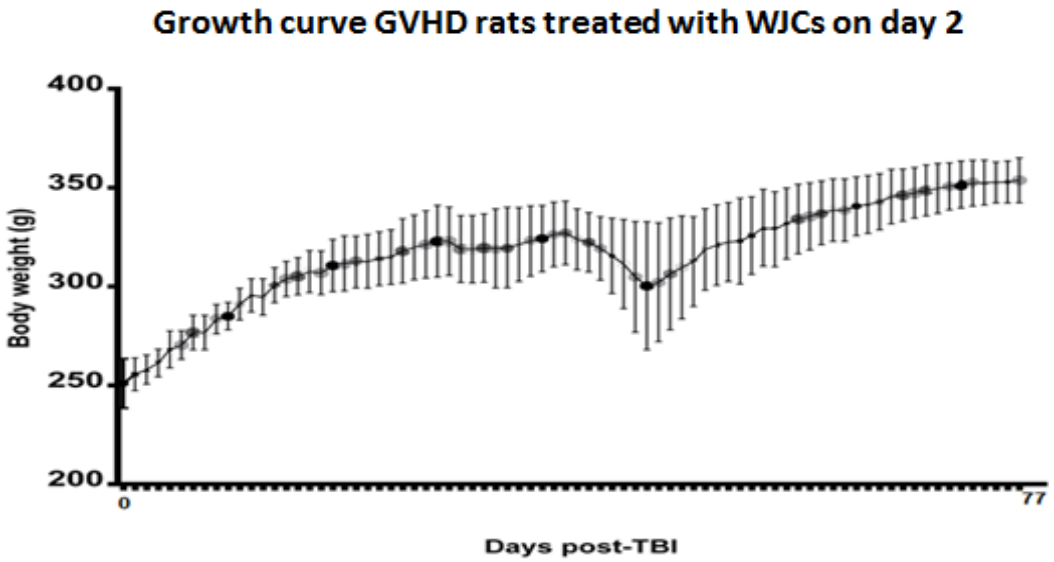

Figure 3.33. Growth curve of graft versus host disease rats which were treated with Wharton's jelly cells, bone marrow and splenocytes 48 hour after lethal 10 Gy TBI (WJC day 2 group). following graft versus host disease (GVHD) induction in rats transplanted with bone marrow cells and $CD8^+$ splenocytes on day 0 and treated with Wharton's jelly cells (WJCs) on day 2 after total body irradiation (called the WJC day 2 group). These rats showed a positive growth curve until days 47- 50 after transplantation, when body weight transiently dropped due to 4 rats transiently losing body weight. One of these four rats showed other GVHD clinical signs such as slight alopecia and diarrhea.

3.9.3. Hematocrit

Hematocrit measured weekly in WJC day 2 group is presented in figure 3.34. In these rats anemia was not observed. However, a reduction in hematocrit was observed at week 2 after transplantation as seen in other GVHD groups (see GVHD only group figure 3.17 on page 65, see WJC day 0 group figure 3.27 on page 76) and the positive control group which received T-cell depleted bone marrow transplantation (see figure 3.12 on page 60).

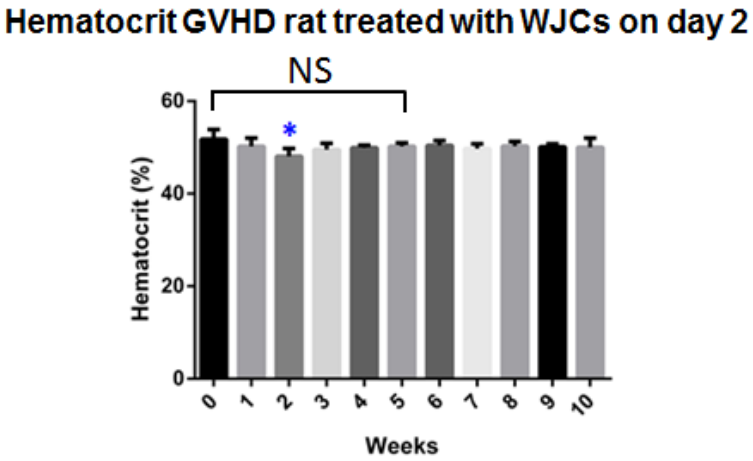

Figure 3.34. Hematocrit of graft versus host disease rats which were treated with Wharton's jelly cells, bone marrow and splenocytes 48 hour after lethal 10 Gy TBI (WJC day 2 group). Asterisk (*) indicates a statistically significant reduction in hematocrit 2 weeks after transplantation t=0.720, p value<0.02. After week 2, hematocrit increased and returned to pre-treatment value by week 5, t=1.878, p value>0.07.

3.9.4. Gross anatomy observations

Viscera macroscopic observation of graft versus host disease rats which were treated with Wharton's jelly cells, bone marrow and splenocytes 48 hour after lethal 10 Gy TBI (WJC day 2 group); indicates no gross abnormalities in rats euthanized at day 35 or 77 post-transplantation (figure 3.35).

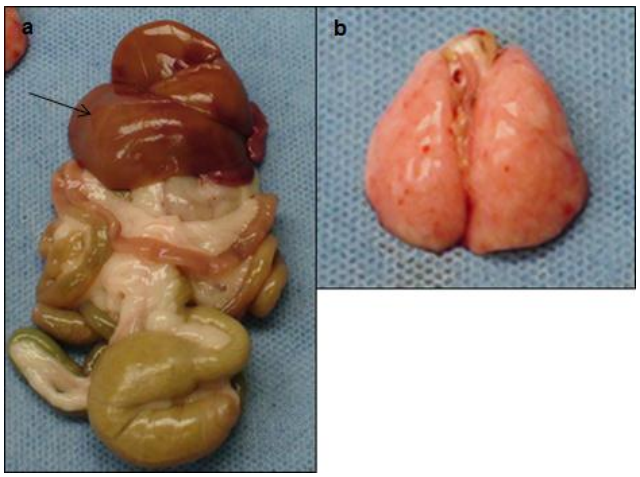

Figure 3.35. Macroscopic aspect of gastrointestinal tract and lungs rats transplanted with bone marrow cells and $CD8^+$ splenocytes and treated with treated with Wharton's jelly cells (WJCs) on day 2. No discernible abnormalities were observed in (a) gastrointestinal tract, liver (arrow) or (b) lungs.

3.9.5. Histopathology

In GVHD rats treated with WJCs on day 2, no histopathological damage was observed in rats euthanized at day 35 or 77 post-transplantation..

3.9.5.1. Mast cells distribution

Evaluation of mast cells distribution in the WJC day 2 group at day 35 post-transplantation by Touidine blue stain revealed few mast cells containing metachromatic granules. However, at small intestine level mast cells were observed within the lamina propia containing only orthochromatic granules (figure 3.36).

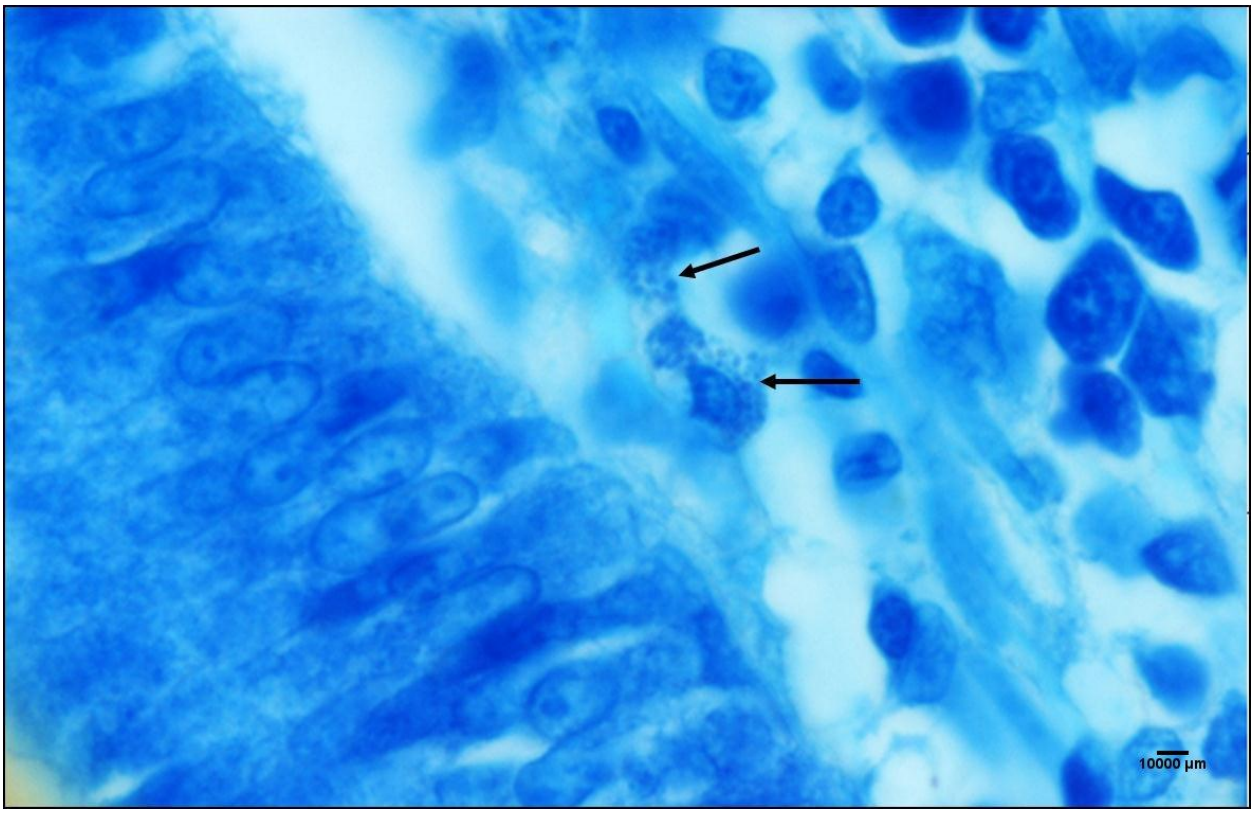

Figure 3.36. Effect of Wharton's jelly cells given on day 2 on graft versus host disease in small intestine mucosa. Small intestine lamina propia day 35 post-transplantation. Mast cells with orthochromatic granules were observed within the lamina propia connective tissue. Toluidine blue stain. Calibration bar is 1000 micrometers.

At day 77 post-transplantation, many mast cells were detected in all studied tissues. Similar to what I observed in the WJC day 0 group, mast cells whose cytoplasm was occupied by metachromatic granules were evident in lymph nodes (fig. 3.37)

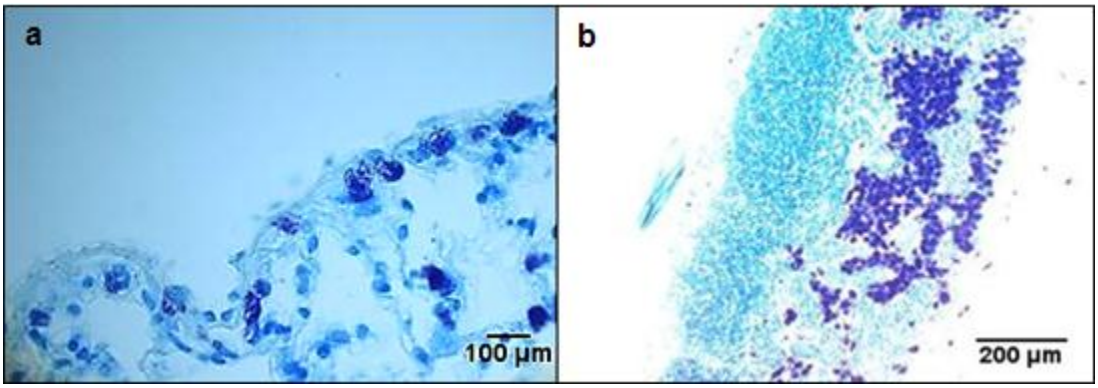

Figure 3.37. Effect of Wharton's jelly cells given on day 2 on graft versus host disease on mast cell number and distribution. Mast cells were observed in lungs and lymph nodes at day 77 post-transplantation in graft versus host disease rats treated with Wharton's jelly cells on day 2. Mast cells were identified by metachromatic stain of granular content following Toluidine blue staining. Both (a) Sub-pleural lung zone and (b) Lymph node had many mast cells located mainly in lymph node inner parenchyma or medulla. Mast cells stain purple and non-metachromatic tissues stain blue. Calibration bar is 100 micrometers in a and 200 micrometers in b.

3.9.5.2 Collagen deposition and epidermis thickness

Collagen deposition is usually a marker of chronic GVHD. Here, I studied collagen deposition in my rat model of GVHD by Masson's trichrome staining. Qualitative comparison of collagen network in skin, liver, small intestine, lung and spleen was performed (fig 3.38).
At day 17 an increase in collagen deposition was observed in GVHD only group in liver, small intestine sub-mucosa, lung and spleen (see arrows in figure 3.38).

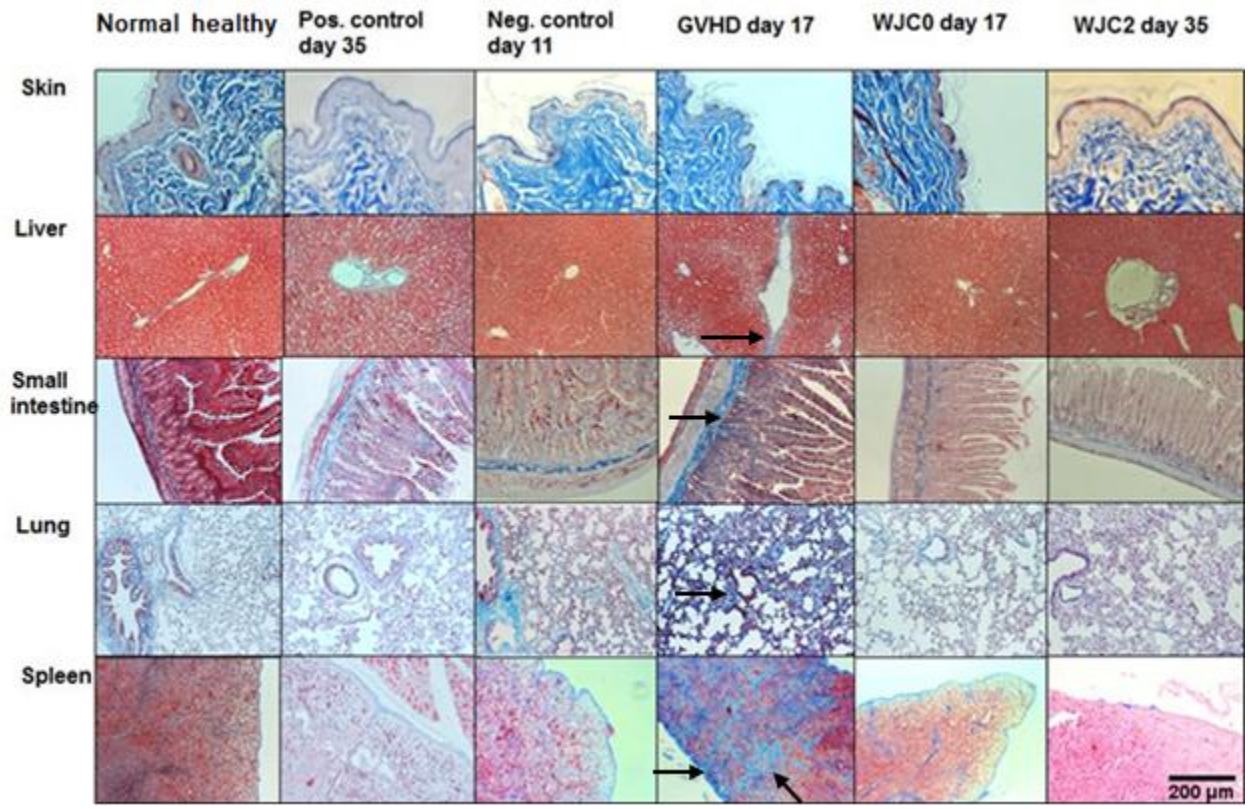

Figure 3.38. Collagen deposition in graft versus host disease (GVHD) target tissues of control and experimental groups. Note that abnormal collagen deposition was observed in GVHD only group at day 17 post- transplantation (indicated by arrows). Unusual collagen deposition was not found in any other group. Masson's trichrome stain. Calibration bar is 200 micrometers.

3.9.5.3. Hematopoietic compartment reconstitution

Tissue samples from hematopoietic organs such as spleen and bone marrow were evaluated for hematopoietic reconstitution. Figures 3.39 and 3.40 show spleen and bone marrow from the experimental and control groups.

3.9.5.4 WJCs day 2 group showed improved splenic T cell-dependent periarteriolar lymphoid sheath (PALS) and mantle repopulation at day 35 post-transplantation.

Cellular composition of splenic PALS, known to be constituted mainly z of T cells, and the follicular mantle zone or corona were studied. As shown in figure 3.39, PALS reconstitution was observed only in GVHD rats receiving WJCs at day 2. At 11 days post-irradiation, rats which were lethally irradiated and not transplanted (negative control) showed a hypoplasia of

spleen parenchyma. At day 17 post-transplantation, in GVHD rats receiving bone marrow and splenocytes $CD8^+$ and untreated with WJCs (GVHD only group), as well as in lethally irradiated rats receiving bone marrow and splenocytes $CD8^+$ treated with WJCs on day 0 (WJC day 0 group), numerous cells were found in mantle zone. In contrast, PALS seems to lack cells and periarteriolar zone (e.g., it looks clear). Similarly, at day 35 post-transplantation lethally irradiate rats which received T-cell depleted bone marrow (positive control group) had a reduction in cell number in both PALS level, as well as the mantle zone (fig 3.39).

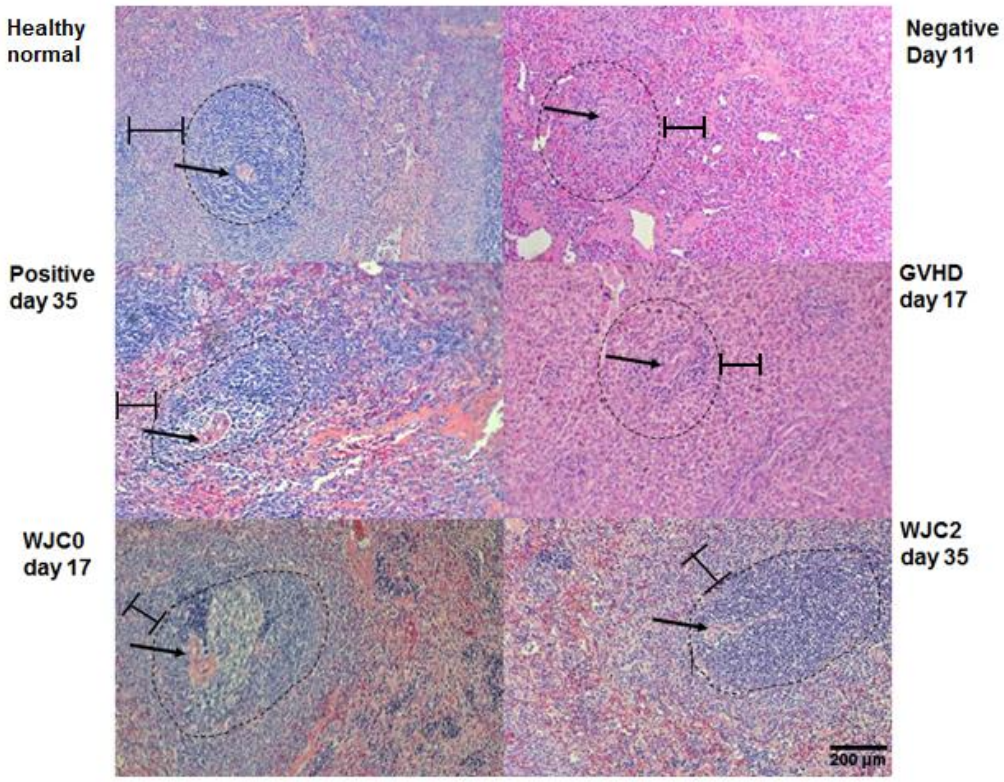

Figure 3.39. Cellularity of spleen white pulp. Arrows indicate the central arteriole of spleen white pulp.Whisker denotes the mantle zone's thickness. Dashed ring delimits splenic follicles. Note that on day 35 after transplantation, the T cell-dependent periarteriolar lymphoid sheath (PALS) was repopulated in lethally irradiated rats receiving bone marrow and splenocytes $CD8^+$ and treated with Wharton's jelly cells on day 2 after transplantation (WJC day 2 group), and to a lesser extent the positive control group (e.g., lethally irradiated and transplanted with T-cell depleted bone marrow). Hematoxylin and eosin. Objective magnification 10X.

3.9.5.4 Rat lethally irradiated on day -1 and which received bone marrow and CD8+ T cells on day 0 and given WJCs on day 0 and day 2 showed improved repopulation of bone marrow parenchyma at 77 days post-transplantation.

To establish the effect of WJCs on bone marrow reconstitution after lethal TBI on day -1 followed by allogeneic hematopoietic cell transplantation and CD8+ splenocytes on day 0, hematoxylin and eosin sections were evaluated from lethally irradiated rats (negative control group on day 11 post-irradiation), lethally irradiate rats transplanted with T-cell depleted bone marrow and untreated with WJCs (positive control group), lethally irradiated rats transplanted with bone marrow and splenocytes $CD8^+$ and untreated with WJCs (GVHD only group), lethally irradiate rats treated with bone marrow and splenocytes $CD8^+$ which received WJCs on day 0 (WJC day 0 group) and which received WJCs on day 2 (WJC day 2 group). Bone marrow samples from healthy normal rats were used as an untreated control (Untreated). Results from cellular composition of bone marrow parenchyma are presented in figure 3.40.

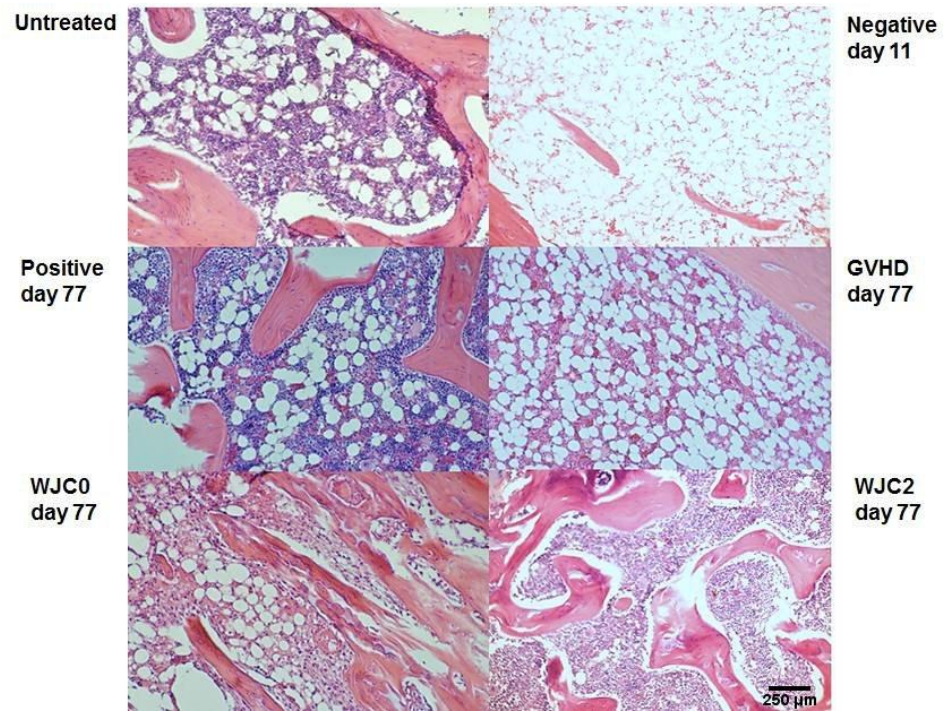

Figure 3.40. Bone marrow parenchyma compartment compared between positive control, negative control and untreated groups compared with various experimental groups (lethally irradiated rats that received bone marrow and CD8+ splenocytes on day 0 and then given Wharton's jelly cells) at 77 days post-transplantation. Bone marrow from lethally irradiated rats who were not transplanted (negative control day 11 post-irradiation) shows a cellular appearance. In contrast, rats transplanted with T-cell depleted bone marrow and who were untreated with WJCs (positive control group) and healthy rats (untreated group) show a highly populated bone marrow parenchyma. The graft versus host disease (GVHD) only group showed a decreased cellularity of their bone marrow parenchymal compared to rats who were also

induced to have GVHD and were treated with WJCs on day 0 (WJC day 0 group) and treated with WJCs on day 2 (WJC day 2 group). Note the fat vacuoles in the bone marrow cavity of untreated, negative control rats, GVHD only, positive control group and the WJC day 0 group. Note that the highest cellularity and the fewest fat vacuoles are found in the WJC day 2 group. Reconstitution of parenchymal components is observed in rats receiving Wharton's jelly cells on day 0 and day 2, as well as in positive control rats. Hematoxylin and eosin. Calibration bar is 250 micrometers.

3.9.5.5. Neutrophil recovery

At day 7 post-radiation, the cell count for leukocytes in peripheral blood was negligible in lethally irradiated rats who were not transplanted (negative control). In animals receiving hematopoietic cells transplantation, neutrophil counts subsequently increase with the time following irradiation and bone marrow transplantation (see figure 3.41). The percentage of neutrophil recovery was determined using the following formula: (number of cells at time point/number of cells at baseline) × 100.

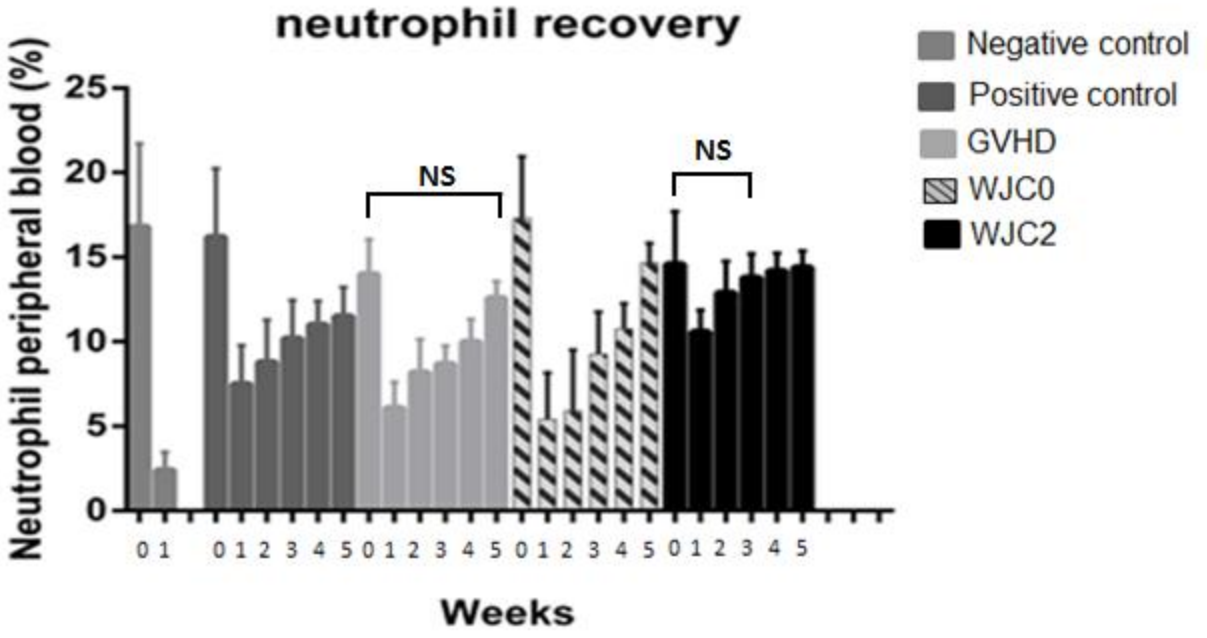

Figure 3.41. Neutrophil recovery in lethally irradiated rats who were not transplanted (negative control group, baseline and day 11 post-irradiation, left-most bars), lethally irradiate rats who were transplanted with T-cell depleted bone marrow and untreated with WJCs (positive control

group, baseline and evaluated weekly after transplantation), lethally irradiated rats who were transplanted with bone marrow and splenocytes $CD8^+$ to induce graft versus host disease (GVHD) and who were untreated with WJCs (GVHD only group), lethally irradiated rats who were transplanted with bone marrow and splenocytes $CD8^+$ to induced GVHD and who were treated with WJCs on day 0 (WJC day 0 group), and lethally irradiated rats who were transplanted with bone marrow and splenocytes $CD8^+$ to induce GVHD and who were treated with WJCs on day 2 (WJC day 2 group). I noted that the WJC day 2 group showed the most rapid neutrophil recovery, followed by the GVHD only group. The positive control group and the WJC day 0 group did not show complete neutrophil recovery over the 77 day survival period. Differential cells counts were performed on Giemsa stained blood smears. Data is expressed as mean±SD.

In the WJC day 2 group, neutrophil recovery was most rapid and had returned to baseline values in 3 weeks. In the GVHD only group, neutrophil recovery returned to baseline levels at week 5 post-transplantation. In the positive control group and the WJCs day 0 group, neutrophil reached more than 10% at week 3 to 4 and had not returned to baseline pretreatment value (week 0).

3.9.6 Comparing clinical manifestations at day 17 of WJC day 2 group versus the GVHD only group and the positive control group.

A comparison the WJC day 2 group versus the positive control group at day 17 is shown in figure 3.42.

The WJC day 2 group presented clinical characteristic of a healthy rat, no alopecia or ear erythema was noted at this time. In contrast, the positive control group presented with mild facial alopecia (nose) and ears erythema. Vasodilation in ears skin was also noted in these rats (fig. 3.42)

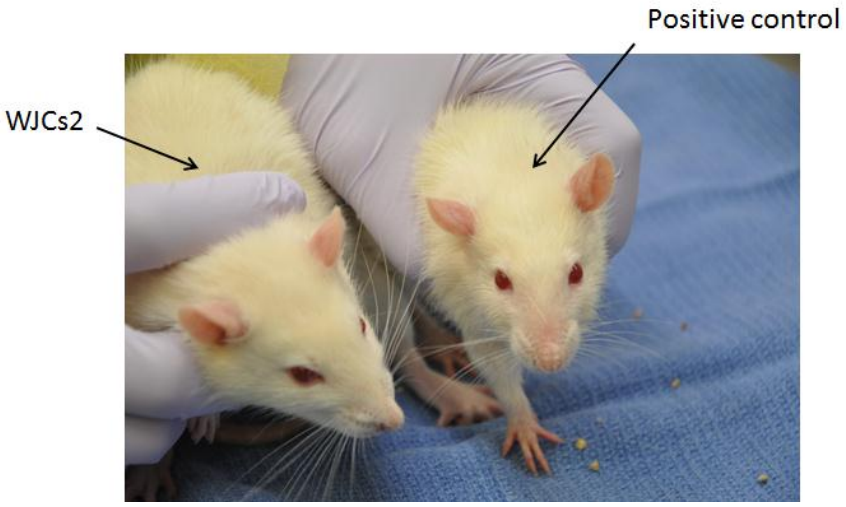

Figure 3.42. Clinical manifestations of WJCs day 2 group versus the (GVHD only group on day 17. Nose and peri-ocular alopecia was observed in all rats from positive control group and not in the WJC day 2 group.

At day 17 a comparison between the WJC day 2 group versus GVHD only group is shown in figure 3.43.

The WJC day 2 group presented clinical characteristic of a healthy rat, no alopecia or ear erythema was observed. Note the normal posture, fur texture and ears skin color of rats in the WJC day 2 group (fig 3.43). In contrast, rat from the GVHD only group have hunched posture, ruffled fur and marked skin eras erythema (fig. 3.43).

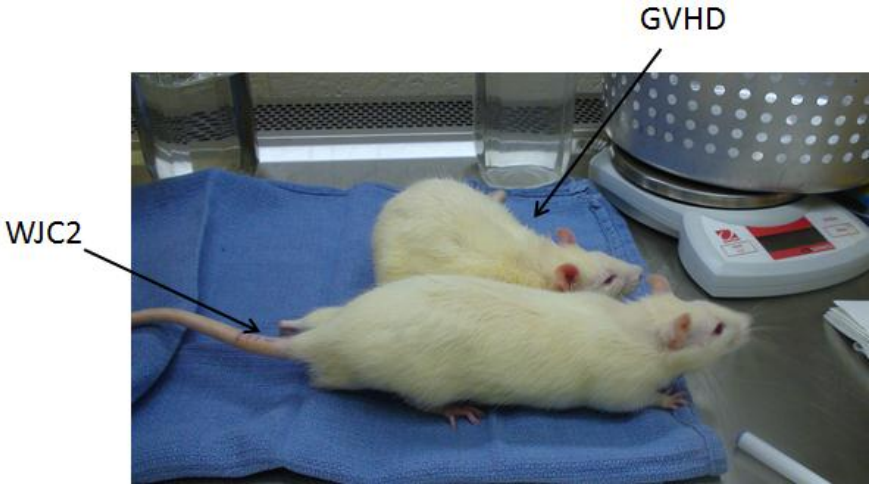

Figure 3.43. Clinical aspect of the WJC day 2 group versus the GVHD only group. GVHD only group rats had hunched posture, ruffled fur and ears skin erythema. In contrast, rats in the WJCs day 2 group did not show GVHD –associated symptomatology.

3.10. Engraftment and chimerism

Using genomic PCR analysis, long term engraftment (day 77) of allogeneic hematopoietic cells was found in all transplanted rats, except one rat in the WJC day 0 group in which cells from donor were not detected in tail tip, spleen or bone marrow at day 77 (see samples from rat 26 in figure 3.44).

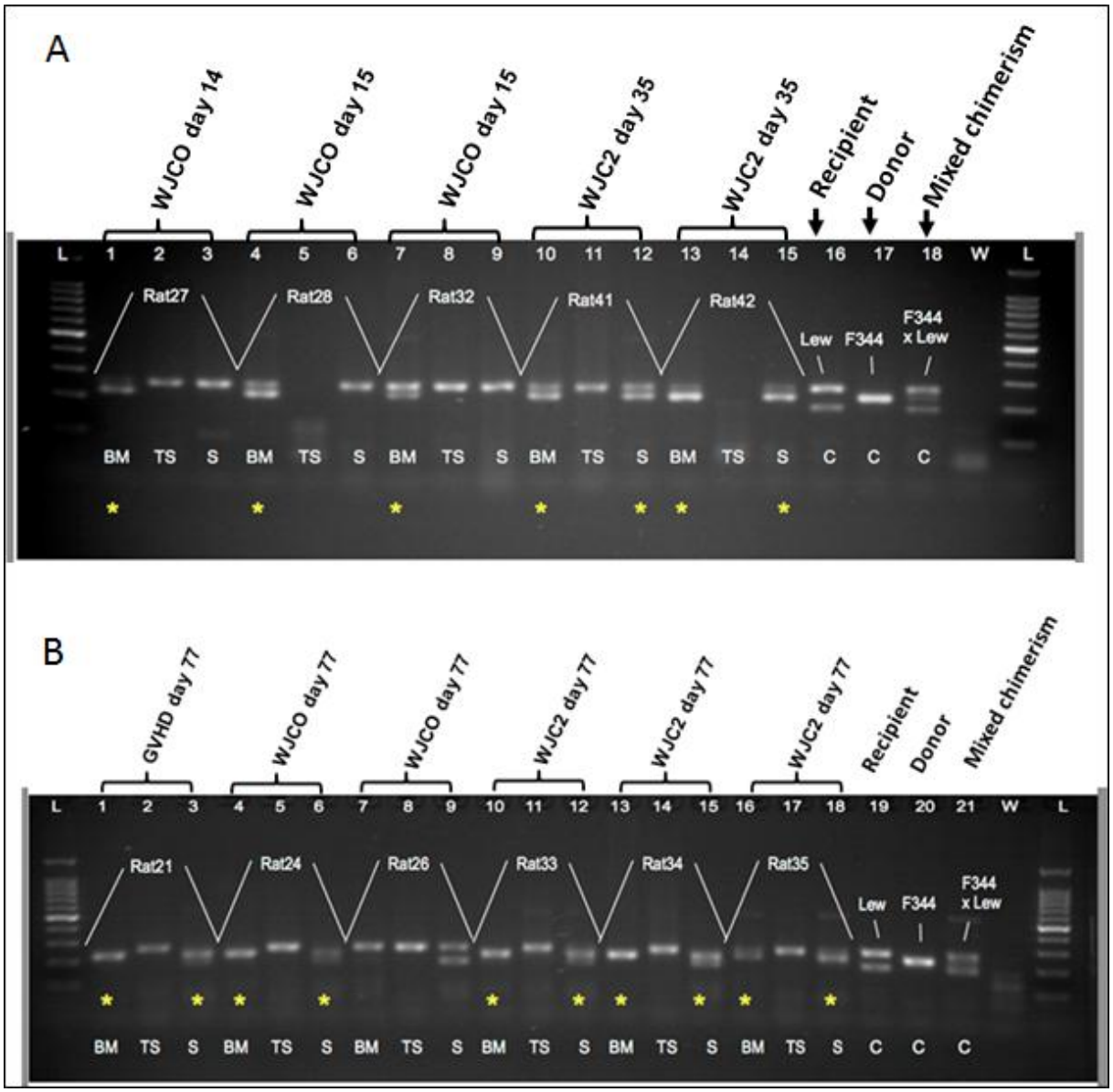

Fig.3.44. PCR genotyping to detect the Lewis (252bp) and F344 (160 bp) microsatellite DNA to demonstrate engraftment of donor F344 rats hematopoietic cells in bone marrow, spleen and tail tip tissues from recipients Lewis rats. (A) WJCO group rats sampled at 14 and 15 days showed DNA from donor F344 rats only at bone marrow level, while at day 35 donor DNA was found in

both bone morrow and spleen from rats receiving WJCs at day 2. (B) Samples taken at the end point (day 77) show F344 DNA in spleen and bone marrow, however double band was not evident.

Note that F344 DNA was not found in tail tip sample but was found in bone marrow and spleen for most animals.

3.11 Assessment of GVHD

3.11.1 GVHD daily clinical signal grade

Semi-quantitative score of GVHD is summarized in table 3.6

TABLE3.6
Semi-quantitative score of GVHD associate symptomatology

Group	Positive	GVHD	WJC0	WJC2
Erythema	3	3	1	0
Weight lost	2	2	2	1
Posture	1	3	0	0
Diarrhea	0	2	0	1
Skin integrity ruffled fur	1	1	1	1
SUM	**7**	**11**	**4**	**3**

By using the IBMTR and Glucksberg five out of 10 rats in the GVHD only group were scored as suffering GVHD stage 1 grade II. The positive control group was scored as suffering stage GVHD 1 grade I. Rats in the WJC day 0 group that were dying before midterm study (day 35) (n=7) were scored as suffering GVHD stage 1 grade I, and rats from this group that survived until day 77 (n=3) were considered not suffering GVHD. In the WJC day 2 group, only one out of 10 rats scored as GVHD stage 1 grade II, and 9 out 10 rats from this group was considered not suffering from GVHD. This ranking was validated with clinical pathological data obtained at day 77 (Tables 3.11).

3.12 Statistical analysis

Comparison between group variables outcomes was performed by Kruskal-Wallis test with Dunn's post-hoc test (non-parametric). Significance was set at $p<0.05$.

3.12.1 Body weight

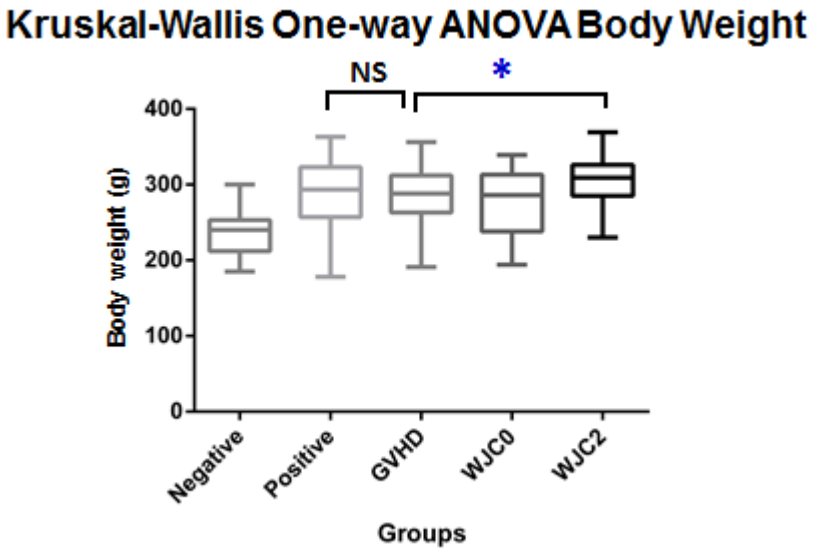

Figure 3.45. A Kruskal-Wallis test was used to evaluate differences among the 4 treatments. The outcome of the test indicated significant differences among the treatment conditions, Kruskal-Wallis test p value = < 0.0001 (df= 4, N=2268). To find out the direction of the differences, Dunn's multiple comparison test was performed.

Table 3.7
Dunn's Multiple Comparison test of Average Weight of rat groups

Number of families	1			
Number of comparisons per family	10			
Alpha	0.05			
Dunn's multiple comparisons test	Mean rank 1	Mean rank 2	Mean rank diff.	Significant?
Negative vs. Positive	310.9	1138	-827.5	Yes
Negative vs. GVHD	310.9	1081	-769.8	Yes
Negative vs. WJC0	310.9	940.7	-629.8	Yes
Negative vs. WJC2	310.9	1392	-1081	Yes
Positive vs. GVHD	1138	1081	57.68	No
Positive vs. WJC0	1138	940.7	197.7	Yes
Positive vs. WJC2	1138	1392	-253.3	Yes
GVHD vs. WJC0	1081	940.7	140	Yes
GVHD vs. WJC2	1081	1392	-311.0	Yes
WJC0 vs. WJC2	940.7	1392	-451.0	Yes

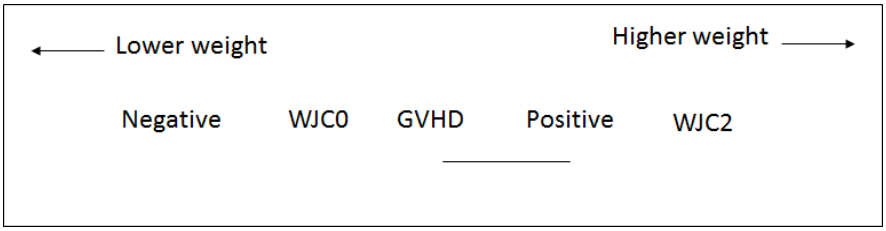

Figure 3.46. Dunn's report. Dunn's Multiple Comparison test of body weight of the experimental groups. Pairwise multiple comparison test revealed no significant difference in body weight mean between the positive control group and the GVHD only group α=0.05.

3.12.2 Hematocrit

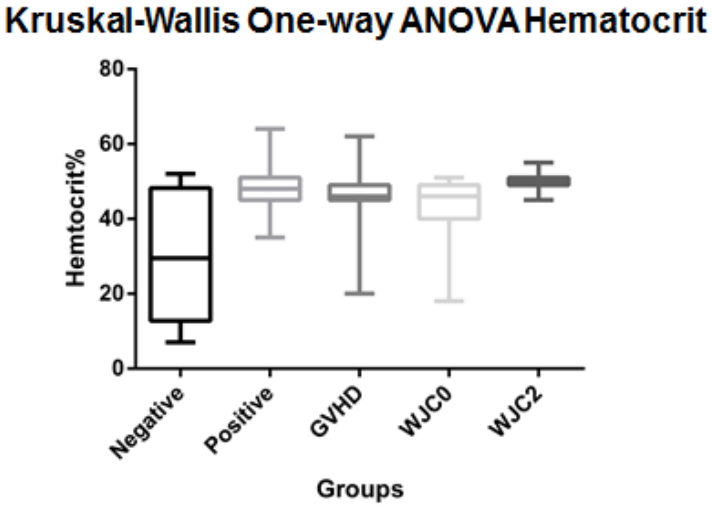

Figure 3.47. After ranking the individual scores Kruskal-Wallis test was used to evaluate differences among the 4 treatments. The outcome of the test indicated significant differences

among the treatment conditions, Kruskal-Wallis test statistic (H= 91.07 p<0.0001, df= 4, n=360). To find the direction of the differences, Dunn's multiple comparison test was performed.

Table 3.8

Dunn's Multiple Comparison test of Average Hematocrit (Ht) of rat groups

Number of families	1			
Number of comparisons per family	10			
Alpha	0.05			
Dunn's multiple comparisons test	Mean rank 1	Mean rank 2	Mean rank diff.	Significant?
Negative vs. Positive	51.58	197.4	-145.8	Yes
Negative vs. GVHD	51.58	164.2	-112.7	Yes
Negative vs. WJC0	51.58	121.4	-69.86	Yes
Negative vs. WJC2	51.58	251.7	-200.1	Yes
Positive vs. GVHD	197.4	164.2	33.12	No
Positive vs. WJC0	197.4	121.4	75.92	Yes
Positive vs. WJC2	197.4	251.7	-54.35	Yes
GVHD vs. WJC0	164.2	121.4	42.80	No
GVHD vs. WJC2	164.2	251.7	-87.47	Yes
WJC0 vs. WJC2	121.4	251.7	-130	Yes

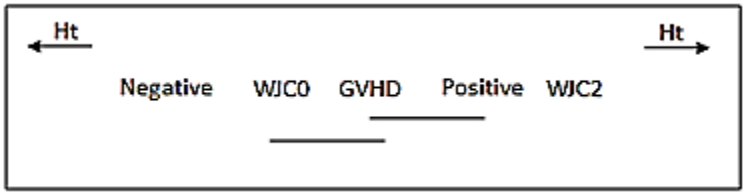

Figure 3.48. Dunn's report. Dunn's Multiple Comparison test of average Hematocrit (Ht) of rat group. Pairwise multiple comparison test revealed no significant difference in hematocrit mean between with the WJCs day 0 group and the positive control group and the GVHD only group. No significant differences in hematocrit was found the GVHD only group and the positive control group.

3.12.3. Body temperature

Body temperature

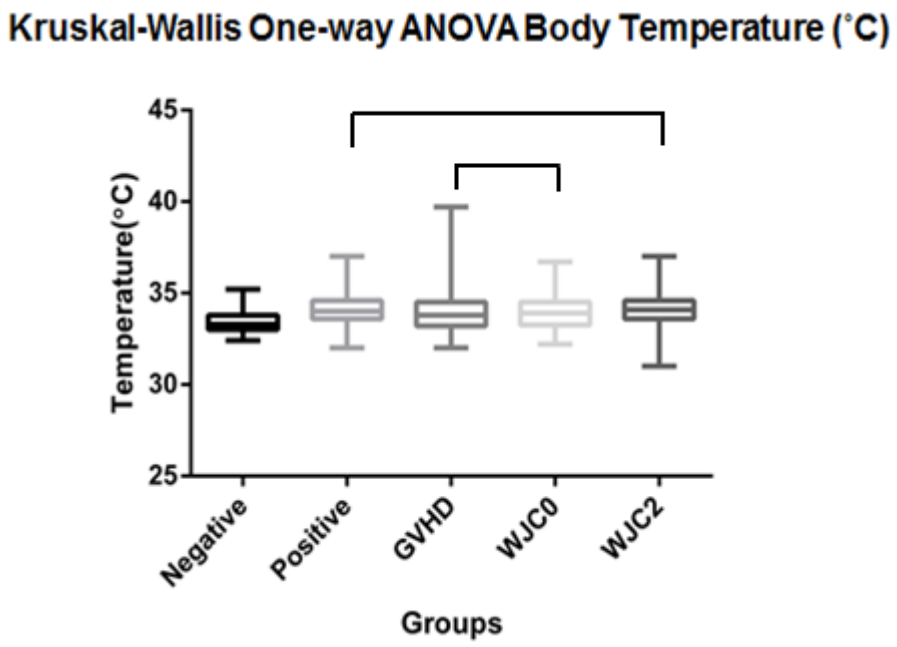

Figure 3.49. A Kruskal-Wallis test was used to evaluate differences among the 4 treatments. The outcome of the test indicated significant differences among the treatment conditions on the variable body temperature, Kruskal-Wallis test statistic (H= 71.76 ,df= 4, p value= <0.0001, n=2167). To find out the direction of the differences, Dunn's multiple comparison test was performed.

Table 3.9
Dunn's Multiple Comparison test of Average Body Temperature (˚C) of rat groups

Number of families	1			
Alpha	0.05			
Dunn's multiple comparisons test	Mean rank 1	Mean rank 2	Mean rank Diff.	Significant?
Negative vs. Positive	690.0	1153	-463.0	Yes
Negative vs. GVHD	690.0	998.9	-308.9	Yes
Negative vs. WJC0	690.0	1022	-332.5	Yes
Negative vs. WJC2	690.0	1172	-481.09	Yes
Positive vs. GVHD	1153	998.9	154.1	Yes
Positive vs. WJC0	1153	1022	130.5	Yes
Positive vs. WJC2	1153	1172	-18.96	No
GVHD vs. WJC0	998.9	1022	-23.55	No
GVHD vs. WJC2	998.9	1172	-173.0	Yes
WJC0 vs. WJC2	1022	1172	-149.5	Yes

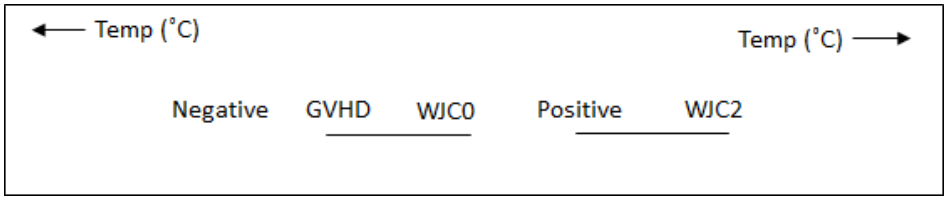

Figure 3.50. Dunn's Multiple Comparison test of body temperature (˚C) of experimental and control groups.

3.13 Clinical pathological study.

Hematological and biochemical clinical parameters were evaluated at day 35 and 77 respectively; data is summarized in tables 3.10 and 3.11.

TABLE 3.10
35-Day GVHD study
Clinical pathology evaluation

	Group 1 Untreated	2 Negative control*	3 Positive control	4 WJCs day 0	5 WJCs day 2	6 GVHD	7 Ref. value‡
Number	5	10*	10	3**	10	9***	-
Hematology							
Leuk count (K/µl)	5.90±0.94	0.19±0.23	4.58±1.17	4.74±0.70	5.78±0.23	3.70±1.50	1.96-8.25
RBC conc. (M/µl)	8.18±0.95	2.34±0.85	8.00±0.89	6.93±0.32	6.96±0.26	6.31±0.59	7.27-9.65
Hgb (g/dL)	14.04±1.53	3.90±1.47	14.29±1.21	14.43±0.60	14.35±0.64	13.30±0.80	13.7-17.6
HcT (%)	47.6±5.25	12.63±4.75	48.10±3.98	49.67±1.53	49.00±1.70	43.90±2.88	39.6-52.3
MCV (fL)	58.20±1.10	54±1.64	60.40±4.86	68.33±1.15	63.10±4.07	59.73±8.50	49.8-57.9
MCH (pg)	17±0.00	16.90±0.35	18.00±1.89	20.67±0.58	19.56±1.51	18.20±2.20	17.1-20.4
MCH conc(g/dL)	29.80±0.84	31.25±1.04	30.10±0.66	30.33±0.58	29.89±0.78	30.18±0.98	32.9-37.
Serum biochemistry							
Creatinine (mg/dL)	0.42±0.08	0.19±0.06	0.39±0.13	0.37±0.06	0.38±0.06	0.42±0.14	0.2-0.5
ALT (U/L)	62.48±6.75	139±219	43.00±8.60	38.33±5.68	46.80±10.80	45.82±14.52	18-45
AST (U/L)	91.78±20.38	176±214	98.20±29.84	88.67±19.60	100±22.53	117.45±18.64	74-143
Bilirubin total (mg/dL)	0.1±0	0.1±0	0.14±0.08	0.13±0.06	0.12±0.04	0.3±0.25	0.05-0.15

(*) Sample were taken at day 7, 9,10 and 11 (prior to death)
(**) only 3 animal survived until day 35
(***) only 9 animals were alive at day 35
‡ Charles Rivers Clinical Laboratory Parameter for Crl:WI(Han). Mary L. A. Giknis, Ph.D and Charles B. Clifford, D.V.M, Ph.D. March, 2008.

TABLE 3.11
77-Day GVHD study
Clinical pathology evaluation

	Group 1 Untreated	2 Negative control*	3 Positive control	4 WJCs day 0	5 WJCs day 2	6 GVHD	7 Ref. value‡
Number	5	10	8*	3**	8*	5***	-
Hematology							
Leuk count(K/µl)	5.90±0.94	0.19±0.23	4.25±1.51	3.87±1.74	4.61±0.83	4.74±1.02	1.96-8.25
RBC conc.(M/µl)	8.18±0.95	2.34±0.85	7.66±0.42	7.66±0.42	7.79±0.26	7.76±0.33	7.27-9.65
Hgb (g/dL)	14.04±1.53	3.90±1.47	14.71±1.26	14.33±0.93	14.99±0.69	14.76 ±0.59	13.7-17.6
HcT (%)	47.6±5.25	12.63±4.75	49±4.57	47.67±4.04	50.00±2.00	49.80±2.59	39.6-52.3
MCV (fL)	58.20±1.10	54±1.64	63.63±3.42	61.33±5.13	63.13±1.89	64.20±1.92	49.8-57.9
MCH (pg)	17±0.00	16.90±0.35	19±1.07	19±2.00	19.13±0.35	19±0.00	17.1-20.4
MCH conc (g/dL)	29.80±0.84	31.25±1.04	30.38±0.52	30±1.00	30±0.53	30±0.71	32.9-37.
Serum biochemistry							
Creatinine(mg/dL)	0.42±0.08	0.19±0.06	0.59±0.09	0.5±0.1	0.53±0.04	0.58±0.08	0.2-0.5
ALT (U/L)	62.48±6.75	139±219	81±52.49	63.33±7.77	63.25±6.5	54±17.48	18-45
AST (U/L)	91.78±20.38	176±214	219.38±166.16	98.33±17.21	121.38±29.32	152.80±51.14	74-143
Bilirubin total (mg/dL)	0.1±0	0.1±0	0.1±0.00	0.1±0.00	0.1±0.00	0.12±0.45	0.05-0.15

(*) only 8 animal survived until day 77
(**) only 3animal survived until day 77
(***) only 5animals were alive at day 77‡ Charles Rivers Clinical Laboratory Parameter for Crl:WI (Han). Mary L. A. Giknis, Ph.D and Charles B. Clifford D.V.M, Ph.D. March,2008

REFERENCES

[1]. Häusermann, P., Walter, R. B., Halter, J., Biedermann, B. C., Tichelli, A., Itin, P., & Gratwohl, A. (2008). Cutaneous graft-versus-host disease: a guide for the dermatologist. *Dermatology (Basel, Switzerland)*, *216*(4): 287–304.

[2]. Warren, E. H., Zhang, X. C., Li, S., *et al*. (2012). Effect of MHC and non-MHC donor/recipient genetic disparity on the outcome of allogeneic HCT. *Blood*, *120*(14): 2796–2806.

[3]. Parmar, S., Del Lima, M., Zou, Y., *et al*. (2009). Donor-recipient mismatches in MHC class I chain-related gene A in unrelated donor transplantation lead to increased incidence of acute graft-versus-host disease. *Blood*, 114(14): 2884–7.

[4]. Flomenberg, N., Baxter-Lowe, L. A., Confer, D., Fernandez-Vina, M., Filipovich, A., Horowitz, M., Hurley, C., *et al*. (2004). Impact of HLA class I and class II high-resolution matching on outcomes of unrelated donor bone marrow transplantation: HLA-C mismatching is associated with a strong adverse effect on transplantation outcome. *Blood*, *104*(7): 1923–1930.

[5]. Kline, J., Subbiah, S., Lazarus, H. M., & van Besien, K. (2008). Autologous graft-versus-host disease: harnessing anti-tumor immunity through impaired self-tolerance. *Bone marrow transplantation*, 41(6): 505–513.

[6]. Cogbill, C. H., Drobyski, W. R., & Komorowski, R. A. (2011). Gastrointestinal pathology of autologous graft-versus-host disease following hematopoietic stem cell transplantation: a clinicopathological study of 17 cases. *Modern pathology : an official journal of the United States and Canadian Academy of Pathology, Inc*, *24*(1): 117–25.

[7]. Drobyski, W. R., Hari, P., Keever-Taylor, C., Komorowski, R., & Grossman, W. (2009). Severe autologous GVHD after hematopoietic progenitor cell transplantation for multiple myeloma. *Bone marrow transplantation*, *43*(2): 169–177.

[8]. Blazar, B. R., & Murphy, W. J. (2005). Bone marrow transplantation and approaches to avoid graft-versus-host disease (GVHD). *Philosophical transactions of the Royal Society of London. Series B, Biological sciences*, 360(1461):1747–1767.

[9]. Socié, G., & Blazar, B. R. (2009). Acute graft-versus-host disease: from the bench to the bedside. *Blood*, 114(20):4327–4336.

[10]. Reddy, P., Ferrara J.L.M. *(*2008). *Mouse models of graft-versus-host disease. In StemBook. Lisa Gerard, editor. StemBook, Cambridge, MA.* http://www.stembook.org/node/548

[11]. Schroeder, M. A, & DiPersio, J. F. (2011). Mouse models of graft-versus-host disease: advances and limitations. *Disease models & mechanisms*, *4*(3):318–333.

[12]. Zinöcker, S., Sviland, L., Dressel, R., & Rolstad, B. (2011). Kinetics of lymphocyte reconstitution after allogeneic bone marrow transplantation: markers of graft-versus-host disease. *Journal of leukocyte biology*, *90*(1):177–187.

[13]. Glazier, A., Tutschka, P.J., Farmer, E.R., Santos, G. (1983). Graft-versus-host disease in cyclosporin A-treated rats after syngeneic and autologous bone marrow reconstitution. *J Exp Med*, 158: 1–8.

[14]. Hess, A.D., Kennedy, M.J., Ruvolo, P. P., *et al*. (1995). Antitumor activity of syngeneic/autologous graft versus host disease. *Ann N Y Acad Sci*, 770:189–202.

[15]. Dressel, R., Walter, L., & Günther, E. (2001). Genomic and funtional aspects of the rat MHC, the RT1 complex. *Immunological reviews*, 184:82–95.

[16]. Gill, T.R., Smith G., Wissler R., Kunz H. (1989).The rat as an experimental animal. Science 245:269–276.

[17]. Ioannidu, S., Walter, L., Dressel, R., & Günther, E. (2001). Physical map and expression profile of genes of the telomeric class I gene region of the rat MHC. *Journal of immunology (Baltimore, Md. : 1950)*, *166*(6): 3957–65.

[18]. Hurt, P., Walter, L., Sudbrak, R., Klages, S., *et al*. (2004). The genomic sequence and comparative analysis of the rat major histocompatibility complex. *Genome research*, 14(4):631–9.

[19]. Caspi, R. R. (2006). Animal models of autoimmune and immune-mediated uveitis. *Drug Discovery Today: Disease Models*, 3(1), 3–9. [20]. Locker, J., Gill, T. J., Kraus, J. P., Ohura, T., Swarop, M., Rivi, M., Islam, M. Q., *et al*. (1990). Brief communication The rat MHC and cystathionine fl-synthase gene are syntenic on chromosome 20: 271–274.

[21]. Günther, E., & Walter, L. (2001). The major histocompatibility complex of the rat (Rattus norvegicus). *Immunogenetics*, 53(7):520–42.

[22]. Leong, L. Y. W., A.-F. Le Rolle, E. V. Deverson, S. J. Powis, A. P. Larkins, J. T. Vaage, A. Stokland, D. Lambracht-Washington, B. Rolstad, E. Joly, G. W. Butcher. 1999. RT1-U: identification of a novel, active, class Ib alloantigen of the rat MHC. *J. Immunol*. 162: 743

[23]. Hughes, A. L. (1995). Origin and evolution of HLA class I pseudogenes. *Molecular biology and evolution*, *12*(2): 247–58.

[24]. Planz, O., Dumrese, T., Hulpusch, S., Schirle, M., Stevanovic, S., & Stitz, L. (2001). A naturally processed rat major histocompatibility complex class I-associated viral peptide as target structure of borna disease virus-specific CD8+ T cells. *The Journal of biological chemistry*, 276(17): 13689–13694.

[25]. Drozina G., *et al.* (2005). Expression of MHC II genes. Curr. Top. Microbiol. Immunol., 290:147–170.

[26]. Nickoloff B.J., LA Turka L.A. (1994).Immunological functions of non-professional antigen-presenting cells: new insights from studies of T-cell interactions with keratinocytes. Immunol Today, 15: 464–469.

[27]. Seckert, C. K., Schader, S. I., Ebert, S., Thomas, D., *et al*. (2011). Antigen-presenting cells of haematopoietic origin prime cytomegalovirus-specific CD8 T-cells but are not sufficient for driving memory inflation during viral latency. *The Journal of general virology*, 92 (Pt 9):1994–2005.

[28]. Stagg, A.J, & Knight, S.C. (2001). Antigen-presenting Cells. In: eLS. John Wiley & Sons Ltd, Chichester. http://www.els.net. doi: 10.1038/npg.els.0000903.

[29]. Rescigno, M. (2010). Functional specialization of antigen presenting cells in the gastrointestinal tract. *Curr Opin Immunol*, 22, 131–136.

[30]. Hamrah, P. (2003). The Corneal Stroma Is Endowed with a Significant Number of Resident Dendritic Cells. *Investigative Ophthalmology & Visual Science*, *44*(2):581–589..

[31]. Koyama, M., Kuns, R. D., *et al*. (2012). Recipient nonhematopoietic antigen-presenting cells are sufficient to induce lethal acute graft-versus-host disease. *Nature medicine*, *18*(1): 135–142.

[32]. Vihinen, M. 2005. Immunodeficiency, Primary: Affecting the Adaptive Immune System. eLS.

[33]. Volpi, E. V., Chevret, E., Jones, T., Vatcheva, R., *et al*. (2000). Large-scale chromatin organization of the major histocompatibility complex and other regions of human chromosome 6 and its response to interferon in interphase nuclei. *Journal of cell science*, 113*:*1565–1576.

[34]. Jameway, C.A., Shlomchik, M.J., Travers, P., Walport, M. (2004). The major histocompatibility complex and its functions .Immunobiology (6th ed.), Garland Publishing, London: 167–184.

[35]. Sargent, C. A., Dunham, I., Trowsdale, J., & Campbell, R. D. (1989). Human major histocompatibility complex contains genes for the major heat shock protein HSP70. *Proceedings of the National Academy of Sciences of the United States of America*, 86(6):1968–72.

[36]. Schulak , J.A., Engelstad, K.M. (1989). Immunologic consequences of combined pancreas-spleen transplantation in the rat. *J Surg Res*, 47(1): 52-68.

[37]. Nakao M., Taguchi T., Ogita K., Nishimoto Y., Suita S. (2005). *Fukuoka Igaku Zasshi*, 96(2):49-57.

[38]. Palmer M., Wettstein P.J., Frelinger J.A.(1983). Evidence for extensive polymorphism of class I genes in the rat major histocompatibility complex (RT1). *Proc Natl Acad Sci U S A.* 80(24):7616–7620.

[39]. Shlomchik, W. D. (2007). Graft-versus-host disease. *Nat. Rev. Immunol*, 7: 340–352.

[40]. Asano, S. (2012). Current status of hematopoietic stem cell transplantation for acute radiation syndromes. *International journal of hematology*, *95*(3): 227–31.

[41]. Duran-Struuck, R., & Dysko, R. C. (2009). Principles of bone marrow transplantation (BMT): providing optimal veterinary and husbandry care to irradiated mice in BMT studies. *Journal of the American Association for Laboratory Animal Science: JAALAS*, *48*(1): 11–22.

[42]. Lange, C., Brunswig-Spickenheier, B., Cappallo-Obermann, H., *et al*. (2011). Radiation rescue: mesenchymal stromal cells protect from lethal irradiation. *PloS One*, *6*(1), e14486.

[43].Nebendahl, K. (2000). Routes of administration. In: Krinke G, editor. The laboratory rat. London: Academic Press; 463-483

[44]. Polchert, D., Sobinsky, J., Douglas, G., Kidd, M., *et al*. (2008). IFN-gamma activation of mesenchymal stem cells for treatment and prevention of graft versus host disease. *European journal of immunology*, 38(6): 1745–1755.

[45]. Taylor, P. A. (2002). The infusion of ex vivo activated and expanded CD4+ CD25+ immune regulatory cells inhibits graft-versus-host disease lethality. *Blood*, *99*(10): 3493–3499.

[46]. Cahn, J.-Y., Klein, J. P., Lee, S. J., *et al*. (2005). Prospective evaluation of 2 acute graft-versus-host (GVHD) grading systems: a joint Société Française de Greffe de Moëlle et Thérapie Cellulaire (SFGM-TC), Dana Farber Cancer Institute (DFCI), and International Bone Marrow Transplant Registry (IBMTR) pros. *Blood*, 106(4):1495–1500.

[47]. Martino, R., Romero, P., Subira, M., *et al*,.(1999). Comparison of the classic Glucksberg criteria and the IBMTR Severity Index for grading acute graft-versus-host disease following HLA-identical sibling stem cell transplantation. International Bone Marrow Transplant Registry. *Bone Marrow Transplant, 24: 283-287.*

[48]. Carpenter,P.A., & MacMillan M.L. (2010). Management of Acute Graft Versus Host Disease in Children. Pediatr Clin North Am NIH Public Access, *57*(1): 273–295.

[49]. Seggewiss, R., Einsele, H., & Dc, W. (2010). Immune reconstitution after allogeneic transplantation and expanding options for immunomodulation : an update. . *Blood*,115:3861–3868.

[50]. Lauterbach, M., Donnell, P. O., Asano, K., & Mayadas, T. N. (2008). Role of TNF priming and adhesion molecules in neutrophil recruitment to intravascular immune. *J. Leukoc Biol*, 83*:* 1423– 1430.

[51]. Rat Gene ftp file, Rat Genome Database Web Site, Medical College of Wisconsin, Milwaukee, Wisconsin. World Wide Web (URL: http://rgd.mcw.edu/). September, 2013.

[52]. Claman, H.N. (1985). Mast cell depletion in murine chronic graft-versus-host disease. *J Invest Dermatol*, (4): 246-248.

[53]. Gowdy, K. M., Nugent, J. L., Martinu, T., *et al*. (2012). Protective role of T-bet and Th1 cytokines in pulmonary graft-versus-host disease and peribronchiolar fibrosis. *American journal of respiratory cell and molecular biology*, 46(2): 249–56.

[54]. Charles Rivers Clinical Laboratory Parameter for Crl:WI (Han). Mary L. A. Giknis, Ph.D and Charles B. Clifford, D.V.M, Ph.D. March, 2008

[55]. Paczesny, S., Braun, T. M., Levine, J. E., *et al*. (2010). Elafin is a biomarker of graft-versus-host disease of the skin. *Sci Transl Med*, 13*:*13ra12.

Chapter 4- Discussion.

Mesenchymal stromal cells derived from bone marrow (BM-MSCs) show immunosuppressive capacities *in vitro* and *in vivo*, and they have been tested in clinical trials as a potential cell therapy to prevent or treat GVHD [1, 2]. However, the isolation procedure, age of the donor, and limitations of *in vi*tro proliferation potential of adult BM-MSCs [3, 4, 5] highlight the necessity to find alternative non-controversial sources of MSCs such as Wharton's jelly cells (WJCs) [6]. The immunosuppressive properties of MSCs have been probed using *in vitro* [7], and *in vivo* assays [8] and, it has been established that their immune properties depend on timing of their exposure to activation-related cytokines (licensing), such as interferon gamma [7]. Valencic *et al*. found that in presence of non-licensed WJCs, activated lymphocytes showed regular or even increased proliferation, while in presence of licensed WJCs their proliferation is strongly inhibited [7]. In this dissertation, Wharton's jelly derived mesenchymal stromal cells (WJCs) were tested as cell therapy to prevent GVHD in a minor histocompatibility mismatch model in rats. Here, the GVHD model was established and lethally irradiated Lewis rats ($RT1^{l}$, 10 Gy exposure) received 30 x 10^6 bone marrow cells and 2 x 10^6 $CD8^+$ splenocytes. Adoptive transfusion of WJCs was done either on day 0 (24 hours after TBI, WJC day 0 group) together with bone marrow cells and splenocytes $CD8^+$ or at day 2 (48 hours after hematopoietic cell transplantation, WJC day 2 group). I found that adoptive transfer of WJCs on day 2 ameliorated GVHD-associated symptomatology including body weight loss, diarrhea, hunched posture, hair loss, prolonged survival and improved hematopoiesis recovery as it was measured by hematocrit, neutrophil recovery and hematopoiesis compartment repopulation.

Polchert *et al*. using bone marrow-derived MSCs to prevent GVHD in a mouse model found that MSCs had a beneficial effect, increasing survival only when given at day 2 or day 20 after transplantation [9]. In agreement with this study, WJCs were valuable to control GVHD only when given on day 2 post-transplant. Although, 7 out 10 GVHD rats receiving WJCs at day 0 died before day 35, the surviving rats showed normal serum biochemistry values and hematopoietic recovery by day 77. The surviving GVHD rats receiving WJC on day 0 showed no evidence of GVHD injury by gross anatomical or histopathological evaluation. In contrast, GVHD rats receiving WJC on day 0 dying before day 17 presented with clinical and

histopathological signs of engraftment failure. Rats in this group had a hematocrit on day 14 of 25 ± 7%.

WJCs express adhesion molecules (CD44, C105) and integrin markers such as CD29 and CD49e [10]. I conjecture that WJCs may adhere to endothelial cells via adhesion molecules or via interactions with integrins. A consequence of this interaction might be reducing diapedesis of hematopoietic cells when bone marrow and MSCs are simultaneously transplanted. It is known that when MSCs are infused IV, most of them are trapped in lung capillary network for about 24 hrs [11]. Murine models showed rapid changes in lung caused by ionizing radiation include cytokines release and increase of endothelial cells adhesion molecules and thereby arrest of inflammatory cells [12]. I hypothesize that WJCs given 24 hours after total body irradiation in rats may fail to control GVHD due to endothelium swelling in lung which contributes with hematopoietic cell and WJCs stasis in lung capillaries, and secondarily producing as a consequence, engraftment failure. Infusion of WJCs on day 2 after transplantation (day 3 post-irradiation) ameliorated the symptoms of acute radiation syndrome such as weight loss, diarrhea, anemia, breathing resistance and activation of lung innate immunity seen as degranulation of pulmonary eosinophils and deposition of major basic protein crystals.

Eosinophils are inflammatory cells present primarily in sub-epithelial connective tissues of gastrointestinal, respiratory systems and final portion of genitourinary system [13]. Major basic protein (MBP) is the most abundant component of eosinophils and constitutes about 51% of the total protein stored in eosinophil granules [13]. Biological actions of MBP including release of histamine from mast cells and basophils, activation of neutrophils and alveolar macrophage, epithelial cell damage [14]. Interleukin 5 (IL-5) released by lymphocytes, mast cells and eosinophil is the main cytokine implicated in eosinophil activation [15]. Interestingly, I found an activation of eosinophils with a concomitant reduction of pulmonary mast cells. In fact, no stainable pleural cells mast cells were found in the negative control group, or in the GVHD only group at day 35, or the WJC day 0 group dying before 17 days post-transplantation. A partial degranulation of mast cells, in which cells lost metachromatic granules but preserved orthochromatic granules, was observed in the positive control group at day 35 and in the WJC day 2 group at day 35. At the end point (day 77), rats from these two groups had mast cells with normal stain affinity in lung pleura. Abundant numbers of mast cell were observed within lymph nodes in long term survival (day 77) of the WJCs day 0 group and WJC day 2 group (figs.3.30

and 3.36). On the contrary, the GVHD only group showed a dramatic increase in mast cells not only in their typical localization within the lamina propia connective tissue, but also within the glandular epithelium (see figure 3.21).

Degranulation of mast cells after ionizing radiation exposure has been reported [16, 17]. Since mast cells secrete IL-5 which in turn activates eosinophils [18], I suppose that pulmonary radiation-induced mast cells depletion is associated with eosinophil activation and deposition of MBP crystals. This leads to IL-5 and/ or mast cells activation and may initiate the inflammatory cytokine cascade and development of GVHD after total body irradiation by allogeneic hematopoietic cell transplantation in the rat model. Lung radiosensivity is indicated by early changes in cytokine production after radiation exposure [12].

It has been proposed that GVHD pathogenesis may be initiated by conditioning regimen-induced injury in target tissues, especially at intestinal level where translocation of lipopolysaccharide (LPS) released by resident microflora stimulate the secretion of cytokines particularly tumor necrosis factor alpha (TNF- α) and interleukin 1(IL-1) by macrophages [13]. Subsequent stages of GVHD may be driven by an increase in adhesion molecules and leakage through intestinal mucosa [14]. Although, the lower respiratory tract is free of resident bacteria [15], TNF-α is also produced by mast cells as preformed or immunologically inducible TNF-α [16]. Here, metachromatic stainable mast cells were not detected at intestinal, hepatic and pulmonary level in irradiated only group. This could be due activation and degranulation of mast cells which in turn may trigger cytokinemia and initiated GVHD syndrome manifestations after TBI and allogeneic hematopoietic cells transplantation.

Contrary to other species where mast cells represent 2-3 % of total cells within lamina propia, mast cells in murine small intestine are scarce with about five mast cells per villus [17]. The role of mast cells in intestinal epithelial homeostasis and barrier has been established [17, 18]. In rat model of GVHD Levy *et al.* showed that after radiation-induced depletion around day 12, intestinal mast cells show a marked intestinal reduction [19]. In concordance with Levy *et al*, in my study stainable mast cells were not identified in tissue sections of Lewis rats irradiated and not transplanted or irradiated, and transplanted but dying before 35 days. The later depletion seen in my study may be related to the degree of histocompatibility mismatch established to induce aGVHD. Levy established the GVHD model across major histocompatibility antigen mismatch settings, which is known to accelerate GVHD manifestation. In my model (across minor

histocompatibility antigen mismatch) clinical and histopathological manifestation of GVHD had a delayed presentation. Metachromatic staining of tissue sample allowed to distinguish rare mast cells containing only orthochromatic granules and confined to sub-epithelial connective tissue in lung and intestine from rats receiving T-cell depleted bone marrow untreated with WJCs (positive control), GVHD rats receiving bone marrow cells and splenocytes $CD8^+$ treated with WJC on day 2, and in rats receiving bone marrow cells and splenocytes $CD8^+$ treated with WJC on day 0 which survived until day 77. A non-quantitative evaluation from GVHD rats untreated with WJCs revealed a pronounced increase in mast cell population at day 77. This increase was observed in small intestine lamina propia, and also within the glandular epithelial lining. Mast cells presented dense granules evident with routine hematoxiline-eosine (H&E) and with specific staining. This clear infiltration of mast cells in intestinal mucosa may produce alterations in epithelial barrier and permeability. Mast cells hyperplasia has been linked with fibrotic disorder associated with GVHD [20], and blockage of their secretion of TNF-α ameliorate aGVHD and improve survival time [21]. In this study, greater deposition of collagen in organs of GVHD rats untreated with WJCs was observed (see figure 3.38). This fibrosis could be linked with mast cells degranulation detected in this group of rats. The role of mast cells in long-term graft tolerance was reported by Lu *et al*. in 2006; they showed that mast cell deficient mice were not capable of establishing long term allo-graft tolerance[22]. In histological sections infiltration of mast cells co-localized with Tregs was observed [22]. Wu *et al.*, in human patients suffering aGVHD, found a trend for higher number of mast cells and Tregs in skin areas corresponding to higher inflammation [23]. In the present study, I found infiltration of mast cells in lymph nodes from long term surviving GVHD rats receiving WJCs on day 0 and day 2 which exhibited clinical parameters considered normal. Based in this observation, I postulate that a putative mechanism used by WJCs to ameliorate GVHD symptomatology may be by recruiting mast cells to lymph nodes where expansion of Tregs occurs after developing in thymus. This hypothesis could be confirmed by lymph node biopsy to quantify presence of Tregs.

Activation of humoral components of innate immunity was observed in GVHD-induced rats at day 17 post-transplantation. Complement deposition was detected in kidney nephron's tubules. Under physiological conditions complement components do not cross the glomerular filtration barrier, however presence of complement in nephron tubules is linked with nephritic pathologies connected to several etiology [24]. Kwan *et al*. recently reported in a mouse model

of GVHD that TBI triggers up-regulation of complement component by host dendritic cells (DC) which in turn activates allogeneic donor T cells [25]. In my study activation of complement may induce nephritic syndrome that could be linked with the increase in serum level creatinine observed in 5 out 5 GVHD rats untreated with WJCs.

After myeloablative conditioning regimen followed by hematopoietic cell transplantation, neutropenia is a common complication associated with a high rate of systemic infections [26]. In this study, infusion of WJCs on day 2 post-transplantation accelerated neutrophil recovery. Rats receiving WJCs on day 2 recovered the initial pre-treatment percentage of neutrophils at week 3 post-transplantation. (fig.3.41)

In summary, in rats which are developing Graft versus host disease, adoptive transfer of WJCs on day 2 can alleviate GVHD-associated symptomatology and enhanced hematopoietic recovery. Although the mechanism used by WJCs to offer immunoregulation is still unclear, I consider that these cells may control innate immunity up-regulation after TBI by promoting mobilization of mast cell to lymph node which in turn facilitates expansion of Tregs. Further studies are needed to confirm this hypothesis. Additional work is also needed to optimize WJCs dose and the timing of administration.

REFERENCES

[1]. Yi, Lin and William J. Hogan. (2011). "Clinical Application of Mesenchymal Stem Cells in the Treatment and Prevention of Graft-versus-Host Disease," Advances in Hematology, vol. 2011, Article ID 427863, 17 pages, 2011. doi:10.1155/2011/427863

[2]. Chen, H., Zhang, N., Li, T., *et al*.(2012). Human umbilical cord Wharton's jelly stem cells: immune property genes assay and effect of transplantation on the immune cells of heart failure patients. *Cell Immunol,* 276 (1-2):83-90.

[3]. Wagner, W., Bork, S., Horn, P., *et al*. (2009). Aging and Replicative Senescence Have Related Effects on Human Stem and Progenitor Cells. *PLoS One*, 4(6), e5846.

[4]. Stolzing, A., Jones, E., McGonagle, D., & Scutt, A. (2008). Age-related changes in human bone marrow-derived mesenchymal stem cells: consequences for cell therapies. *Mechanisms of Ageing and Development*, 129(3):163–73.

[5]. D'Ippolito, G., Schiller, P. C., Ricordi, C., Roos, B. A, & Howard, G. A. (1999). Age-related osteogenic potential of mesenchymal stromal stem cells from human vertebral bone marrow. *Journal of Bone and Mineral Research*, 14(7):1115–1122.

[6]. Forraz, N., & Mcguckin, C. P. (2011). The umbilical cord : a rich and ethical stem cell source to advance regenerative medicine. *Cell Prolif,* 44 (Suppl.1):60–69.

[7]. Valencic E., Piscianz E., Andolina M., Ventura A., Tommasini A. (2010). The immunosuppressive effect of Wharton's jelly stromal cells depends on the timing of their licensing and on lymphocyte activation. *Cytotherapy*, 12(2):154-160.

[8]. Ma, L., Zhou, Z., Zhang, D., Yang, S., Wang, J., Xue, F., Y. Yang,Y., R. Yang, R. (2012) Immunosuppressive function of mesenchymal stem cells from human umbilical cord matrix in immune thrombocytopenia patients. *Thromb Haemos,* 107(5):937-950.

[9]. Polchert, D., Sobinsky, J., Douglas, G., Kidd, M., Moadsiri, A., Reina, E., Genrich, K., *et al*. (2008). IFN-gamma activation of mesenchymal stem cells for treatment and prevention of graft versus host disease. *European Journal of Immunology*, 38(6): 1745–1755.

[10]. Iacono, M. L., Anzalone, R., Corrao, S., Giuffrè, M., Stefano, A. D., Giannuzzi, P., Cappello, F., *et al*. (2011). Perinatal and Wharton's Jelly-derived mesenchymal stem cells in cartilage regenerative medicine and tissue engineering strategies. Open Tissue Engineering & Regenerative Medicine Journal, (4):72-81.

[11]. Lee, R. H., Pulin, A. A., Seo, M. J., Kota, D. J., Ylostalo, J., Larson, B. L., Semprun-prieto, L., *et al*. (2009). Intravenous hMSCs improve myocardial infarction in mice

because cells embolized in lung are activated to secrete the anti-inflammatory protein TSG-6. *Stem Cells*, 5(1):54–63.

[12]. Hill, R. P. (2005). Radiation effects on the respiratory system.(2005) *BJR Suppl*, 27:75-81.

[13]. Malik, A. and Batra, J. K. (2012). Antimicrobial activity of human eosinophil granule proteins: involvement in host defense against pathogens *Crit. Rev. Microbiol.* 38: 168– 181.

[14]. Ferrara J.L., Reddy P. (2006). Pathophysiology of graft-versus-host disease *Semin Hematol*, 43:3–10.

[15]. Stover, C. M. (2010). Mechanism of stress-mdediated modulation of upper and lower respiratory tract infections.*Microbial Endocrinology*, (M. Lyte & P. P. E. Freestone, Eds.):181–189.

[16]. Gordon, J. R., Burd, P. R. & Galli, S. J. (1990).Mast cells as a source of multifunctional cytokines. *Immunol. Today*, 11:458–464.

[17]. Groschwitz, K. R., Ahrens, R., *et al*. (2009). Mast cells regulate homeostatic intestinal epithelial migration and barrier function by a chymase/Mcpt4-dependent mechanism. *Proceedings of the National Academy of Sciences of the United States of America*, 106(52): 22381–22386.

[18]. Chichlowski, M., Westwood, G. S., Abraham, S. N., & Hale, L. P. (2010). Role of mast cells in inflammatory bowel disease and inflammation-associated colorectal neoplasia in IL-10-deficient mice. *Plos One*, 5(8): 2–11.

[19]. Levy, D. A.,Wefald, A.(1986).Gut mucosal mast cells and goblet cells during acute graft-versus-host disease in rats. *Ann Inst Pasteur/Immunol*,137:281-288

[20]. Atkins F.M., Clark, R.A. (1987). Mast cells and fibrosis. *Arch Dermatol*, 123(2):191-193.

[21]. Korngold, R., Marini, J. C., de Baca, M. E., Murphy, G. F. & Giles-Komar, J. (2003). Role of tumor necrosis factor-α in graft-versus-host disease and graft-versus-leukemia responses. *Biol. Blood Marrow Transplant*, 9: 292–303.

[22]. Lu, L.F., *et al*. (2006). Mast cells are essential intermediaries in regulatory T-cell tolerance. *Nature*, 442: 997–1002

[23]. Wu, K.N., Emmons, R.V., Lisanti M.P., *et al*. (2009). Foxp3-expressing T regulatory cells and mast cells in acute graft-versus-host disease of the skin. *Cell Cycle*, 8:3593–3597.

[24]. Gaarkeuken, H., Siezenga, M. a, Zuidwijk, K., van Kooten, C., Rabelink, T. J., Daha, M. R., & Berger, S. P. (2008). Complement activation by tubular cells is mediated by

properdin binding. *American Journal of Physiology. Renal Physiology*, 295(5):F1397–1403.

[25]. Kwan, W., Hashimoto, D., Paz-Artal, E., *et al*. (2012). Brief report Antigen-presenting cell – derived complement modulates graft-versus-host disease. *J Clin Invest*, 122(6):2234–2238.

[26]. Mac Manus, M., Lamborn, K., Khan, W., *et al*. (1997). Radiotherapy-associated neutropenia and thrombocytopenia: analysis of risk factors and development of a predictive model. *Blood*, 89(7):2303–2310.